VOLUME 34 FEBRUARY 1956 NUMBER 2

# Canadian Journal of Chemistry

*Editor:* LÉO MARION

*Associate Editors:*

HERBERT C. BROWN, *Purdue University*
A. R. GORDON, *University of Toronto*
C. B. PURVES, *McGill University*
Sir ERIC RIDEAL, *Imperial College, University of London*
J. W. T. SPINKS, *University of Saskatchewan*
E. W. R. STEACIE, *National Research Council of Canada*
H. G. THODE, *McMaster University*
A. E. VAN ARKEL, *University of Leiden*

*Published by* THE NATIONAL RESEARCH COUNCIL

OTTAWA CANADA

# CANADIAN JOURNAL OF CHEMISTRY

(*Formerly Section B, Canadian Journal of Research*)

Under the authority of the Chairman of the Committee of the Privy Council on Scientific and Industrial Research, the National Research Council issues THE CANADIAN JOURNAL OF CHEMISTRY and six other journals devoted to the publication, in English or French, of the results of original scientific research. Matters of general policy concerning these journals are the responsibility of a joint Editorial Board consisting of: members representing the National Research Council of Canada; the Editors of the Journals; and members representing the Royal Society of Canada and four other scientific societies.

The Chemical Institute of Canada has chosen the Canadian Journal of Chemistry and the Canadian Journal of Technology as its medium of publication for scientific papers.



## EDITORIAL BOARD

### Representatives of the National Research Council

A. N. Campbell, *University of Manitoba*
G. E. Hall, *University of Western Ontario*
E. G. D. Murray, *McGill University*
D. L. Thomson, *McGill University*
W. H. Watson (Chairman), *University of Toronto*

### Editors of the Journals

D. L. Bailey, *University of Toronto*
T. W. M. Cameron, *Macdonald College*
J. B. Collip, *University of Western Ontario*
G. A. Ledingham, *National Research Council*
Léo Marion, *National Research Council*
R. G. E. Murray, *University of Western Ontario*
G. M. Volkoff, *University of British Columbia*

### Representatives of Societies

D. L. Bailey, *University of Toronto*
Royal Society of Canada
T. W. M. Cameron, *Macdonald College*
Royal Society of Canada
J. B. Collip, *University of Western Ontario*
Canadian Physiological Society
R. G. E. Murray, *University of Western Ontario*
Canadian Society of Microbiologists
H. G. Thode, *McMaster University*
Chemical Institute of Canada
T. Thorvaldson, *University of Saskatchewan*
Royal Society of Canada
G. M. Volkoff, *University of British Columbia*
Royal Society of Canada; Canadian Association of Physicists

### Ex officio

Léo Marion (Editor-in-Chief), *National Research Council*
F. T. Rosser, Director, Division of Administration, *National Research Council*


---


*Manuscripts* for publication should be submitted to Dr. Léo Marion, Editor-in-Chief, Canadian Journal of Chemistry, National Research Council, Ottawa 2, Canada.
(For instructions on preparation of copy, see **Notes to Contributors** (inside back cover).)

*Proof, correspondence concerning proof, and orders for reprints* should be sent to the Manager, Editorial Office (Research Journals), Division of Administration, National Research Council, Ottawa 2, Canada.

*Subscriptions, renewals, requests for single or back numbers, and all remittances* should be sent to Division of Administration, National Research Council, Ottawa 2, Canada. Remittances should be made payable to the Receiver General of Canada, credit National Research Council.

The journals published, frequency of publication, and prices are:

| | | |
|---|---|---|
| Canadian Journal of Biochemistry and Physiology | Bimonthly | $3.00 a year |
| Canadian Journal of Botany | Bimonthly | $4.00 a year |
| Canadian Journal of Chemistry | Monthly | $5.00 a year |
| Canadian Journal of Microbiology | Bimonthly | $3.00 a year |
| Canadian Journal of Physics | Monthly | $4.00 a year |
| Canadian Journal of Technology | Bimonthly | $3.00 a year |
| Canadian Journal of Zoology | Bimonthly | $3.00 a year |

The price of single numbers of all journals is 75 cents.

Reprinted in entirety by photo-offset from the original issue

Canadian Journal of Chemistry

*Issued by* THE NATIONAL RESEARCH COUNCIL OF CANADA

VOLUME 34 FEBRUARY 1956 NUMBER 2

# THE SYNTHESES OF SUGARS FROM SMALLER FRAGMENTS

## PART X. SYNTHESIS OF L-GLUCOHEPTULOSE[1]

BY J. K. N. JONES[2] AND R. B. KELLY[3]

ABSTRACT

L-*Gluco*heptulose has been prepared by the action of muscle aldolase on a mixture of L-erythrose and hexose diphosphate.

## INTRODUCTION

In a previous communication (1) it was shown that propionaldehyde and hexose diphosphate together with a crude pea aldolase extract yielded 5,6-didesoxy-D-fructose. We now show that L-erythrose and hexose diphosphate with crystalline muscle aldolase yield L-*gluco*heptulose phosphate from which the free sugar was prepared. It had been demonstrated previously (2) that if L-erythrose is replaced by its optical isomer, D-sedoheptulose phosphate resulted. We have confirmed this observation. These are further examples of the rule that aldolase of plant or animal origins will transfer dihydroxyacetone phosphate from hexose diphosphate to an aldehyde with the formation of a derivative of D-*threo*pentulose.

In experiments with crude pea aldolase preparations it was observed that L-erythrose condensed with hexose diphosphate with the formation of small amounts of a heptulose sugar which was identified chromatographically (cf. 4) as *gluco*-heptulose. Further work with a purer enzyme preparation will be required before this sugar can be positively identified.

## EXPERIMENTAL

Crude pea aldolase was prepared according to the method of Hough and Jones (3). The crystalline muscle aldolase was supplied by Nutritional Biochemical Corporation.

Erythrose and threose were prepared by Ruff degradation (6) of the corresponding calcium arabonates and xylonates according to the method of Overend, Stacey, and Wiggins (5).

IR 120 resin and IR 4B resins were purified before use. The former was treated with ammonia, washed with water, and then treated with 2 *N* hydrochloric acid and again washed with water until the washings were neutral.

[1]*Manuscript received October 18, 1955.*
*Contribution from the Department of Chemistry, Queen's University, Kingston, Ontario.*
[2]*Department of Chemistry, Queen's University, Kingston, Ontario.*
[3]*Merck & Company Limited, Montreal, Quebec.*

The latter was treated with 2 *N* sodium hydroxide, washed with water, and then converted to the acetate form before use by reaction with 8 *N* acetic acid.

*Preparation of* L-*Glucoheptulose*

A solution of the sodium salt of hexose diphosphate (5.0 gm.) and L-erythrose (2.5 gm.) in water (80 ml.) was adjusted by addition of acetic acid to a pH of 6.8. Dialyzed muscle aldolase (100 mgm.) in water (20 ml.) was added and the solution incubated first at room temperature for four hours and then at 37°C. for 14 hr. Sulphuric acid (100 ml., 2 *N*) was then added and the solution heated briefly at 80°C. to coagulate protein. After filtration the solution was boiled for three and a half hours, cooled, and neutralized with barium carbonate. Precipitated inorganic material was removed by filtration and the filtrate deionized on IR 120 and IR 4B acetate resins. Concentration of the resultant neutral solution gave a resin (1.7 gm.) which contained a heptulose sugar contaminated with traces of fructose (paper chromatography). After treatment with charcoal, the sirup crystallized from alcohol to yield L-*gluco*-heptulose (400 mgm.) with m.p. 171–173°C. (not depressed on admixture with an authentic sample) and $[\alpha]_D$ −65° (*c*, 1.0 in water). The powdered crystals gave an X-ray diffraction pattern identical with that of an authentic specimen, kindly supplied by Dr. N. K. Richtmyer.

*Preparation of Sedoheptulosan*

The sodium salt of hexose diphosphate (6.0 gm.) in water (50 ml.) was added to a solution of D-erythrose (3.2 gm.) in water (30 ml.). The resulting solution was adjusted by addition of acetic acid to a pH of 6.8. A dialyzed solution of muscle aldolase (100 mgm.) in water (20 ml.) was added and the solution incubated at 25°C. for four hours and then at 37°C. for 14 hr. The solution was then heated briefly to 80°C. to coagulate protein and filtered. Sulphuric acid (100 ml. 2 *N*) was added and the solution boiled for three hours. The cooled solution was then made alkaline by addition of barium hydroxide, solids were removed by filtration, and the filtrate was boiled for two and a half hours. The cooled solution was neutralized with dilute sulphuric acid, filtered, and the filtrate concentrated. The concentrate was deionized on IR 120 and IR 4B resins and the neutral solution decolorized with charcoal. Concentration of the filtrate gave a sirup which crystallized from 95% alcohol furnishing sedoheptulosan hydrate (520 mgm.). Recrystallization from methanol gave the pure sugar, m.p. 93°C. with $[\alpha]_D$ −130° (*c*, 18.5 in water). The material did not depress the melting point of an authentic sample, kindly supplied by Dr. N. K. Richtmyer; the two samples were indistinguishable on paper chromatograms. The powdered crystals gave an X-ray diffraction pattern identical with that of an authentic specimen.

*Incubation of* L-*Erythrose with Hexose Diphosphate*

A solution of L-erythrose (4.0 gm.) in water (25 ml.) was added to a solution of hexose diphosphate (sodium salt, 8 gm.) in water (40 ml.), the pH of the solution was adjusted to 6.8 by the addition of acetic acid, and to this solution was added a solution of pea aldolase (100 ml. from 100 gm. seed). The solution

was incubated at 37°C. for 14 hr. The pH was then adjusted to 5 (acetic acid) and the solution was heated briefly at 80°C. to coagulate protein. The precipitate was removed on the centrifuge and the supernatant solution was then passed down a column of IR 120 resin. The acidic solution was concentrated to 50 ml. and then boiled for two hours. The cooled solution was passed down a column of IR 4B resin and the neutral effluent concentrated to a sirup (1.12 gm.). The sirup contained heptulose which was separated on a column of cellulose using butan-2-ol–water (10:1) as solvent. The heptulose fraction was contaminated with fructose. Further purification was effected by chromatography on sheets of Whatman No. 1 paper using ethyl acetate – acetic acid – formic acid – water (4:3:1:4) as solvent. Elution of the appropriate section of the paper gave a sirupy heptulose (100 mgm.) which failed to crystallize. It yielded an osazone, m.p. 202–203°C. (sintering at 197°C.) with $[\alpha]_D$ −35° (*c*, 5.6 in pyridine alcohol 2:3). Anal.: Calc. for $C_{14}H_{24}N_4O_5$: C, 60.3; H, 6.2. Found: C, 59.9, H, 6.1. The osazone of D-*gluco*heptulose has m.p. 194–196°C. (sintering at 187°C.) with $[\alpha]_D$ +36°; that of D-*manno*heptulose has m.p. 193–196°C. (sintering at 190°) with $[\alpha]_D$ +36° (solvent as above).

Unfortunately well-defined X-ray diffraction patterns of the osazones could not be obtained. The rate of movement of the sugar was close to that of *gluco*heptulose and *manno*heptulose in several solvent systems. It could be differentiated from all other heptuloses except *allo*heptulose, no specimen of which was available.

The authors thank the National Research Council for financial assistance and for the award of a Postdoctorate Fellowship to one of them (R. B. K.). They also thank Dr. N. K. Richtmyer for the generous gift of heptulose samples.

## REFERENCES

1. GORIN, P. A. J., HOUGH, L., and JONES, J. K. N. J. Chem. Soc. In press.
2. HORECKER, B. L., SMYRNIOTIS, P., and KLENOW, H. J. Biol. Chem. 205: 66. 1953.
3. HOUGH, L. and JONES, J. K. N. J. Chem. Soc. 4050. 1952.
4. HOUGH, L. and JONES, J. K. N. J. Chem. Soc. 342. 1953.
5. OVEREND, W. G., STACEY, M., and WIGGINS, L. F. J. Chem. Soc. 1358. 1949.
6. RUFF, O. Ber. 34: 1362. 1901.

# ORGANIC DEUTERIUM COMPOUNDS

## XIV. PREPARATION OF DEUTERATED METHYL BENZENES[1]

By R. Renaud and L. C. Leitch

ABSTRACT

The synthesis of toluene-$\alpha$-$d_3$, $o$-chlorotoluene-$\alpha$-$d_2$, and $m$-xylene-$\alpha,\alpha'$-$d_6$ from benzotrichloride, $o$-chlorobenzotrichloride, and $\alpha,\alpha'$ hexachloro-$m$-xylene respectively is reported using zinc and acetic acid-$d$ as the dechlorinating agent. The preparation of acetic acid-$d$ of optimum isotopic purity is described.

The reduction of alkyl halides with zinc and acetic acid-$d$ has been recommended by Schissler, Thompson, and Turkevich (4) for the preparation of deuterated methanes, ethanes, and propanes in preference to the hydrolysis of Grignard reagents with deuterium oxide, or else dehalogenation of halides with lithium aluminum deuteride or zinc and methanol-$d$. Their method has now been extended successfully to the preparation of methyl benzenes deuterated in the side chain.

According to the literature (1) benzotrichloride reacts with zinc, alone or in the presence of ether, to give tolane dichloride; toluene has never been reported to be a product of this reaction. Preliminary experiments using zinc dust and acetic acid in ether also gave predominantly tolane dichloride but traces of toluene as well. As a result of several experiments in which the effect of temperature, order of adding the reagents, and ratio of acid to halide were studied, a procedure was developed which consistently gave 70 to 80% yields of toluene. It consists in adding benzotrichloride slowly to a stirred suspension of zinc dust and acetic acid in absolute ether while keeping the temperature of the reaction mixture below +4°C. Under these conditions little if any tolane dichloride is formed. These experiments indicated that this reaction would be satisfactory for the preparation of deuteromethyl benzenes.

TABLE I

| Source of acetic acid-$d$ | Deuterium content of toluene-$\alpha$-$d_3$ | | | |
|---|---|---|---|---|
| | Mol. % $C_6H_5CD_3$ | Mol. % $C_6H_5CHD_2$ | Mol. % $C_6H_5CH_2D$ | At. % D |
| 1. Acetic anhydride | 66.1 | 29.2 | 4.7 | 87.0 |
| 2. Freshly distilled acetic anhydride | 79.7 | 18.7 | 1.6 | 92.6 |
| 3. Acetic anhydride distilled over Mg | 82.9 | 15.8 | 1.3 | 93.3 |
| 4. Acetyl chloride redistilled | 89.5 | 10.5 | — | 96.5 |
| 5. Acetyl chloride distilled over $C_6H_5NMe_2$ | 95.6 | 4.1 | 0.3 | 98.5 |
| 6. Silver acetate + DBr | 39.3 | 41.5 | 16.5 | 70.5 |

The preparation of toluene-$\alpha$-$d_3$ therefore depended upon obtaining acetic acid-$d$ of high isotopic purity. With acetic acid-$d$ prepared by the hydrolysis of

[1]*Manuscript received October 14, 1955.*
*Contribution from the Division of Pure Chemistry, National Research Council, Ottawa, Canada. Issued as N.R.C. No. 3818.*

freshly distilled acetic anhydride with deuterium oxide (99.6%) the deuterium content of the toluene was unexpectedly low as shown in the figures for experiment 2 in Table I. A slight improvement was evident using acetic anhydride that had been refluxed with magnesium turnings for two days before distillation. Acetic acid-*d* prepared by hydrolyzing redistilled acetyl chloride gave still better results. Toluene-$\alpha$-$d_3$ of optimum purity was obtained from acetic acid-*d* which had been prepared by distilling acetyl chloride over dimethylaniline and hydrolyzing it with deuterium oxide. The dimethylaniline evidently combines with traces of dissolved hydrogen chloride in the acetyl chloride. With trifluoroacetic acid-*d* the yields of toluene were very poor and the isotopic purity was low. Acetic acid-*d* prepared by decomposing anhydrous silver acetate with deuterium bromide likewise gave a product of low deuterium content.

The same reaction was used to prepare *o*-chlorotoluene and *m*-xylene deuterated in the methyl groups and can probably be extended to the preparation of other related compounds if the required chloro derivatives are available. In this connection *o*-xylene deuterated in the methyl groups could probably not be prepared with a high deuterium content because in the chlorination of *o*-xylene by the method of Miller (5) the maximum number of chlorine atoms that can be introduced in the side chains is five, further substitution occurring in the ring.

In view of the high *m*-orienting capacity of the trichloromethyl group it is possible that the procedure just described may afford a new route to *m*-substituted derivatives of toluene which are at present accessible with difficulty. This aspect of the work is currently under investigation.

With respect to the mechanism of the reaction the formation of tolane dichloride would at first lead one to believe it is homolytic:

$$C_6H_5CCl_3 + Zn \rightarrow C_6H_5\dot{C}Cl_2 + ZnCl$$

$$2C_6H_5\dot{C}Cl_2 \rightarrow C_6H_5CCl_2CCl_2C_6H_5$$

$$C_6H_5CCl_2CCl_2C_6H_5 \xrightarrow{Zn} C_6H_5CCl{=}CClC_6H_5.$$

Toluene would be formed by attack of the dichlorobenzyl radical on acetic acid:

$$C_6H_5\dot{C}Cl_2 + CH_3COOH \rightarrow C_6H_5CHCl_2 + CH_3CO\dot{O}$$

$$CH_3CO\dot{O} + ZnCl \rightarrow ZnCl(OOCCH_3).$$

However, Kharasch has established that succinic acid is the chief product of the decomposition of acyl peroxides in acetic acid (2), i.e. the free radical initially formed by decomposition of the peroxide abstracts hydrogen from the methyl group of the acetic acid to give a new free radical, $\dot{C}H_2COOH$, which dimerizes to succinic acid. Consequently benzotrichloride and acetic acid-*d* should give ordinary toluene and succinic acid if the homolytic mechanism is correct. That is apparently not the case.

An alternative mechanism, which proceeds via an organometallic intermediate, may be written thus:

$$C_6H_5CCl_3 + Zn \rightarrow C_6H_5CCl_2ZnCl$$

$$C_6H_5CCl_2ZnCl + CH_3COOD \rightarrow C_6H_5CCl_2D + ZnCl(OOCCH_3).$$

It would be related to the mechanism proposed by Miller and Nord (3) for the Reformatsky reaction:

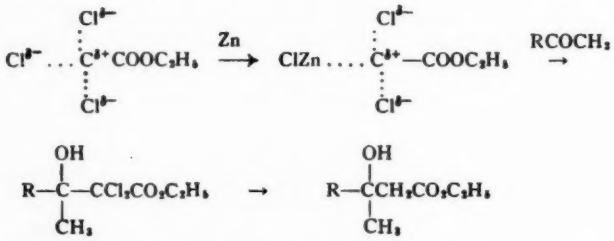

Ethyl acetate is formed as a by-product in Reformatsky syntheses by reaction of the enol form of the ketone with the organometallic complex:

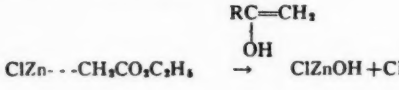

## EXPERIMENTAL

### *Toluene*

In a 500 ml. four-necked round-bottomed flask equipped with a reflux condenser, a thermometer, a separatory funnel, and a stirrer with a thick glass blade (Tru-bor) were placed 200 ml. of anhydrous ether, 45 ml. of glacial acetic acid, and 30 gm. of zinc dust. While the stirred suspension of the zinc in the ether was kept at +3°C. by immersion of the flask in a bath of ice water, benzotrichloride (19.6 gm., 0.1 mole) dissolved in 100 ml. of ether was added over a period of four hours; stirring was continued for three hours longer. Water (200 ml.) was then added and the mixture was filtered through a wad of glass wool in a filter funnel. The ether layer was washed three times with 100-ml. portions of water, once with 10% aqueous sodium bicarbonate, and finally with water again. The ether solution was then dried over calcium chloride and distilled. The residue was distilled through a U-tube containing pellets of potassium hydroxide on the vacuum line. The distillate was fractionated through a Stedman column (12 in. × $\frac{3}{8}$ in.). The main fraction, b.p. 110°C., $n_D^{20}$ 1.4962, amounted to 7.8 ml. (78% of the theoretical amount). For pure toluene $n_D^{20}$ is 1.49624.

### *Acetic Acid-d*

(*a*) *From* $(CH_3CO)_2$ *and* $D_2O$

The preparation was carried out on a vacuum manifold. A mixture of 35 gm. of acetic anhydride, 1.0 gm. of zinc dust, 1 ml. of carbon tetrachloride, and a

trace of phosphorus pentoxide in a round-bottomed flask attached through a reflux condenser to a Stock trap to the vacuum manifold was stirred for three hours. Any water or acetic acid present reacts with the zinc and halide to give methane. Deuterium oxide (7.4 ml., 99.6%) was then added to the anhydride and the mixture was stirred at 60°C. for two hours, then overnight at room temperature. The acetic acid-*d* was distilled into the Stock trap, which was cooled to −50°C. by dry ice and acetone, while the manifold was continuously evacuated. Yield: 97.2%.

(*b*) *From $CH_3COCl$ and $D_2O$*

Acetyl chloride (60 ml.), redistilled over 10 ml. of dimethylaniline to remove dissolved hydrogen chloride, was treated with 5 ml. of dimethylaniline in a round-bottomed flask attached to a vacuum manifold. The solution was stirred for two hours. The acetyl chloride was then distilled into a round-bottomed flask under a cold finger condenser attached to the line through a Stock trap by placing dry ice into the finger after the line was evacuated. Deuterium oxide (14.7 ml., 99.6%) was added slowly from a funnel to the acetyl chloride while the mixture was stirred with a bar magnet. The deuterium chloride evolved was allowed to escape but if desired it could be condensed on the manifold in a trap cooled by liquid nitrogen. The reaction mixture was stirred for two hours after the deuterium oxide was added. When the line was continuously evacuated while the Stock trap was cooled in dry ice and acetone to −50°C., the acetic acid-*d* distilled over practically free of dissolved deuterium chloride. The yield was nearly theoretical.

*Toluene-α-$d_3$*

Deuterated toluene was prepared from each sample of acetic acid-*d* as described in the preparation of the normal hydrocarbon using dry equipment and ether dried over sodium. The deuterium content of each sample of toluene is shown in Table I. The best sample of toluene-α-$d_3$ was prepared from acetic acid-*d* obtained by hydrolysis of the chloride. For this material, $n_D^{20}$ is 1.4953.

*o-Chlorotoluene-α-$d_3$*

This compound was prepared from *o*-chlorobenzotrichloride exactly as described for the preparation of the parent compound.

*α,α′-Hexachloro-m-xylene*

This compound was prepared as described by Miller (5) by the chlorination of *m*-xylene exposed in a quartz tube to ultraviolet light.

*m-Xylene-α,α′-$d_6$*

The hexachloro-*m*-xylene (31.3 gm.) was dechlorinated as described for benzotrichloride using 65.7 gm. of acetic acid-*d* prepared by the hydrolysis of acetyl chloride with deuterium oxide and 55 gm. of zinc dust. The yield of product, $n_D^{20}$ 1.4934, was 63%. The mass analysis indicated 94 mol. % $C_6H_4(CD_3)_2$.

## ACKNOWLEDGMENTS

The authors are grateful to Miss F. Gauthier for the mass analyses and to Heyden Chemical Corporation for samples of *o*- and *p*-chlorobenzotrichloride.

## REFERENCES

1. HUNTRESS, E. H. Organic chlorine compounds. John Wiley & Sons, Inc., New York. 1948. p. 880.
2. KHARASCH, M. F. and GLADSTONE, M. T. J. Am. Chem. Soc. 65: 15. 1943.
3. MILLER, R. E. and NORD, F. F. J. Org. Chem. 16: 728. 1951.
4. SCHISSLER, D. O., THOMPSON, S. O., and TURKEVICH, J. Discussions Faraday Soc. No. 10: 46. 1951.
5. SLESSOR, C. and SCHRAMM, R. S. Natl. Nuclear Energy Ser. Vol. VII, Chap. I, p. 207. 1951.

# THE REACTIONS OF TRIFLUOROMETHYL RADICALS WITH PROPANE, *n*-BUTANE, AND ISOBUTANE[1]

By P. B. Ayscough[2] and E. W. R. Steacie

ABSTRACT

A study of the reactions of trifluoromethyl radicals, produced by the photolysis of hexafluoroacetone, with propane, *n*-butane, and isobutane has been made. The rate constants of the hydrogen-abstraction reactions have been determined at temperatures between 27°C. and 119°C. and the activation energies found to be 6.5±0.5, 5.1±0.3, and 4.7±0.3 kcal./mole respectively. These values are compared with those obtained for the reactions with methane and ethane, and with the corresponding reactions of methyl radicals.

## INTRODUCTION

Hexafluoroacetone has been shown to yield trifluoromethyl radicals and carbon monoxide when irradiated with ultraviolet light in the temperature range 25° to 300°C. The reactions of these radicals with methane and ethane have already been described (3), and the rate constant for their dimerization has been determined (1). This paper describes a further extension of this work in which more complex hydrocarbons were used. It is now possible to make a more detailed comparison of the rates of abstraction of hydrogen atoms from hydrocarbons by trifluoromethyl radicals with the rates of the corresponding reactions of alkyl radicals.

## EXPERIMENTAL

The apparatus was described in the earlier paper (3) and the only significant modification was the illumination of the whole volume of the cell since the lower temperatures used eliminated any possibility of reaction of the radicals with the walls of the vessel. In order to achieve a higher radical concentration some of the experiments on propane and all of those with the butanes were made using the total illumination from the B.T.H. high-pressure mercury lamp. The same sample of hexafluoroacetone was used as before, and the hydrocarbons were again Phillips research grade, distilled before use in the vacuum system and degassed in the usual way. The analytical procedure was essentially the same, except that in this work the carbon monoxide and the fluorocarbons were separated completely from the hydrocarbons by distillation in Ward stills. Mass-spectrometric and infrared spectrophotometric analysis was used to determine the hexafluoroethane/fluoroform ratios (2).

## RESULTS AND DISCUSSION

Fluoroform is a major product when hexafluoroacetone is photolyzed in the presence of hydrocarbons, and in the case of reactions with propane and butane the hydrogen-abstraction is so rapid that even at room temperature the fluoro-

[1]*Manuscript received September 30, 1955.*
*Contribution from the Division of Pure Chemistry, National Research Council, Ottawa, Canada. Issued as N.R.C. No. 3825.*
[2]*National Research Council of Canada Postdoctorate Fellow 1953–55.*

form/hexafluoroethane ratio is undesirably high. The accuracy of the analyses is therefore reduced and the usable temperature range restricted, even at high radical concentrations which favor the formation of hexafluoroethane.

The proposed reaction scheme is as follows:

$$CF_3COCF_3 + h\nu \rightarrow 2CF_3 + CO \quad [1]$$

$$2CF_3 \rightarrow C_2F_6 \quad [2]$$

$$CF_3 + RH \rightarrow CF_3H + R \quad [3]$$

$$CF_3 + R \rightarrow CF_3R \quad [4]$$

$$2R \rightarrow R_2 \quad [5]$$

where RH is propane, *n*-butane, or isobutane. The products were not examined for compounds of the type $CF_3R$ because these were present in a very small amount compared with the residual hexafluoroacetone and could not have been identified with any assurance. Some hexane was identified however when propane was the substrate, and since ethane and 1,1,1-trifluoroethane had

TABLE I

REACTIONS OF $CF_3$ WITH HYDROCARBONS

| Temp. (°K.) | Press. $CF_3COCF_3$ (mm.) | Press. RH (mm.) | Time (sec.) | Products (moles/sec. $\times 10^{10}$) | | $k_3/k_2^{\frac{1}{2}} \times 10^{12}$ (molecules$^{-\frac{1}{2}}$cc.$^{\frac{1}{2}}$sec.$^{-\frac{1}{2}}$) |
|---|---|---|---|---|---|---|
| | | | | $C_2F_6$ | $CF_3H$ | |
| *RH = propane* | | | | | | |
| 300 | 51.7 | 25.2 | 8400 | 0.116 | 1.31 | 2.68 |
| 312 | 50.4 | 23.7 | 9000 | 0.217 | 1.92 | 3.32 |
| 324.5 | 26.2 | 29.7 | 7200 | 0.130 | 2.86 | 5.10 |
| 328 | 49.7 | 25.8 | 9000 | 0.149 | 2.62 | 5.04 |
| 340 | 28.3 | 20.2 | 7800 | 0.406 | 5.15 | 7.90 |
| 359 | 51.0 | 14.0 | 3840 | 3.72 | 21.0 | 16.3 |
| 372.5 | 38.7 | 20.5 | 3000 | 1.57 | 20.8 | 17.7 |
| 372.5 | 25.8 | 24.6 | 3600 | 0.74 | 17.8 | 18.2 |
| 392 | 30.2 | 15.7 | 3300 | 1.92 | 38.2 | 40.0 |
| *RH = n-butane* | | | | | | |
| 302 | 50.1 | 22.9 | 2400 | 2.20 | 16.2 | 8.35 |
| 306 | 50.4 | 17.6 | 2400 | 2.37 | 15.6 | 10.3 |
| 314.5 | 47.5 | 21.0 | 2400 | 1.45 | 15.1 | 10.95 |
| 327 | 45.6 | 21.2 | 1800 | 3.90 | 30.6 | 13.95 |
| 337.5 | 52.7 | 17.3 | 1800 | 4.62 | 37.6 | 19.9 |
| 348 | 51.7 | 21.3 | 1800 | 5.31 | 54.1 | 22.4 |
| 356 | 51.3 | 18.6 | 1500 | 8.00 | 71.4 | 28.2 |
| 365.5 | 51.0 | 17.8 | 1200 | 8.87 | 83.1 | 33.4 |
| *RH = isobutane* | | | | | | |
| 301 | 50.7 | 20.1 | 2400 | 0.450 | 11.2 | 15.6 |
| 302.5 | 51.5 | 18.3 | 2400 | 0.482 | 11.96 | 16.5 |
| 313 | 49.3 | 17.4 | 1200 | 0.587 | 16.3 | 22.3 |
| 318.5 | 50.5 | 12.4 | 1860 | 1.39 | 20.7 | 26.3 |
| 329 | 52.0 | 15.8 | 2400 | 1.69 | 39.9 | 30.2 |
| 338 | 50.0 | 17.5 | 1800 | 0.846 | 30.9 | 37.9 |
| 349 | 51.8 | 17.6 | 1110 | 1.88 | 52.7 | 44.4 |
| 357 | 51.3 | 12.8 | 1590 | 8.36 | 97.0 | 54.5 |

been detected in the earlier experiments with methane, and butane in the products of experiments with ethane as substrate it seems reasonable to assume the same general mechanism for all these hydrocarbons. The rate constants derived for the reactions [3] would not in any case be affected by the fate of the alkyl radicals unless there was built up an appreciable concentration of some other product which produced fluoroform at a rate comparable with reaction [3]. We have therefore calculated the rate constants from the following relation, derived in the usual way:

$$k_3/k_2^{\frac{1}{2}} = \text{rate } CF_3H/[(\text{rate } C_2F_6)^{\frac{1}{2}}\ (RH)].$$

The reaction volume was assumed to be the cell volume (190 ml.). The results are presented in Table I, and Arrhenius plots are shown in Fig. 1. The activation energy for the reaction of trifluoromethyl radicals with propane was found to be 6.5±0.5 kcal./mole, for reaction with *n*-butane 5.1±0.3 kcal./mole, and for reaction with isobutane 4.7±0.3 kcal./mole, all about 2–3 kcal. less than

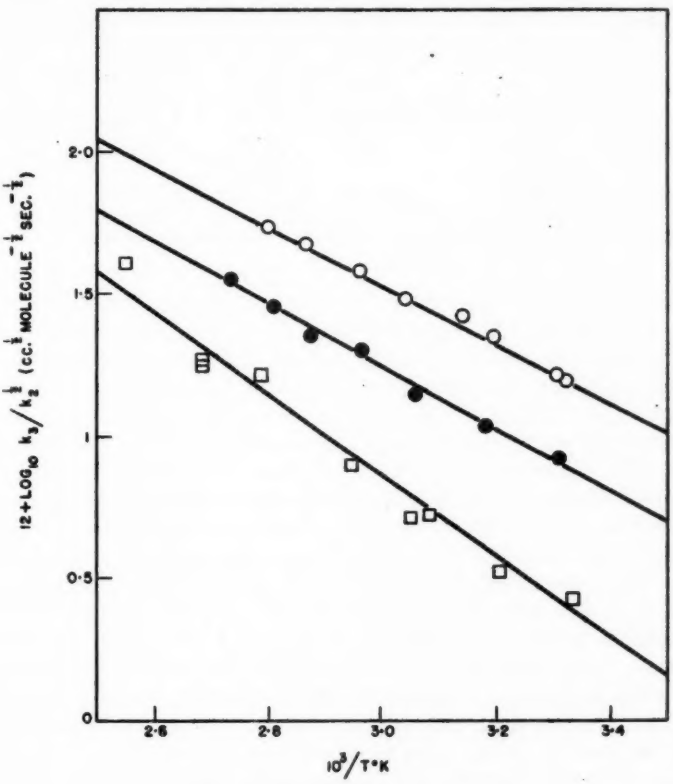


FIG. 1. Arrhenius plots of data.

the corresponding reactions of methyl radicals. This difference was noted in the case of reactions with methane and ethane (3), and in view of the work on the dimerization of trifluoromethyl radicals (1) it is certain that this difference is real and is not the result of a difference in activation energies for the radical recombination reactions.

In Table II the reactions of methyl and of trifluoromethyl radicals with hydrocarbons are compared. The steric factors have been calculated assuming

TABLE II

RATE OF HYDROGEN-ABSTRACTION FROM HYDROCARBONS

| Reaction | Rate constants $k_3/k_2^{\frac{1}{2}}\times10^{13}$* (400°K.) (cc.$^{\frac{1}{2}}$ molecule$^{-\frac{1}{2}}$ sec.$^{-\frac{1}{2}}$) | Steric factors $P_3/P_2^{\frac{1}{2}}$ (400°K.) | Activation energy (kcal./mole) | Rate constant $k_3\times10^{13}$ (400°K.) (cc. molecule$^{-1}$ sec.$^{-1}$) | Ref. |
|---|---|---|---|---|---|
| $CH_3+CH_4$ | 0.029 | | 14 | 0.017 | 5, 9 |
| $+C_2H_6$ | 0.83 | $6\times10^{-4}$ | 11.4 | 0.49 | 9, 10 |
| $+C_3H_8$ | — | $4\times10^{-3}$ | 9.9 | — | 4 |
| $+n$-$C_4H_{10}$ | 5.8 | $3\times10^{-4}$ | 8.3 | 3.42 | 9, 10 |
| +iso-$C_4H_{10}$ | 12.6 | $3\times10^{-4}$ | 7.6 | 7.43 | 7, 9, 10 |
| $CF_3+CH_4$ | 3.5 | $6\times10^{-3}$ | 10.3±0.5 | 2.19 | 3 |
| | | | 9.5±2 | | 6 |
| $+C_2H_6$ | 104 | $6\times10^{-3}$ | 7.5±0.5 | 65 | 3 |
| $+C_3H_8$ | 418 | $6\times10^{-3}$ | 6.5±0.5 | 261 | This paper |
| $+n$-$C_4H_{10}$ | 631 | $2\times10^{-3}$ | 5.1±0.3 | 395 | This paper |
| | | | 5.5±1 | | 6 |
| +iso-$C_4H_{10}$ | 1010 | $2\times10^{-3}$ | 4.7±0.3 | 631 | This paper |

*$k_3$ refers to the abstraction reaction, $k_2$ to the radical recombination reaction in each case.*

the following collision diameters: $CH_3$, 3.5 Å; $CF_3$, 4.0 Å; $CH_4$, 3.5 Å; $C_2H_6$, 4.5 Å; $C_3H_8$, 5.2 Å; $n$-$C_4H_{10}$, 5.9 Å; iso-$C_4H_{10}$, 5.8 Å. The activation energies given assume zero activation energy for the radical recombination reactions. In order to calculate the absolute rate constants, $k_{400°K.}$, we have used the values $3.5\times10^{-11}$ cm.$^3$ molecule$^{-1}$ sec.$^{-1}$ for the recombination of methyl radicals (8), and $3.9\times10^{-11}$ cm.$^3$ molecule$^{-1}$ sec.$^{-1}$ for the recombination of trifluoromethyl radicals (1). There are some difficulties about the values for methyl radical reactions in Table II. A number of investigations, and particularly unpublished work by Kutschke and Whiteway (4), indicate that the value for the activation energy of $CD_3+CD_3COCD_3$ is higher than that previously reported (10). As a result the value for ethane (10) is too low, and has been corrected from 10.4 to 11.4 kcal. The value for $C_3H_8$ includes this correction. There is thus some inconsistency between the values for propane and those for $n$- and iso-butane. The latter compounds were investigated by a non-isotopic method, however, and are free from errors involving the reaction of $CD_3$ with $CD_3COCD_3$. As a result, until further work is done, there are uncertainties of the order of 1 kcal. in the values of activation energies for methyl radical reactions. The values of the rate constants at 400°K. are, however, affected very little by these uncertainties. Table II also shows for comparison some recent values obtained by

Pritchard, Pritchard, and Trotman-Dickenson (6), using $CF_3$ radicals from the photolysis of hexafluoroazomethane. There is complete agreement between these values and those obtained with hexafluoroacetone. It will be seen from Table II that the abstraction of hydrogen from hydrocarbons by $CF_3$ radicals is about 100 times faster than the corresponding reaction of methyl radicals at 400°K. The activation energies for $CF_3$ reactions are 2–3 kcal. smaller than those for $CH_3$.

## ACKNOWLEDGMENTS

The authors are grateful to Mr. R. Lauzon for performing the infrared analyses, and to Miss F. Gauthier for the mass-spectrometric analyses.

## REFERENCES

1. AYSCOUGH, P. B. J. Chem. Phys. In press. 1955.
2. AYSCOUGH, P. B. Can. J. Chem. 33: 1566. 1955.
3. AYSCOUGH, P. B., POLANYI, J. C., and STEACIE, E. W. R. Can. J. Chem. 33: 743. 1955.
4. KUTSCHKE, K. O. and WHITEWAY, S. G. Unpublished work.
5. MCNESBY, J. R. and GORDON, A. S. J. Am. Chem. Soc. 76: 4196. 1954.
6. PRITCHARD, G. O., PRITCHARD, H. O., and TROTMAN-DICKENSON, A. F. Chemistry & Industry, 564. 1955.
7. REBBERT, R. E. and STEACIE, E. W. R. J. Chem. Phys. 21: 1723. 1953.
8. SHEPP, A. J. Chem. Phys. In press. 1955.
9. TROTMAN-DICKENSON, A. F. Quart. Revs. 7: 198. 1953.
10. TROTMAN-DICKENSON, A. F., BIRCHARD, J. R., and STEACIE, E. W. R. J. Chem. Phys. 19: 163. 1951.

# THE POLYMERIZATION OF STYRENE IN THE PRESENCE OF α- AND β-BROMOSTYRENE[1]

By M. H. Jones

ABSTRACT

A study of the polymerization of styrene in the presence of either α- or β-bromostyrene at 45°C. and 70°C. has shown that copolymerization does not occur. From the variation of molecular weight and rate of polymerization with bromostyrene concentration it is concluded that the bromostyrenes behave essentially as efficient transfer agents.

## INTRODUCTION

The bromination of polystyrene in solution, both photochemically and thermally, is accompanied by some degradation and there is evidence that the resultant polymer may contain olefinic bonds in the carbon chain due to the concomitant elimination of hydrogen bromide (6). As an alternative means of preparing polystyrenes containing aliphatic bromine atoms for use as polyradical sources in grafting experiments (5, 6), an attempt has been made to copolymerize styrene with α- or β-bromostyrene. This would permit a close control of the position and frequency of the bromine atoms in the polymer backbone and would avoid the disadvantages resulting from the direct bromination method.

Although the aliphatic bromostyrenes do not polymerize by a radical mechanism alone (7, 11), it was considered that they may take part in a copolymerization reaction if the principal cause of their low reactivity is steric hindrance imparted by the bulky bromine atom. This is expected to be less in a transition state involving only one species containing a bromine atom adjacent to the reaction center, as in the unsymmetrical propagation step of a copolymerization reaction, than in the normal polymerization involving two species containing bromine atoms. However, in experiments at 45°C. and 70°C., no evidence of copolymerization was obtained and the bromostyrenes appeared to behave as efficient transfer agents.

## EXPERIMENTAL

### *Materials*

Styrene (Eastman Kodak Practical Grade) was shaken with a 10% sodium hydroxide solution to remove the inhibitor, washed with distilled water, and dried over anhydrous calcium chloride. It was distilled under reduced pressure in a stream of nitrogen and the middle fraction, b.p. 51.3°C. at 27 mm. pressure, was used for the polymerization experiments. Prior to use, the monomer was given a bulb-to-bulb distillation in vacuum.

α-Bromostyrene was prepared by the elimination of hydrogen bromide from styrene dibromide. Styrene dibromide (0.1 mole) was shaken for 20 min. with

*Manuscript received October 11, 1955*
*Contribution from the Department of Chemistry, Ontario Research Foundation, Toronto 5, Ontario*

100 cc. of a 20% solution of potassium hydroxide in ethanol, the temperature being maintained below 20°C. The reaction mixture was poured into a large excess of ice-cold water and the oil separated and dried over anhydrous sodium sulphate. The product was distilled under reduced pressure in a stream of nitrogen, second fraction b.p. 77.0–77.2°C. at 9 mm.; $n_D^{22.5}$ 1.5868. The conditions described by Ashworth and Burkhardt (1) yielded a product consisting principally of phenyl acetylene.

β-Bromostyrene (Eastman Kodak Practical Grade) was purified in a similar manner to the α-compound, b.p. 85.0–85.1°C. at 7 mm.; $n_D^{22.5}$ 1.6063. As both the bromostyrenes were found to be sensitive to atmospheric oxidation, particularly the α-isomer, they were sealed in ampoules under vacuum and stored at −5°C.

α,α′-Azo-bis-isobutyronitrile was recrystallized twice from ethanol in the temperature range 30°–0°C. and dried under vacuum.

*Procedures*

Reaction mixtures of styrene and the required bromostyrene were thoroughly degassed on a high vacuum line and sealed in pyrex vessels at a pressure of $10^{-3}$–$10^{-4}$ mm. For experiments at 45°C., 1.0 gm./liter of α,α′-azo-bis-isobutyronitrile was used as initiator and the reactions were followed dilatometrically. The volume contraction – time curves were linear and the rates recorded in Table I were calculated on the assumption that polystyrene is the

TABLE I

POLYMERIZATION OF STYRENE WITH α- AND β-BROMOSTYRENE AT 45°C.
1.0 gm./liter of α,α′-azo-bis-isobutyronitrile used as initiator

| Expt. No. | Bromostyrene | [Styrene], moles l.$^{-1}$ | [Bromostyrene]/[Styrene] | Rate.$10^7$ vol. contraction, moles l.$^{-1}$ sec.$^{-1}$ | Rate.$10^7$ polymer recovered, moles l.$^{-1}$ sec.$^{-1}$ | $[\eta]_{25°C.}$, dl. gm.$^{-1}$ | $M_n$ |
|---|---|---|---|---|---|---|---|
| 2 | — | 8.49 | — | 142 | 128 | 1.72 | 425,000 |
| 13 | α | 7.98 | 0.060 | | 5.6 | | |
| 5 | α | 6.07 | 0.353 | 5.5 | 0.3 | | |
| 14 | β | 7.98 | 0.061 | 115 | 110 | 0.182 | 9,000 |
| 1 | β | 6.79 | 0.224 | 83 | 54 | 0.110 | 4,500 |
| 3 | β | 4.25 | 0.893 | 17 | 7.4 | | |
| 4 | β | 1.82 | 3.23 | 3.9 | 0.1 | | |

only product of polymerization and that no copolymerization occurs. Using the data of Patnode and Scheiber (9) for the densities of monomer and polymer respectively, a contraction in volume of 15.4% at 45°C. corresponds to 100% polymerization. In all cases, conversions were limited to less than 7%. The polymer was recovered by precipitation in a 30–40 volume excess of methanol, filtered, and dried to constant weight in vacuum at room temperature. The rates of polymerization at 45°C. and 70°C. were also determined from the weights of polymer recovered in this way.

Intrinsic viscosities were measured in benzene solution at 25°C. using a modified Ubbelohde type viscometer incorporating a bulb to permit dilution

of the solutions *in situ*. No kinetic energy corrections were applied to the flow times as they were found to be less than 1%.

## RESULTS AND DISCUSSION

The rates of polymerization for various styrene–bromostyrene compositions are recorded in Tables I and II together with the intrinsic viscosities of the

TABLE II

POLYMERIZATION OF STYRENE WITH α- AND β-BROMOSTYRENE AT 70°C.
No initiator used

| Expt. No. | Bromo-styrene | [Styrene], moles l.$^{-1}$ | $\frac{[\text{Bromostyrene}]}{[\text{Styrene}]}$ | $k_2.10^7$, l. moles$^{-1}$ sec.$^{-1}$ | $[\eta]_{25°C.}$, dl. gm.$^{-1}$ | $M_n$ |
|---|---|---|---|---|---|---|
| 10 | — | 8.29 | — | 0.875 | 3.26 | 740,000 |
| 18 | α | 8.18 | 0.012 | 0.103 | 0.166 | 8,000 |
| 17 | α | 7.78 | 0.059 | 0.040 | 0.087 | 3,000 |
| 6 | α | 5.53 | 0.448 | 0.030 | | |
| 7 | α | 3.11 | 1.49 | <0.005 | | |
| 19 | β | 8.18 | 0.012 | 0.715 | 0.480 | 41,000 |
| 12 | β | 7.78 | 0.060 | 0.760 | 0.172 | 8,500 |
| 8 | β | 5.53 | 0.441 | 0.785 | 0.095 | 3,500 |
| 9 | β | 3.11 | 1.47 | 0.030 | | |

products obtained. The molecular weights given in the last columns of these tables were calculated from the intrinsic viscosity – molecular weight relationship suggested by Pepper (10) for unfractionated polystyrenes in the molecular weight range $2.10^3$–$2.10^6$,

$$\text{i.e. } [\eta] = 4.37.10^{-4}\, M_n^{0.66}.$$

Microanalyses of the products from reactions with high bromostyrene concentrations showed that they may contain as much as 4.5% bromine. However, the ultraviolet absorption curve of the polymer from experiment No. 8 had peaks at 2850 Å and 2950 Å which occur in the absorption spectrum of β-bromostyrene but are not present in those of either polystyrene or a brominated polystyrene prepared by direct bromination. Assuming the product to be a mixture of polystyrene and β-bromostyrene, the percentage composition of the latter was determined from the optical densities at various wave lengths in the region 2550–2950 Å. The analyses were constant within the experimental accuracy and were in good agreement with the value obtained from the microanalysis for bromine. Two reprecipitations of the polymer from benzene solution in methanol reduced the absorption attributed to the bromostyrene by a factor of two. That there can be incomplete separation of the polymer and bromostyrene by precipitation was demonstrated by a blank experiment in which a sample of pure polystyrene was recovered and dried in the normal way from a benzene solution containing 20% β-bromostyrene. The presence of the bromo compound was detected in the ultraviolet spectrum of the product. Although the bromostyrenes are soluble in methanol they are insoluble in solutions containing more than 5–10% water Presumably condensation of

atmospheric water vapor during filtration of the polymer under reduced pressure precipitates the bromostyrene which is then absorbed on the polymer. Because of its very low vapor pressure, it will not be completely removed when dried under vacuum at room temperature.

From the spectra of the products from experiments Nos. 1 and 8 it has been estimated that the true bromine contents are less than 0.7% and, consequently, there cannot be more than one bromostyrene unit in 110 units of the polymer chain, that is, in a molecular weight of approximately 11,000. As the molecular weights of these polymers from viscosity measurements are 4500 and 3500 respectively, they must contain less than one bromine atom per molecule. The bromine contents of the products from reactions with low bromostyrene concentrations, in which there was less contamination of the polymer by bromostyrene, were also lower than the requirement for one bromine atom per molecule. There is, therefore, no evidence that copolymerization occurs.

The rapid fall in molecular weight with increasing bromostyrene concentration, both for polymerizations at 45°C. and 70°C., suggests that the growing polymer radicals terminate by one or both of the following mechanisms.

(1) The addition of a bromostyrene molecule to a growing polymer chain produces a radical with a low reactivity towards propagation,

$$\underset{\text{Active}}{M_n^{\cdot}} + \text{B} \rightarrow \underset{\text{Inactive}}{M_n\text{B}^{\cdot}}$$

termination occurring by mutual interaction with a polystyrene radical or another of its own kind.

(2) The bromostyrenes act as efficient transfer agents,

$$M_n^{\cdot} + \text{B} \rightarrow M_n + \text{B}^{\cdot}.$$

With the catalyzed reactions at 45°C., where the rate of initiation is constant, there should be an exact correspondence between the decrease in molecular weight and the fall in rate of polymerization for mechanism (1), provided transfer to monomer is small and can be neglected (2). For the thermal reactions at 70°C., in which transfer to monomer is an important termination step, it can be shown that this mechanism requires the proportional decrease in molecular weight to be less than the decrease in the second order rate constant $k_2$, where $k_2 = \text{rate}/[\text{M}]^2$. It is generally accepted that the rate of initiation for uncatalyzed thermal polymerizations is proportional to the square of the monomer concentration. For reactions with both the $\beta$-isomer at 45°C. and the $\alpha$- and $\beta$-isomer at 70°C., the fall in molecular weight is at least 20 times greater than required for these relationships (Tables I and II). Thus, the addition of a bromostyrene molecule to form an inactive radical is not the predominant chain termination process.

Although the reaction rates determined dilatometrically and from the polymer recovered are not strictly comparable, particularly for reactions with high bromostyrene concentrations, the trend is similar. It is probable that the greater rate decrease obtained by the second method is attributable to incomplete precipitation of low molecular weight material which is progressive as the

molecular weight decreases. Confirmation of this was obtained in two of the experiments at 70°C. (Nos. 7 and 9) in which 50% of each reaction mixture was transferred to a distillation apparatus, degassed, sealed under vacuum, and the volatile constituents removed in a bulb-to-bulb distillation. In both cases, gummy residues remained which consisted of very short chain polymers as they were partly soluble in methanol and readily soluble in acetone. This partial fractionation will also mean that the true molecular weights are somewhat less than the determined values in the low molecular weight range.

If the bromostyrenes act principally as transfer agents and the radicals formed in the transfer step are equally efficient in continuing polymerization, then, for the initiated reactions with a constant catalyst concentration, the rate of polymerization will be proportional to the monomer concentration. For the thermal reactions without initiator, the dependence will be second order with respect to monomer concentration, that is, $k_2$ will remain constant (3, 4). Although the rate measurements are not too precise, the rates as a function of monomer concentration are less than for first and second order relationships, which suggests that the probability of the radicals resulting from transfer continuing the kinetic chain is less than unity. This is particularly apparent for reactions with $\alpha$-bromostyrene at 70°C. but the evidence for reactions with the $\beta$-isomer at the same temperature is not conclusive. In addition, it must be recognized that a similar effect would be observed in the catalyzed reactions if the bromostyrenes compete with the monomer for the initiator fragments, since this will cause a progressive reduction in the rate of starting chains. Transfer constants for the two bromo compounds have been determined from the variation of molecular weight with bromostyrene–styrene ratio (8). Although this method is strictly applicable only when each radical formed by transfer continues polymerization, it has been used to obtain approximate values. At 70°C., the transfer constants for the $\alpha$- and $\beta$-bromostyrene are 1.0 and 0.2 and are respectively 100 and 20 times greater than that of carbon tetrachloride at this temperature (4).

## REFERENCES

1. Ashworth, F. and Burkhardt, G. N. J. Chem. Soc. 1791. 1928.
2. Baysal, B. and Tobolsky, A. V. J. Polymer Sci. 8: 529. 1952.
3. Gregg, R. A. and Mayo, F. R. Discussions Faraday Soc. No. 2: 328. 1947.
4. Gregg, R. A. and Mayo, F. R. J. Am. Chem. Soc. 70: 2373. 1948.
5. Jones, M. H., Melville, H. W., and Robertson, W. G. P. Nature, 174: 78. 1954.
6. Jones, M. H., Melville, H. W., and Robertson, W. G. P. Paper presented at Intern. Symposium on Macromolecular Chem., Milan. Sept. 1954.
7. Marvel, C. S. and Moon, N. S. J. Am. Chem. Soc. 62: 45. 1940.
8. Mayo, F. R. J. Am. Chem. Soc. 65: 2324. 1943.
9. Patnode, W. and Scheiber, W. J. J. Am. Chem. Soc. 61: 3449. 1939.
10. Pepper, D. C. J. Polymer Sci. 7: 347. 1951.
11. Shorygin, P. P. and Shorygina, N. V. J. Gen. Chem. (U.S.S.R.), 9: 845. 1939.

# THE PHOTOLYSIS OF KETENE IN THE PRESENCE OF HYDROGEN[1]

By H. Gesser[2] and E. W. R. Steacie


## ABSTRACT

The photolysis of ketene in the presence of hydrogen has been investigated in the temperature range −40° to 207°C. The main products are CO, $C_2H_4$, $C_2H_6$, and $CH_4$, with some methyl ethyl ketone at the higher temperatures. Hydrogen and ketene compete for $CH_3$ radicals by the reactions

$$CH_3 + CH_2CO \rightarrow C_2H_4 + CO \qquad [2]$$

$$CH_3 + H_2 \rightarrow CH_4 + H \qquad [3]$$

with $E_3 - E_2 = 0.8$ kcal. At the higher temperatures the reaction

$$CH_3 + H_2 \rightarrow CH_4 + H \qquad [6]$$

leads to a chain reaction via

$$H + CH_2CO \rightarrow CH_3 + CO. \qquad [4]$$

The value of $E_6$ is found to be 10.2±0.5 kcal. in good agreement with previous work.


## INTRODUCTION

The recent study by Strachan and Noyes (10) of the photolysis of ketene and ketene–oxygen mixtures has greatly clarified the mechanism of the ketene photolysis and its dependence on wave length. In view of this it was believed that a re-examination of the ketene–hydrogen system, previously investigated by Rosenblum (7, 8), would perhaps distinguish unambiguously between the addition (1) and abstraction (8) reactions of $CH_2$ radicals with hydrogen.

Bawn and Milsted (1) studied the reaction of sodium atoms with the methylene halides and found that at 300°C. with hydrogen as the carrier gas $CH_4$ was the principal product, whereas with nitrogen as the carrier gas $C_2H_4$ was the main hydrocarbon product. They therefore postulated the reaction

$$CH_2 + H_2 \rightarrow CH_4. \qquad [3a]$$

Rosenblum (8), however, postulated

$$CH_2 + H_2 \rightarrow CH_3 + H \qquad [3]$$

to account for the high proportion of saturated hydrocarbons produced by the photolysis of ketene in the presence of hydrogen.

During the course of this investigation Chanmugam and Burton* (2) studied the photolysis of ketene in the presence of hydrogen and deuterium from 27° to 412°C. They conclude that reaction [3*a*] occurs to a small extent at 27° and has a low activation energy, while [3] only occurs at higher temperatures.

[1]*Manuscript received October 13, 1955.*
*Contribution from the Division of Pure Chemistry, National Research Council, Ottawa, Canada. Issued as N.R.C. No. 3835.*
[2]*National Research Council of Canada Postdoctorate Fellow 1954–55. Present address: Department of Chemistry, University of Manitoba, Winnipeg, Manitoba.*
**We are greatly indebted to Drs. Burton and Chanmugam for allowing us to see the manuscripts of their papers prior to publication.*

## EXPERIMENTAL

The apparatus, essentially completely free of stopcocks, was similar to that of Strachan and Noyes (10). It consisted of a quartz cell 5 cm. in diameter and 10 cm. long enclosed in an insulated box which served as an air oven. The temperature was controlled by means of a mercury regulator to within $\pm 2°$ at temperatures above room temperature. A few experiments were performed at $-40°$C. by partial filling of the box with dry ice. Under these circumstances there was a slight amount of condensation on the quartz windows of the box which caused small variations in the intensity of illumination. The volume of the cell was 193 cm.$^3$, and the total volume of cell and connecting tubing was about 225 cm.$^3$.

The analytical units consisted of a furnace containing copper and copper oxide maintained at 210°C. for the analysis of CO, $H_2$, $CH_4$ mixtures, a hydrogenator (9) for the analysis of $C_2H_4$, $C_2H_6$ mixtures, and a platinum wire unit for the combustion of $CH_4$. The CO, $H_2$, $CH_4$ fraction was separated at $-215°$C., and the $C_2$ fraction at $-185°$C. by means of a LeRoy still.

Ketene was prepared by the thermal decomposition of acetic anhydride (4) at 500°C. It was degassed repeatedly at the temperature of liquid oxygen, and distilled from a trap at $-130°$C. into a bulb where it was stored in liquid nitrogen. When the ketene was allowed to react with acetic acid, $CO_2$ was detected as an impurity, present in the ketene to the extent of 0.1%.

Hydrogen was purified by passage of commercial cylinder hydrogen through three traps immersed in liquid nitrogen and through two palladium thimbles maintained at 320°C. Its purity was tested by means of the copper oxide furnace. It was found that approximately 0.0002% of the hydrogen did not disappear to form water in the presence of hot copper oxide. Traces of CO and $CH_4$ were found, and the yields of the products were corrected for them. Hydrogen was stored in a 5 liter bulb and was dosed into the cell by means of a 100 cc. mercury Toepler pump, with the ketene previously measured and frozen down with liquid nitrogen. The gases were then allowed to mix by warming to room temperature and repeated expansion into the Toepler pump.

The light source was a Hanovia S-500 medium-pressure mercury arc, collimated by means of two quartz lenses. The almost parallel beam was allowed to fill the cell. The intensity was checked by means of a General Electric type GL 935 phototube. The light was filtered with a Corning glass filter No. 9863 (3 mm.) and a chlorine filter in quartz (5 cm. long at 1 atm. pressure). The effective absorbed radiation was thus about 2700 Å, with about six per cent above 3600 Å. The intensity was varied by means of neutral density filters of aluminum sputtered on quartz.

## RESULTS

The products of the photolysis of ketene in the presence of hydrogen at $-40°$ and 26°C were CO, $C_2H_4$, and $C_2H_6$, together with some polymer detected by a slow drop in the transmission of the cell windows. The cell was occasionally flamed with half an atmosphere of oxygen to remove the polymer. At higher temperatures $CH_4$ was also produced. Experiments at 26°C. showed that the

TABLE I

PHOTOLYSIS OF KETENE–HYDROGEN MIXTURES

Illumination time = 1 hr.

| $[CH_2CO]$ | $[H_2]$ | $R_{CO}$ | $R_{C_2H_4}$ | $R_{C_2H_6}$ | $R_{CH_4}$ | $\frac{R_{CO}}{R_{C_2H_4}}$ | Material balance | $R_{MEK}$ |
|---|---|---|---|---|---|---|---|---|
| molecules/cc. $\times 10^{-18}$ | | molecules/cc./sec. $\times 10^{-13}$ | | | | | | molecules/cc./sec. $\times 10^{-13}$ |
| | | | | Temperature = −40±4°C. | | | | |
| 0.83 | 2.49 | .304 | .080 | .069 | — | | .980 | |
| 0.81 | 6.86 | .258 | .039 | .092 | — | | 1.016 | |
| 0.81 | — | .315 | .140 | | | 2.25 | | |
| 0.83 | 4.56 | .247 | .045 | .076 | — | | .980 | |
| | | | | Temperature = 26±2°C. | | | | |
| 0.97 | — | .594 | .272 | | | 2.18 | | |
| 0.97 | 1.62 | .590 | .170 | .118 | — | | .976 | |
| 0.97 | 0.97 | .571 | .183 | .091 | — | | .960 | |
| 0.97 | 0.36 | .583 | .232 | .037 | — | | .923 | |
| 0.97 | 3.60 | .535 | .100 | .161 | — | | .976 | |
| 1.00 | — | .428 | .194 | | | 2.21 | | |
| 1.00 | 6.36 | .409 | .061 | .145 | — | | 1.007 | |
| 0.98 | 4.79 | .416 | .067 | .130 | — | | .947 | |
| 0.95 | — | .387 | .174 | | | 2.22 | | |
| 1.00 | 3.78 | .412 | .078 | .117 | — | | .947 | |
| 0.97 | 1.91 | .392 | .098 | .092 | — | | .969 | |
| 0.97 | 1.01 | .377 | .125 | .060 | — | | .981 | |
| 0.94 | — | .361 | .161 | | | 2.24 | | |
| 1.68 | 1.29 | .598 | .214 | .070 | — | | .950 | |
| 1.65 | 0.78 | .577 | .228 | .048 | — | | .957 | |
| 1.62 | 0.61 | .549 | .226 | .037 | — | | .958 | |
| | | | | Temperature = 99±2°C. | | | | |
| 1.36 | 0.55 | .571 | .217 | .037 | .003 | | .895 | |
| 1.32 | 0.86 | .563 | .191 | .059 | .005 | | .897 | |
| 1.27 | 2.02 | .558 | .136 | .104 | .016 | | .889 | |
| 0.84 | 2.66 | .463 | .076 | .106 | .026 | | .842 | |
| 0.81 | 3.82 | .446 | .054 | .129 | .039 | | .908 | |
| 0.71 | 6.00 | .401 | .028 | .131 | .059 | | .940 | |
| | | | | Temperature = 149±2°C. | | | | |
| 0.68 | 4.90 | .549 | .031 | .083 | .216 | | .809 | .052 |
| 0.71 | 3.87 | .522 | .036 | .084 | .172 | | .789 | .055 |
| 0.69 | 3.16 | .508 | .043 | .085 | .140 | | .780 | .056 |
| 0.68 | — | .354 | .159 | | | 2.23 | | |
| 1.17 | — | .572 | .251 | | | 2.28 | | |
| 1.14 | 3.25 | .735 | .101 | .089 | .152 | | .724 | .101 |
| 0.92 | — | .454 | .197 | | | 2.30 | | |
| 0.89 | 1.49 | .515 | .104 | .066 | .058 | | .773 | .058 |
| 1.03 | — | .489 | .212 | | | 2.31 | | |
| 1.01 | 0.66 | .512 | .155 | .034 | .020 | | .777 | .057 |
| 0.48 | — | .234 | .103 | | | 2.27 | | |
| 0.48 | 1.81 | .293 | .027 | .062 | .064 | | .826 | .026 |
| 0.92 | — | .410 | .183 | | | 2.24 | | |
| 0.92 | 3.25 | .590 | .060 | .091 | .145 | | .758 | .071 |
| 0.69 | — | .405 | .178 | | | 2.28 | | |
| 0.69 | 2.41 | .478 | .066 | .074 | .111 | | 818 | 043 |
| | | | | Temperature = 207±2°C. | | | | |
| 0.49 | 4.59 | 1.00 | .057 | .056 | .636 | | .862 | .069 |
| 0.48 | — | 260 | 106 | | | 2.45 | | |
| 0.50 | 3.66 | .846 | .059 | 053 | 488 | | 842 | 067 |
| 0.52 | 2 25 | .676 | 065 | 054 | 297 | | 791 | 070 |
| 1.03 | — | 524 | 215 | | | 2 44 | | |
| 1 01 | 2 25 | 1 03 | 169 | 048 | 285 | | 698 | 155 |
| 1.01 | 1 31 | 813 | 182 | 030 | 139 | | 693 | 125 |

addition of hydrogen to ketene undergoing photolysis had no effect on $R_{CO}$ (the rate of formation of CO). However, at higher temperatures where $CH_4$ was produced, the addition of hydrogen to ketene caused an increase in $R_{CO}$ such that $R_{CO}$ for ketene alone was about equal to $R_{CO}-R_{CH_4}$ for ketene–hydrogen mixtures.

Mass spectrometric analysis showed that in experiments with ketene alone up to 207°C. the CO fraction contained less than 0.5% methane, and the $C_2H_4$ fraction contained less than 0.5% ethane with no detectable amounts of acetylene. The yields of $CO_2$ were always negligible compared with the impurity already present in the ketene.

In experiments at 149° and 207°C. relatively large amounts of products were obtained which were volatile above 125° and were not found in comparable quantities in the absence of hydrogen or at lower temperatures (except at 99°C. at very low intensities). Mass spectrometric analysis of this fraction showed that the gases volatile between −75° and −125°C. contained from 30 to 50% methyl ethyl ketone. The remaining gases which could not be positively identified were probably other mixed ketones.

The extent of decomposition was usually about two per cent, except at the highest temperatures where, because of the chain reaction, the decomposition was about six per cent under similar conditions.

The rates of formation of products are given in Table I. Table II shows the effect of intensity (a variation of about 500-fold). The filter used in this series

TABLE II

EFFECT OF INTENSITY

| $[CH_2CO]$ | $[H_2]$ | Temp., °C. | Relative intensity | Time, sec. | $R_{CO}$ | $R_{C_2H_4}$ | $R_{C_2H_6}$ | $R_{CH_4}$ | $\frac{R_{CO}}{R_{C_2H_4}}$ | Material balance |
|---|---|---|---|---|---|---|---|---|---|---|
| molecules/cc. $\times 10^{-18}$ | | | | | molecules/cc./sec. $\times 10^{-12}$ | | | | | |
| 1.16 | — | 26 | 1000 | 500 | 17.02 | 7.52 | | | 2.26 | |
| 1.08 | 2.16 | 26 | 1000 | 200 | 17.21 | 5.40 | 3.10 | — | | .992 |
| 1.07 | 2.13 | 26 | 14 | 7000 | 0.267 | 0.071 | 0.058 | — | | .966 |
| 1.03 | — | 26 | 14 | 7000 | 0.263 | 0.117 | | | 2.25 | |
| 0.92 | 1.79 | 99 | 1000 | 100 | 18.10 | 4.43 | 4.28 | — | | .964 |
| 0.91 | 1.79 | 99 | 14 | 6900 | 0.289 | 0.060 | 0.064 | 0.011 | | .896 |
| 0.90 | — | 99 | 14 | 7200 | 0.277 | 0.128 | | | 2.16 | |
| 0.95 | 1.88 | 99 | 2 | 54000 | 0.0333 | 0.00622 | 0.00475 | 0.00373 | | .771 |
| 0.93 | — | 99 | 2 | 54000 | 0.0290 | 0.0129 | | | 2.25 | |
| 0.80 | 2.57 | 149 | 1000 | 60 | 14.08 | 2.24 | 4.21 | 0.960 | | .984 |
| 0.79 | — | 149 | 1000 | 60 | 13.83 | 6.29 | | | 2.20 | |
| 0.80 | 2.67 | 149 | 2 | 54000 | 0.0464 | 0.00432 | 0.00310 | 0.0163 | | .671 |
| 0.78 | — | 149 | 2 | 54000 | 0.0240 | 0.0102 | | | 2.35 | |

NOTE: *A dash signifies product not detectable.*
*A blank space indicates that no analysis was made.*

was a Corning No. 9863 alone, giving effective radiation from 3900 Å to 2600 Å. Experiments at 26°C. with ketene–hydrogen mixtures using 3660 Å and 3130 Å gave results similar to those with 2700 Å.

One experiment was performed at shorter wave lengths in which 54 mm. of ketene at 26°C. was photolyzed with the 2139 Å line of a low pressure zinc resonance lamp, the longer wave length resonance line 3076 Å being removed by means of a chlorine filter. The products were mainly CO and $C_2H_4$, and were analyzed by means of a mass spectrometer. The CO fraction was shown

to contain 0.75% $H_2$, and the $C_2$ fraction had the following composition: 3.5% $C_2H_2$, 5.4% $C_2H_6$, 91.1% $C_2H_4$. The value of $R_{CO}/R_{C_2H_4}$ was 2.38. There are thus small but definite differences as compared with the results at longer wave lengths, possibly owing to the onset of another primary process.

## DISCUSSION

Consideration of the principal products of the photolysis of ketene in the presence of hydrogen leads to the following material balance:

$$(2R_{C_2H_4}+2R_{C_2H_6}+R_{CH_4})/R_{CO} = 1.$$

The values of this ratio are given in Tables I and II under the heading "Material balance". It is evident that the material balance decreases with increase in temperature (Table I), and increases with increase in intensity (Table II). Some polymerization occurred, and this resulted in a slight decrease in transmission in successive runs. This is reflected in the values of $R_{CO}$ in Table I, but the ratios of rates are not affected. In view of the large variation in intensity in Table II, no appreciable error is involved in conclusions regarding the effect of intensity. The small increase in the ratio $R_{CO}/R_{C_2H_4}$ with increase in temperature is probably due to an increase in the amount of polymer formed at higher temperatures. The values of the material balance show that polymerization is never of major importance, especially at low temperatures.

The mechanism most consistent with our results is as follows:

$$CH_2CO + h\nu \rightarrow CH_2 + CO \quad [1]$$

$$CH_2 + CH_2CO \rightarrow C_2H_4 + CO \quad [2]$$

$$CH_2 + H_2 \rightarrow CH_3 + H \quad [3]$$

$$H + CH_2CO \rightarrow CH_3 + CO \quad [4]$$

$$CH_3 + CH_3 \rightarrow C_2H_6 \quad [5]$$

$$CH_3 + H_2 \rightarrow CH_4 + H \quad [6]$$

If ethane and methane are produced solely by reactions [5] and [6], then the following relation should be obeyed:

$$R_{CH_4}/R^{\frac{1}{2}}_{C_2H_6} = k_6[H_2]/k_5^{\frac{1}{2}}. \quad [I]$$

Fig. 1 shows a plot of $R_{CH_4}/R^{\frac{1}{2}}_{C_2H_6}$ against $[H_2]$ at 99°, 149°, and 207°C. and it is evident that the above relationship is obeyed. The values of $k_6/k_5^{\frac{1}{2}}$ at the different temperatures were obtained from the slopes of the curves in Fig. 1, and are given in Fig. 2 in the form of an Arrhenius plot. The values of $k_6/k_5^{\frac{1}{2}}$ reported by Majury and Steacie (6) from an investigation of the photolysis of acetone–hydrogen mixtures are given for comparison. The agreement is excellent except at the highest temperature where Majury and Steacie's results are unreliable. The results of the present work lead to the expression

$$13+\log k_6/k_5^{\frac{1}{2}} = 5.96-(2.24\times 10^3/T),$$

and to $E_6-\frac{1}{2}E_5 = E_6 = 10.2\pm 0.5$ kcal. This agrees well with the value re-

ported by Whittle and Steacie (11) of 10.0±0.5 kcal. If collision diameters of 2.8 Å and 3.5 Å are assumed for $H_2$ and $CH_3$, the ratio of the steric factors, $P_6/P_5^{\frac{1}{2}}$, is $2.3\times10^{-2}$. The complete agreement with previous work is strong

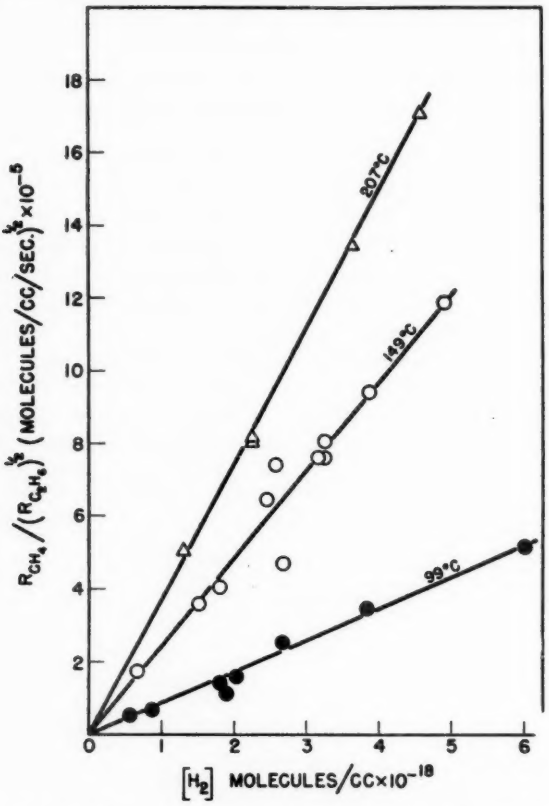


FIG. 1. Plot of $R_{CH_4}/R_{C_2H_6}^{\frac{1}{2}}$ against $[H_2]$. For convenience in plotting, the values of the ordinate have been divided by 2 for the 149°C. curve, and by 5 for the 207°C. curve.

evidence that reaction [3*a*] is unimportant as a source of methane in the present work. This is to be expected from the work of Chanmugam and Burton (2) who showed that at 27°C. the total methane, amounting to about one per cent of the CO, is formed by reaction [3*a*], whereas at higher temperatures the methane is predominantly formed by a radical reaction.

A mechanism involving reactions [1] to [6] leads to the relationship:

$$R_{C_2H_6}/R_{C_2H_4} = k_3[H_2]/k_2[CH_2CO]. \qquad [II]$$

A plot of $R_{C_2H_6}/R_{C_2H_4}$ against $[H_2]/[CH_2CO]$ is shown in Fig. 3. The slopes of the lines, corresponding to $k_3/k_2$, are 0.28, 0.40, and 0.52 for −40°, 26°, and 99°

respectively. An Arrhenius plot of these values is given in Fig. 4, whence $E_3 - E_2 = 0.8$ kcal., and $P_3/P_2 \sim 1$.

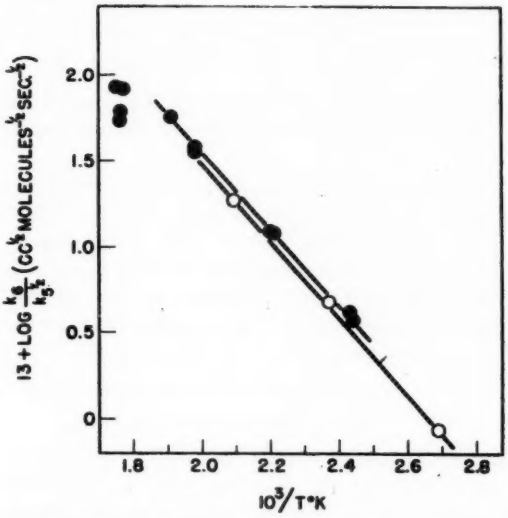


FIG. 2. Arrhenius plot of $k_6/k_3^{\frac{1}{2}}$. Open circles represent the present work. The filled circles are from the work of Majury and Steacie.

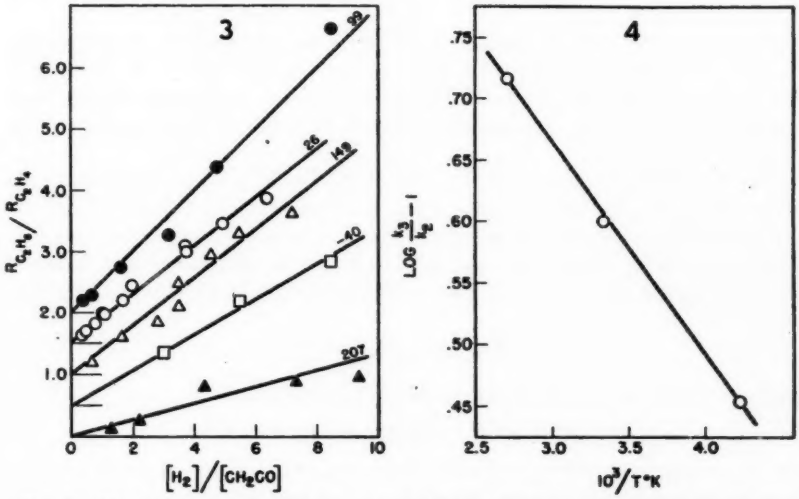


FIG. 3. Plot of $R_{C_2H_6}/R_{C_2H_4}$ against $[H_2]/(CH_2CO]$. The temperatures are indicated by the numbers on the lines. For clarity, the origin of each successive curve is displaced upwards by increments of 0.5 units.

FIG. 4. Arrhenius plot of $k_3/k_2$ from data in Fig. 3.

At 99°C. appreciable methane is formed, and it is possible to check both equations [I] and [II]. The results agree excellently. It follows that a reaction sequence such as

$$CH_3 + CH_2CO \rightarrow CH_3CH_2CO$$
$$CH_3CH_2CO + H_2 \rightarrow C_2H_6 + CO,$$

as postulated by Chanmugam and Burton to account for the formation of ethane at 27°C., cannot be of any importance in the present work even at low temperatures.

The slopes of the lines in Fig. 3 give an excellent Arrhenius plot at the three lowest temperatures. At higher temperatures, however, the slopes decrease again, being 0.40 at 149° and 0.13 at 207°. Also, the plot in Fig. 3 is far from linear at 207°. The decrease in the apparent value of $k_3/k_2$ is almost certainly due to the formation of methyl ethyl ketone in view of the fact that both $k_3/k_2$ and the material balance (Table II) increase with increase in intensity. Methyl ethyl ketone presumably arises by the reactions

$$CH_3 + CH_3CO \rightarrow CH_3COCH_3 \qquad [7]$$
$$CH_3 + CH_3COCH_3 \rightarrow C_2H_5COCH_3. \qquad [8]$$

The rate of formation of methyl ethyl ketone, $R_{MEK}$, at 149° and 207°C. can be calculated by assuming that the material balance differs from unity solely because of the formation of methyl ethyl ketone. Hence $R_{MEK} = \frac{1}{2}R_{CO}$ (1 − material balance). The values thus calculated are given in Table I, and should obey the relationship

$$R_{CH_4}/R_{MEK} = k_6[H_2]/k_7(CH_2CO]. \qquad [III]$$

Fig. 5 shows that this relationship is obeyed satisfactorily. The slopes lead to $E_6 - E_7 = 3.8$ kcal., i.e. $E_7 = 6.4$ kcal., and to $P_6/P_7 = 30$ or $P_7 = 7 \times 10^{-4}$. Since these values are derived from results at two temperatures only, and involve rather drastic assumptions, they are to be regarded as correct in magnitude only.

It is, however, possible to obtain some confirmatory evidence from the work of Chanmugam and Burton (3). Their work on the photolysis of ketene–acetone mixtures showed that methyl ethyl ketone was an important product. From their yields of methane and ethane it can be shown that at the three highest temperatures used by them (200°, 298°, and 412°C.) an Arrhenius plot of

$$R_{CH_4}/R^{\frac{1}{2}}_{C_2H_6}[\text{Acetone}]$$

gives an activation energy of 9.8 kcal. for reaction [9].

$$CH_3 + CH_3COCH_3 \rightarrow CH_4 + CH_3COCH_2. \qquad [9]$$

This is in excellent agreement with their own (3) and previous work on the acetone photolysis. It follows therefore that either all methane comes from [9] or that if $CH_3$ radicals abstract hydrogen from ketene the activation energy must also be approximately 9.8 kcal. This latter alternative is ruled out, however, by the fact that $R_{CH_4}$ is a function of $[H_2]$ and is independent of $[CH_2CO]$ in the present work.

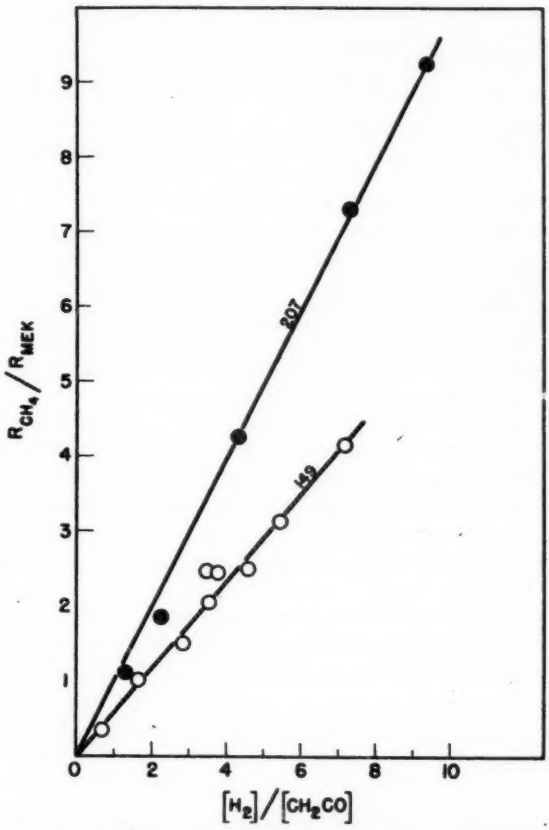


FIG. 5. $R_{CH_4}/R_{MEK}$ plotted against $[H_2]/[CH_2CO]$. The temperatures are indicated on the curves.

If it is now assumed that [7] and [8] are the main method of forming methyl ethyl ketone (which is also assumed by Chanmugam and Burton) then an Arrhenius plot of

$$R_{CH_4}[CH_2CO]/R_{MEK}[\text{Acetone}]$$

using the results of Chanmugam and Burton leads to

$$E_9 - E_7 = 4.8 \text{ kcal.}, \qquad E_7 = 5 \text{ kcal.}$$

Considering the assumptions involved this is in excellent agreement with the value of 6.4 kcal. from the present work.

If equation [II] is now corrected to include reactions [7] and [8],

$$(R_{C_2H_6}+R_{MEK})/R_{C_2H_4} = k_3[H_2]/k_2[CH_2CO]. \qquad [IV]$$

Using equation [IV], we can correct the results in Fig. 3 for 149° and 207°C.

In this way $k_3/k_2$ at 149° is raised to 0.66 in good agreement with the value of 0.59 obtained by extrapolation from Fig. 4. However, the results for 207° do not agree with equation [IV], since a straight line is not obtained when $(R_{C_2H_6}+R_{MEK})/R_{C_2H_4}$ is plotted against $[H_2]/[CH_2CO]$. Also, apart from the deviation from linearity the slope of the curve is much too small. A possible explanation is the formation of ethylene at the highest temperature by some process other than reaction [2], analogous to the unexplained formation of ethylene in the acetone photolysis at high temperatures.

In view of the uncertainties at the higher temperatures the exact value obtained for $E_3-E_2$ is open to some suspicion. There appears to be no doubt, however, that the difference between $E_3$ and $E_2$ is small.

The effect of intensity is in general agreement with the proposed mechanism. The competition between reactions [5] and [7] adequately explains the increase in the material balance, and the parallel increase in the apparent ratio $k_3/k_2$ as determined by equation [II] with increase in intensity.

Reaction [4] has previously been postulated by Knox, Norrish, and Porter (5) to account for the chain decomposition in the flash photolysis of ketene. To gain further evidence for its occurrence it was desirable to use a system in which hydrogen atoms were produced in the presence of ketene. With this in view an experiment was performed in which a 4:1 $H_2$–$CH_2CO$ mixture was saturated with mercury vapor and illuminated with mercury resonance radiation (2537 Å) at 26°. Under these circumstances $CH_4$ was not formed, and the material balance was 1.0. The ratio $R_{C_2H_6}/R_{C_2H_4}$ was 4.2, about 2.5 times greater than that obtained for the photolysis of an equivalent mixture at 2700 Å. This is strong evidence for the occurrence of reaction [4].

The mechanism leads to $E_3-E_2 = 0.8$ kcal. All indications are that $E_2$ is small. Hence $E_3$ is of the order of 3 kcal. For reaction [3]

$$-\Delta H_3 = D(CH_2-H)-D(H-H)$$

$$= D(CH_2-H)-103 \text{ kcal.}$$

Hence $E_3$ can only be as small as 3 kcal. if $D(CH_2-H)$ is at least 100 kcal. If the high value of the latent heat of the sublimation of carbon, $L_C = 170$ kcal., is correct, as seems almost certainly to be the case, such a value for $D(CH_2-H)$ is reasonable. Recent unpublished work by Kistiakowsky in fact indicates that $D(CH_2-H)$ is probably greater than $D(CH_3-H)$.

## REFERENCES

1. Bawn, C. E. H. and Milsted, J. Trans. Faraday Soc. 35: 889. 1939.
2. Chanmugam, J. and Burton, M. J. Am. Chem. Soc. In press.
3. Chanmugam, J. and Burton, M. J. Am. Chem. Soc. In press.
4. Fisher, G. J., MacLean, A. F., and Schnizer, A. W. J. Org. Chem. 18: 1055. 1953.
5. Knox, K., Norrish, R. G. W., and Porter, G. J. Chem. Soc. 1477. 1952.
6. Majury, T. G. and Steacie, E. W. R. Can. J. Chem. 30: 800. 1952.
7. Rosenblum, C. J. Am. Chem. Soc. 60: 2819. 1938.
8. Rosenblum, C. J. Am. Chem. Soc. 63: 3322. 1941.
9. Shepp, A. and Kutschke, K. O. Can. J. Chem. 32: 1112. 1954.
10. Strachan, A. N. and Noyes, W. A., Jr. J. Am. Chem. Soc. 76: 3258. 1954.
11. Whittle, E. and Steacie, E. W. R. J. Chem. Phys. 21: 993. 1953.

# AN OXYGEN-18 STUDY OF ACETAL FORMATION AND HYDROLYSIS[1]

By Fred Stasiuk,[2] W. A. Sheppard,[3] and A. N. Bourns

ABSTRACT

A tracer study has been made of acetal formation and hydrolysis. Benzaldehyde and *n*-butyraldehyde, enriched in $O^{18}$, on reaction with *n*-butyl and allyl alcohols, gave acetals of normal isotopic abundance. The label appeared in the water of condensation. Hydrolysis of benzaldehyde di-*n*-butyl acetal and *n*-butyraldehyde di-*n*-butyl acetal in $O^{18}$ enriched water gave alcohols of normal isotopic content. A slight enrichment due to isotopic exchange was found in allyl alcohol produced by the hydrolysis of benzaldehyde diallyl acetal. These results establish that the reversible reaction proceeds by a fission of the aldehyde-carbon to oxygen bond.

## INTRODUCTION

The rate-determining step in the acid-catalyzed formation of an acetal from aldehyde and alcohol is generally assumed to be the reaction of the second alcohol molecule with the conjugate acid of an intermediate hemiacetal. In the reverse of this reaction, that is, in acetal hydrolysis, the formation of the hemiacetal from the conjugate acid of the acetal is considered to be the slow step (4).

On the basis of the relative hydrolysis rates observed for a number of formaldehyde acetals (12), Hammett has suggested a unimolecular mechanism in which there is formed a carbonium ion intermediate derived from the alcohol component of the molecule (4).

$$[RCH(OR')—OHR']^+ \xrightarrow{\text{slow}} RCHOR'—OH + [R']^+$$

$$[R']^+ + H_2O \xrightarrow{\text{fast}} [R'OH_2]^+$$

Hydrolysis rates, however, are much more sensitive to structural changes in the aldehyde component. For example, the following relative rates have been observed in the hydrolysis of acetals of pentaerythritol: formaldehyde, 1; acetaldehyde, $6 \times 10^3$; acetone, $1 \times 10^7$ (13). Ingold (5) has pointed out that this kinetic effect can be understood if the carbonium ion is derived from the aldehyde component since then the methyl substituents would be joined directly to the electron deficient carbon.

$$[RCH(OR')—OHR']^+ \xrightarrow{\text{slow}} [RCHOR']^+ + R'OH$$

$$[RCHOR']^+ + H_2O \xrightarrow{\text{fast}} [RCH(OR')—\overset{+}{O}H_2]^+$$

This mechanism also accounts for the markedly greater ease of hydrolysis of acetals compared to ordinary ethers.

[1]*Manuscript received June 14, 1955.*
*Contribution from the Department of Chemistry, Hamilton College, McMaster University, Hamilton, Ontario. Presented before Section III, Royal Society of Canada, Kingston Meeting, June, 1950.*
[2]*Graduate student.*
[3]*Undergraduate student. Present address: Hickrill Research Foundation, Katonah, New York.*

In acetal formation these reactions would be reversed with carbon–oxygen bond fission giving a carbonium ion again being the slow step.

The use of oxygen-18 provides a means of distinguishing between the two mechanisms since the oxygen appearing in the product, water, from acetal formation or in the product, alcohol, from acetal hydrolysis would have a different origin in the two cases. Benzaldehyde and *n*-butyraldehyde, enriched in $O^{18}$, have been reacted with *n*-butyl alcohol and allyl alcohol, and the $O^{18}$ content of the resulting acetals and of the water of condensation determined for each of the four reaction systems. Allyl alcohol was chosen as an alcohol reactant since resonance stabilization of the allyl carbonium ion might be expected to provide a system most favorable for reaction by the Hammett mechanism. Hydrolysis in $O^{18}$ enriched water of three acetals, benzaldehyde di-*n*-butyl acetal, *n*-butyraldehyde *n*-butyl acetal, and benzaldehyde diallyl acetal, has also been studied. The alcohol product was isolated and its oxygen isotopic abundance determined.

After the present investigation had been completed, O'Gorman and Lucas (9) reported a stereochemical study of acetal hydrolysis in which the acetal of D(+)-2-octanol was hydrolyzed to give D(+)-2-octanol of the same rotation as the original alcohol from which the acetal had been prepared. Since reaction by the Hammett mechanism would be expected to give extensive racemization, these authors conclude that it is the aldehyde carbon which forms the carbonium ion.

## EXPERIMENTAL

### *Preparation of Benzaldehyde-$O^{18}$ and Butyraldehyde-$O^{18}$*

The aldehydes were shaken for three days with $O^{18}$ enriched water containing approximately 0.8 atom % (0.6 atom % excess) of the heavier isotope. Water was separated and the aldehydes dried by azeotropic distillation with benzene. Their $O^{18}$ content was determined in two ways: (1) by calculation from a knowledge of the $O^{18}$ content of the water before and after equilibration, and (2) by determining the $O^{18}$ content of the water produced on reaction of the aldehyde with phenylhydrazine under conditions which permitted its continuous removal by azeotropic distillation with benzene. Although there was good agreement between the two methods, the values obtained by the second have been used in Table I, since similar techniques were used in determining the $O^{18}$ content of the water produced in acetal synthesis.

### *Acetal Formation*

Carefully dried alcohol (0.32 mole) and the $O^{18}$ enriched aldehyde (0.16 mole) were dissolved in 50 ml. of dry benzene and 0.5 gm. of anhydrous *p*-toluenesulphonic acid added. The solution was refluxed gently with continuous removal of the water of condensation using a Dean-Stark separator. The resulting acetal was recovered in the usual way, distilled, and converted to water and hydrocarbon in the manner described below.

### *Acetal Hydrolysis*

The acetal (0.11 mole), enriched water (0.5 mole) containing approximately 0.4 atom % excess $O^{18}$, and two drops of concentrated hydrochloric acid were

shaken together for two hours in a stoppered flask at 60–70° C. After the reaction mixture was cooled, it was neutralized with sodium hydroxide solution, water separated, and the alcohol product isolated by fractional distillation. The alcohol was dried azeotropically with benzene and converted to water and hydrocarbon by hydrogenolysis.

*Hydrogenolysis of Organic Compounds and Mass-spectrometric Analysis of the Oxygen Isotopes*

The acetals and alcohols were passed with a stream of dry hydrogen at 400° C. over a thoria-promoted nickel catalyst (11). Water, formed in 60–80% yields, was purified by distillation, and its $O^{18}$ content determined by equilibration with carbon dioxide followed by a mass-spectrometric analysis of the oxygen isotopes in the carbon dioxide (3). The water removed azeotropically in the reaction of the aldehydes with phenylhydrazine and in acetal formation was purified by distillation over small quantities of sodium hydroxide and potassium permanganate before equilibration with carbon dioxide. Corrections were made for $O^{18}$ dilution resulting from oxygen exchange with these compounds.

The isotopic analyses were made using a 180° direction-focusing Nier type mass spectrometer equipped with an automatic recorder (7). The precision of the mass-spectrometric analyses was $\pm 0.1\%$, while the over-all precision was considerably poorer, about $\pm 2$–$3\%$, owing to small and variable dilution of $O^{18}$ during manipulative procedures.

*Tests for Oxygen Exchange between Reactants and Products*

Since exchange of oxygen between aldehyde and alcohol or acetal under the conditions of acetal synthesis would destroy the significance of the results insofar as mechanism considerations are concerned, the following tests for exchange were carried out:

(*a*) A synthesis of benzaldehyde di-*n*-butyl acetal using benzaldehyde containing 0.316 atom % excess $O^{18}$ was carried to half completion, the unreacted *n*-butyl alcohol was separated, purified, and converted to water by hydrogenolysis, and the $O^{18}$ content of the water determined in the manner previously described. The enrichment of the alcohol was found to be only 0.012 atom %.

(*b*) A benzaldehyde di-*n*-butyl acetal synthesis from benzaldehyde containing 0.346 atom % excess $O^{18}$ was carried to half completion, the unreacted aldehyde and the acetal each separated, purified, and converted to water by methods already described. The benzaldehyde was found to contain 0.324 atom % excess, while the acetal was normal.

It is apparent from these results that, under the conditions used in the tracer study of acetal formation, there were no significant complications arising from exchange between normal and enriched materials.

Acid-catalyzed exchange between water and *n*-butyl alcohol during acetal hydrolysis experiments would certainly be too slow to appreciably affect the results (10, 2). Allyl alcohol, however, might be expected to undergo exchange much more rapidly and, therefore, an experiment was made to determine the extent of such exchange under the conditions used in the tracer studies. Allyl

alcohol, containing the normal abundance of the oxygen isotopes, was dissolved in five molar equivalents of water, containing 0.444 atom % excess $O^{18}$, and the solution maintained at 65° C. for two hours. At the end of this period the alcohol was isolated, carefully dried, converted into water, and the oxygen isotopic abundance determined in the usual way. The alcohol was found to contain 0.018 atom % excess $O^{18}$, showing that, although there was some exchange, it was not sufficiently rapid to invalidate conclusions based on the results of the tracer work.

## RESULTS AND DISCUSSION

The results of the tracer study of acetal formation for the four different systems of aldehyde plus alcohol are shown in Table I. In each case, the acetal formed from the $O^{18}$ enriched aldehyde has been found, within experimental error, to have the normal abundance of the oxygen isotopes. With the exception of the reaction of benzaldehyde with *n*-butyl alcohol, however, not all of the

TABLE I

OXYGEN-18 RESULTS FOR ACETAL FORMATION

| Acetal | Isotopic abundances (atom % excess)* | | | % of excess $O^{18}$ reappearing in water |
|---|---|---|---|---|
| | Original aldehyde | Water of condensation | Acetal | |
| Benzaldehyde (1) | 0.346 | 0.344 | 0.003 | 99.4 |
| di-*n*-butyl (2) | 0.337 | 0.337 | 0.000 | 100.0 |
| Butyraldehyde (1) | 0.346 | 0.333 | 0.000 | 96.2 |
| di-*n*-butyl (2) | 0.346 | 0.324 | † | 93.6 |
| Benzaldehyde (1) | 0.316 | 0.277 | † | 87.7 |
| diallyl (2) | 0.346 | 0.309 | 0.001 | 89.3 |
| Butyraldehyde (1) | 0.136 | 0.109 | 0.003 | 80.2 |
| diallyl (2) | 0.136 | 0.109 | † | 80.2 |

**The abundances shown are the excess above the value 0.206% found for normal benzaldehyde di-n-butyl acetal when it was compared with Lake Ontario water to which a value of 0.204% had been assigned (15).*

*†Not determined.*

excess $O^{18}$ originally present in the aldehyde reappeared in the water of condensation. This result and the trend of the values shown in the last column of the table can be readily understood on the assumption that, in competition with acetal formation, there is a reaction of the alcohol producing an ordinary ether and water of normal $O^{18}$ abundance. Of the two alcohols, allyl and butyl, the former reacts more slowly in the acetal reaction (14), but is very much more reactive in simple ether formation. Furthermore, of the two aldehydes entering into the acetal reaction, benzaldehyde is the more reactive (1). Greatest dilution with normal water would, therefore, be expected in the *n*-butyraldehyde – allyl alcohol system, and least dilution in the reaction of benzaldehyde with *n*-butyl alcohol. This has been found to be the case.

The results of the acetal hydrolysis studies are shown in Table II. With the exception of the reaction of the acetal derived from allyl alcohol, the alcohol product contained, within experimental error, the normal abundances of the oxygen isotopes. Allyl alcohol was slightly enriched, a result to be ex-

pected since this alcohol has been shown to slowly exchange its oxygen with water under the conditions of the experiment. (See Experimental section.)

TABLE II

OXYGEN-18 RESULTS FOR ACETAL HYDROLYSIS

| Acetal | | Isotope abundances (atom % excess)* | |
|---|---|---|---|
| | | Water | Alcohol product |
| Benzaldehyde di-*n*-butyl | | 0.371 | −0.001 |
| Butyraldehyde di-*n*-butyl | | 0.371 | −0.003 |
| Benzaldehyde diallyl | (1) | 0.444 | +0.033 |
| | (2) | 0.522 | +0.016 |

**See first footnote to Table I.*

These results quite definitely establish that it is the bond of oxygen to the aldehyde carbon which undergoes fission in the reversible reaction of acetal formation and hydrolysis. Two mechanisms are consistent with this finding, namely the carbonium ion mechanism proposed by Ingold and a bimolecular process involving attack of the reagent on the conjugate acid of the hemiacetal or acetal. The latter mechanism, however, would appear to have been eliminated as a possibility by the recent observation of McIntyre and Long (6, 8) that the rate of hydrolysis of methylal is a linear function of the Hammett acidity function, $H_0$, indicating that no water molecules are firmly bound in the transition state. It is of interest that the present work shows that the carbonium ion is derived from the aldehyde part of the molecule even in systems involving allyl alcohol in which a carbonium ion derived from the alcohol would be mesomeric.

## ACKNOWLEDGMENTS

The authors wish to express their appreciation to the National Research Council for a grant-in-aid. One of us (F.S.) wishes to thank the B. Greening Wire Company, Hamilton, for financial assistance.

## REFERENCES

1. ADKINS, H. and ADAMS, E. W. J. Am. Chem. Soc. 47: 1368. 1925.
2. BUNTON, C. A. and FREI, Y. F. J. Chem. Soc. 1872. 1951.
3. COHN, M. and UREY, H. C. J. Am. Chem. Soc. 60: 679. 1938.
4. HAMMETT, L. P. Physical organic chemistry. McGraw-Hill Book Company, Inc., New York. 1940. pp. 303–305.
5. INGOLD, C. K. Structure and mechanism in organic chemistry. Cornell Univ. Press, Ithaca, N.Y. 1953. p. 334.
6. LONG, F. A. and MCINTYRE, D. J. Am. Chem. Soc. 76: 3243. 1954.
7. LOSSING, F. P., SHIELDS, R. B., and THODE, H. G. Can. J. Research, B, 25: 397. 1947.
8. MCINTYRE, D. and LONG, F. A. J. Am. Chem. Soc. 76: 3240. 1954.
9. O'GORMAN, J. M. and LUCAS, H. J. J. Am. Chem. Soc. 72: 5489. 1950.
10. REITZ, O. Z. Elektrochem. 45: 100. 1939.
11. RUSSELL, W. W. and FULTON, J. W. Ind. Eng. Chem. Anal. Ed. 5: 384. 1933.
12. SKRABAL, A. and EGER, H. H. Z. physik. Chem. 122: 349. 1926.
13. SKRABAL, A. and ZLATEWA, M. Z. physik. Chem. 119: 305. 1926.
14. STREET, J. N. and ADKINS, H. J. Am. Chem. Soc. 50: 162. 1928.
15. THODE, H. G. Research, 2: 154. 1949.

# DEPOLARIZATION BY MERCAPTOACETIC ACID DURING ELECTRODEPOSITION OF COPPER[1]

By A. J. Sukava[2] and C. A. Winkler

ABSTRACT

Mercaptoacetic acid (MAA) in acid copper sulphate electrolyte decreased the cathode polarization throughout the course of electrolysis at all concentrations up to 20 mgm./liter. Addition of small amounts of chloride caused further depolarization. When present together with cystine, MAA showed an independence of action. The depolarization caused by MAA was ascribed to a decreased activation overpotential due to substitution of a more readily dischargeable MAA–copper complex for the aquo–copper complex. The additional depolarization due to chloride was ascribed to formation of a still more readily dischargeable chloro–MAA–copper complex. The depolarization in both cases increased with time during prolonged electrolysis, apparently due to surface roughening with, presumably, a consequent increase in surface area and decrease in true current density.

## INTRODUCTION

Investigations have recently been made in this laboratory into the addition agent effects, during electrodeposition of copper, of some simple amino compounds (1, 5). These compounds are known to be positively charged in acid solution and to be capable of co-ordination with copper ions. In the course of these studies, it became of interest to inquire whether a sulphur-containing carboxylic acid lacking the amino group, and with no positive charge in the solution, would show any fundamental difference in behavior from that of the amino compounds studied. Preliminary experiments with mercaptoacetic acid (MAA) indicated an interesting behavior, more extended investigation of which gave the results reported in the present paper.

## EXPERIMENTAL

The equipment and procedure were identical with those outlined previously (5). MAA was reagent grade. A stock solution of it in the standard electrolyte was made to a concentration of 0.05 gm./liter (the low solubility of a dark precipitate that formed limited the concentration to this value). This solution was diluted with standard electrolyte to give the desired concentration of MAA during electrolysis. All experiments were made at 24.5° C., with a current density of 2 amp./dm.$^2$.

## RESULTS

MAA alone in the electrolyte reduced the total polarization below the 100-millivolt steady state value obtained with no additive (5). There was some indication of an indeterminate maximum in polarization during the initial 0.01 sec. (approximately), but the first distinct trace on the cathode ray oscilloscope showed a sharp drop in polarization and this depolarization by MAA continued throughout the electrolysis. The immediate effect of MAA

[1]*Manuscript received in original form July 28, 1955, and, as revised, November 14, 1955.*
*Contribution from the Physical Chemistry Laboratory, McGill University, Montreal, Que., with financial assistance from the Consolidated Mining and Smelting Co., Trail, B.C., and the National Research Council of Canada, Ottawa, Canada.*
[2]*Holder of a Cominco Research Fellowship. Present address: Department of Chemistry, University of Western Ontario, London, Ont.*

was to cause depolarization to about 50 to 60 mv. with a standard surface; the steady state polarization, established after electrolysis for an hour or more, was decreased to a limiting value of about 35 mv. as the concentration of MAA

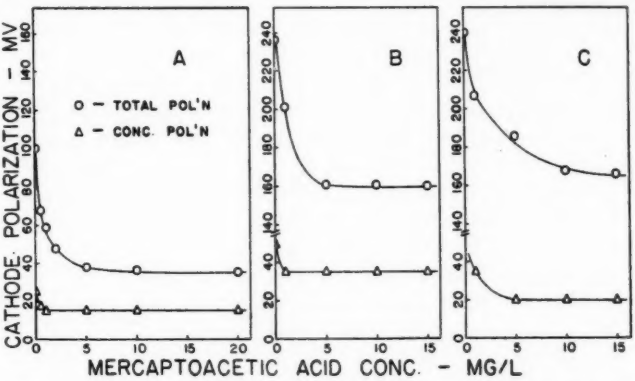


FIG. 1. Effect of mercaptoacetic acid concentration on steady state total and concentration polarizations.
A. Mercaptoacetic acid present alone.
B. Mercaptoacetic acid with 20 mgm./liter cystine.
C. Mercaptoacetic acid with 20 mgm./liter gelatin.

was increased, while the concentration polarization suffered a decrease of about 10 mv. (Fig. 1A). The steady state deposits obtained at these low polarizations had a characteristically coarse appearance under the microscope. These facts suggest that a gradual change in surface conditions, sufficient to decrease the true current density, is superimposed on the depolarizing action of the MAA. It seems reasonable to conclude that, in addition to the 15 mv. measured concentration polarization, there remains at the steady state about 20 mv. due to hydrogen ion interference (5).

The addition of chloride in low concentration caused further depolarization. Both the total and concentration polarizations at steady state, with 10 mgm./liter MAA, passed through a minimum at about 10 mgm./liter chloride ion (Fig. 2). The steady state polarization in the presence of chloride was also established slowly, just as in its absence. This greater depolarization due to chloride appeared to be accompanied by greater roughness of the cathode deposit. At the 20 mv. level of total polarization the crystal outgrowths were about 80 microns long. It should be noted, perhaps, that the concentration polarization at higher chloride concentrations increased to a limiting value of about 20 mv.

Since the polarization was decreased by MAA but increased by cystine (5) or gelatin (2), it was of interest to study the behavior when both depolarizing and polarizing addition agents were present. When various amounts of MAA were added with a fixed amount (20 mgm./liter) of cystine, the steady state polarization was lowered to a limiting value, the magnitude of the decrease being of the same order as that observed in the absence of cystine (Fig. 1B). Moreover, about 5 mgm./liter MAA gave maximum depolarization in either

case. The 75 mv. decrease in polarization caused by MAA in the presence of cystine includes a 15 mv. decrease in concentration polarization; the difference, 60 mv., is to be compared with the corresponding difference of 55 mv. obtained with MAA alone.

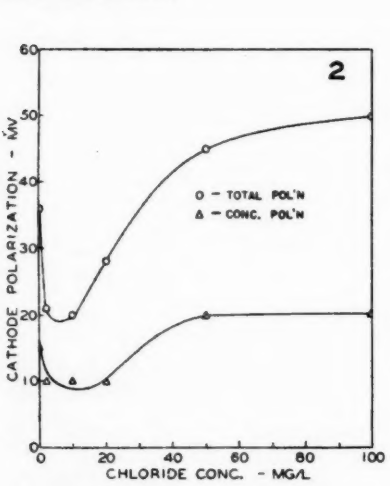


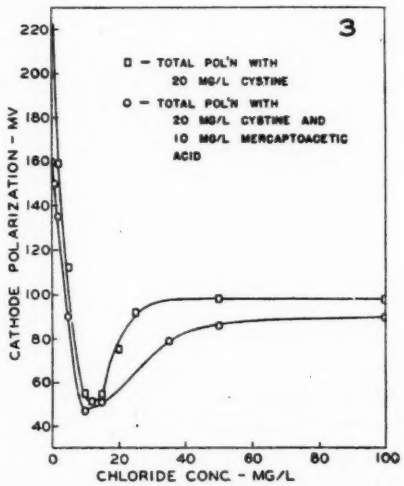
3
CATHODE POLARIZATION - MV
CHLORIDE CONC. - MG/L
□ — TOTAL POL'N WITH 20 MG/L CYSTINE
O — TOTAL POL'N WITH 20 MG/L CYSTINE AND 10 MG/L MERCAPTOACETIC ACID

FIG. 2. Cathode polarization – chloride concentration relation in the presence of 10 mgm./liter mercaptoacetic acid.

FIG. 3. Cathode polarization – chloride concentration relation with 20 mgm./liter cystine and with 20 mgm./liter cystine and 10 mgm./liter mercaptoacetic acid.

Study of the polarization–time relations when both MAA and cystine were present showed that during the first few seconds of electrolysis the total polarization values were as low as 60 mv. A rapid increase to a maximum after one or two minutes was followed by approach to a steady state during the next two to three hours. The steady state deposits, when both addition agents were present, were smooth and had none of the gray tinge imparted to the deposit by cystine alone. The following data were obtained with 20 mgm./liter cystine and different concentrations of MAA:

| Time | Total polarization (mv.) | | | |
|---|---|---|---|---|
| | Mercaptoacetic acid concentration (mgm./liter) | | | |
| | 1 | 5 | 10 | 15 |
| 0 | (Initial maxima not measurable) | | | |
| 2 sec. | 80 | 85 | 73 | 60 |
| ¼ min. | 155 | 132 | 113 | 93 |
| ½ min. | 188 | 158 | 125 | 107 |
| 1 min. | 203 | 170 | 142 | 110 |
| 2 min. | 207 | 173 | 140 | 108 |
| 10 min. | 209 | 183 | 150 | 114 |
| 20 min. | 211 | 182 | 153 | 120 |
| 30 min. | 209 | 179 | 153 | 123 |
| 40 min. | 208 | 176 | 154 | 130 |
| 110 min. | 201 | 166 | 152 | 149 |
| 120 min. | 202 | 167 | 153 | 150 |
| 290 min. | 202 | 161 | 159 | 159 |
| 330 min. | 201 | 161 | 161 | 160 |

As indicated, the higher concentrations of MAA accentuated the depolarization during the early stages of electrolysis, though not at the steady state.

Addition of small concentrations of chloride practically eliminated the influence of MAA in the presence of cystine (Fig. 3). It should be noted, however, that with excess chloride the total steady state polarization in the presence of MAA was about 15 mv. lower than in its absence. Also, the levelling-off of the total polarization curve required a greater amount of chloride when MAA was added to the electrolyte. The presence of MAA with excess chloride and 20 mgm./liter cystine did not affect the concentration polarization, which was about 20 to 25 mv. The polarization–time curves with chloride present were essentially the same as those obtained with the same amount of cystine in the absence of MAA (5).

Experiments with a combination of 20 mgm./liter gelatin and different amounts of MAA showed an effect on the steady state polarization similar to that observed with cystine (Fig. 1C). Addition of chloride to such a system gave a polarization – chloride concentration relation similar in its essential features to that obtained with gelatin and chloride in the absence of MAA (4). The polarization–time relations were rather complex. They resembled those obtained with small concentrations of thiourea (5) in the respect that the polarization increased rather sharply after about one hour's electrolysis, after which it either increased further, or decreased slowly to the steady state value, depending on the concentration of chloride.

## DISCUSSION

The immediate depolarizing effect of MAA, shown by initial polarization values, indicates that the activation overpotential was reduced to but a few millivolts. Accompanying the rough surface laid down, a further decrease in activation overpotential, hydrogen ion interference, and concentration polarization gradually occurred, probably because of decrease in true current density with an increase of true cathode area.

The behavior of MAA is in striking contrast with that of cystine, which appeared to leave the activation overpotential unaltered, but to increase the total polarization by adsorption on the cathode (5). If reference is made to the views of Lyons (3) the difference in behavior might be ascribed to a higher activity of cystine and a lower activity of MAA, relative to that of water, at the cathode surface. This might be expected since positively charged cystine, but not the neutral MAA, should tend to accumulate at the cathode surface. According to this point of view, such differences in activity of the co-ordinating species may be reflected in the relative activation overpotentials involved.

The observed additivity of the cystine and MAA effects at steady state gives clear indication that the two substances act in large measure independently. If, as argued previously (5), the aquo–copper complex is discharged in the presence of cystine, the reduction in activation overpotential with MAA is probably due to the ready discharge of the MAA–copper complex.

Although MAA should not accumulate at the cathode as a result of electrostatic attraction, it might well be readily adsorbed. Indeed, the behavior of MAA in the presence of cystine during the early stages of electrolysis suggests

that preferential adsorption of the MAA probably does occur prior to electrolysis. This could account for the observation that the depolarizing effect with higher concentrations of MAA is greater during the early stages than at steady state. However, the hindrance to the adsorption of cystine by such adsorbed MAA could be slowly overcome by gradual accumulation of cystine at the cathode surface. If MAA in the adsorbed phase were present as a readily dischargeable MAA–copper complex, it would not contribute to increase in polarization.

The additional depolarization caused by chloride in the presence of MAA apparently arises from increased roughening of the surface when chloride is present. This might be due to discharge of a more readily dischargeable chloro–MAA–copper complex, the presence of which is assumed, rather than the MAA–copper complex. Support for this assumption may be found in a previous argument (5) that chloride, when present alone, does not affect the activation overpotential. Hence, it does not appear that the depolarizing effect of chloride in the presence of MAA could be due to any readily dischargeable chloro–copper or chloro–aquo–copper complexes. For chloride concentrations above that corresponding to the minimum in the polarization – chloride concentration curve (Fig. 2), adsorption of cuprous chloride (5) might be expected to decrease the active surface area of the cathode, hence increase the true current density. This, in turn, might be expected to increase the difference between total and concentration polarization and this is observed. The 20-mv. plateau in the concentration–polarization curve (Fig. 2) might be regarded as a maximum diffusion and convection effect with increasing true current density.

Since the effect of low concentrations of chloride in the presence of both cystine and MAA more closely resembles its effect with cystine alone than with MAA alone (Fig. 3), the chloride effect is preferential in favor of cystine. For chloride concentrations above the minimum polarization point, more chloride appears to be necessary to produce the limiting maximum polarization (due to cuprous chloride (5)), when MAA is present with cystine than when cystine is present alone. Moreover, the effect of MAA in this combination is to lower the limiting maximum, which indicates a decrease in activation overpotential alone since the concentration polarization, hydrogen ion interference, and adsorption polarization due to cuprous chloride would be essentially the same in the two cases. These effects are to be expected if some of the chloride not tied up in the chloro–cystine–copper complex (5) associates with the MAA, possibly as the readily dischargeable chloro–MAA–copper complex.

## REFERENCES

1. ADAMEK, S. and WINKLER, C. A. Can. J. Chem. 32: 931. 1954.
2. GAUVIN, W. and WINKLER, C. A. Can. J. Research, B, 21: 81. 1943.
3. LYONS, E. H. J. Electrochem. Soc. 101: 363, 376. 1954.
4. MANDELCORN, L., MCCONNELL, W. B., GAUVIN, W., and WINKLER, C. A. J. Electrochem. Soc. 99 (No. 2): 84. 1952.
5. SUKAVA, A. J. and WINKLER, C. A. Can. J. Chem. 33: 961. 1955.

# THE CRYSTAL STRUCTURES OF SOME INTERMETALLIC COMPOUNDS OF PLUTONIUM[1]

By O. J. C. Runnalls

ABSTRACT

The crystal structures of the following binary intermetallic compounds of plutonium are reported: $PuAl_2$, $PuAl_3$, $PuAl_4$, $PuBe_{13}$, $PuCo_2$, $PuFe_2$, $PuMn_2$, $PuNi_2$, $PuNi_5$, and $Pu_2Ni_{17}$. In addition, the unit cell dimensions are reported for $PuAg_2$.

## INTRODUCTION

It is now possible to report on the crystal structures of intermetallic compounds of plutonium, because of a recent declassification decision. X-ray data have been compiled in this paper for 11 such compounds. The present data are compared with American (5) and Russian (9) data released recently, in Appendix I at the end of the paper.

All X-ray powder photographs were taken on a 14.3 cm. diameter General Electric camera, using Ni-filtered Cu radiation. The single crystal photographs were taken on a G.E. rotation camera of 5 cm. radius. The wave-lengths used in the calculations were 1.5418 Å for Cu $K_\alpha$ and 1.5405 for Cu $K_{\alpha_1}$.

## EXPERIMENTAL

### 1. *Plutonium–Aluminum Alloys*

Plutonium–aluminum alloys were prepared in BeO crucibles by the reduction of 99.5% pure plutonium trifluoride with 99.99% pure aluminum in vacuum at 900° C. Three intermediate Pu–Al phases have been identified using X-ray diffraction analyses—$PuAl_2$, $PuAl_3$, and $PuAl_4$.

#### (*a*) *$PuAl_2$*

A powder diffraction pattern showed that $PuAl_2$ is face-centered cubic with $a_0 = 7.831 \pm 0.005$ Å. The compound is isostructural with $UAl_2$ (11) and, therefore, has the $MgCu_2$ structure. The face-centered positions in space group $Fd3m$ are

$$8 \text{ Pu in } 0, 0, 0; \tfrac{1}{4}, \tfrac{1}{4}, \tfrac{1}{4}$$

$$16 \text{ Al in } \tfrac{5}{8}, \tfrac{5}{8}, \tfrac{5}{8}; \tfrac{5}{8}, \tfrac{7}{8}, \tfrac{7}{8}; \tfrac{7}{8}, \tfrac{5}{8}, \tfrac{7}{8}; \tfrac{7}{8}, \tfrac{7}{8}, \tfrac{5}{8}.$$

The calculated density is 8.10 gm. cm.$^{-3}$, assuming eight $PuAl_2$ molecules per unit cell. The interatomic distances are tabulated in Table I.

#### (*b*) *$PuAl_3$*

The powder diffraction pattern for $PuAl_3$ proved more complex than the simple cubic $UAl_3$, where $a_0 = 4.287$ Å (11). However, approximately one-third of the diffraction lines could be indexed on a simple cubic pattern of $a_0 = 4.30$ Å. Hence, it seemed probable that the $PuAl_3$ configuration was the result of a minor shift in the $UAl_3$-type cubic close-packing.

[1]*Manuscript received September 8, 1955.*
*Contribution from the Chemistry and Metallurgy Division, Atomic Energy of Canada Limited, Chalk River, Ontario. Issued as A.E.C.L. No. 267.*

Single crystals of $PuAl_3$ were separated from a 40 wt. % Pu–Al alloy after dissolving the aluminum matrix in 3 *N* NaOH. Several of the hexagonal-

TABLE I

INTERATOMIC DISTANCES IN $PuAl_2$

| Atom | Neighbor | Number of neighbors | Distance, Å |
|---|---|---|---|
| Pu | Pu | 4 | 3.39 |
| | Al | 12 | 3.25 |
| Al | Pu | 6 | 3.25 |
| | Al | 6 | 2.77 |

shaped crystals illustrated in Fig. 2 proved suitable as single crystal X-ray specimens. A series of rotation photographs revealed that the primitive cell was hexagonal with lattice dimensions

$$a_0 = 6.08 \pm 0.01 \text{ Å}$$

$$c_0 = 14.40 \pm 0.03 \text{ Å}.$$

The calculated density is 6.92 gm. cm.$^{-3}$, assuming six molecules per unit cell. A Laue photograph of a $PuAl_3$ crystal exhibited dihexagonal symmetry, identifying the point group as 622, $6mm$, $\bar{6}m2$, or $6/mmm$.

A model for the unit cell consistent with the observed dimensions was constructed using six close-packed planes, each containing one $PuAl_3$ molecule (Fig. 1). The model is derived by stacking the first four layers in cubic close-packed positions similar to $UAl_3$, and inserting a mirror plane at $c = \frac{1}{2}$, i.e.

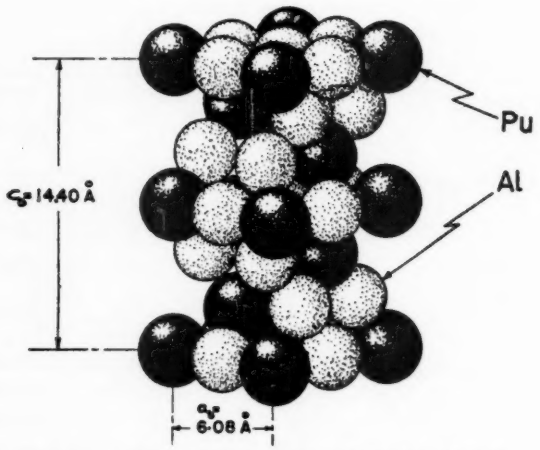


FIG. 1. An approximate model of the $PuAl_3$ unit cell.

[ABCACB]ABCAC—. This configuration is described in the International Tables (7) by the space group $P\bar{6}m2$, or, as pointed out by the Los Alamos

group (8), $P6_3/mmc$. Calculated intensities are reported in Table II for the following atomic positions in $P\bar{6}m2$:*

1 Pu in (*a*) 0, 0, 0
1 Pu in (*b*) 0, 0, $\frac{1}{2}$
2 Pu in (*h*) $\frac{1}{3}$, $\frac{2}{3}$, $z$; $\frac{1}{3}$, $\frac{2}{3}$, $\bar{z}$; $z = \frac{1}{6}$
2 Pu in (*i*) $\frac{2}{3}$, $\frac{1}{3}$, $z$; $\frac{2}{3}$, $\frac{1}{3}$, $\bar{z}$; $z = \frac{1}{3}$
3 Al in (*j*) $x$, $\bar{x}$, 0; $x$, $2x$, 0; $2\bar{x}$, $\bar{x}$, 0; $x = -\frac{1}{2}$
3 Al in (*k*) $x$, $\bar{x}$, $\frac{1}{2}$; $x$, $2x$, $\frac{1}{2}$; $2\bar{x}$, $\bar{x}$, $\frac{1}{2}$; $x = -\frac{1}{2}$
6 Al in (*n*) $x$, $\bar{x}$, $z$; $x$, $2x$, $z$; $2\bar{x}$, $\bar{x}$, $z$; $x$, $\bar{x}$, $\bar{z}$; $x$, $2x$, $\bar{z}$; $2\bar{x}$, $\bar{x}$, $\bar{z}$; $x = -\frac{1}{6}$, $z = \frac{1}{4}$
6 Al in (*n*) $x = \frac{1}{6}$, $z = \frac{1}{3}$.

TABLE II

POWDER DIFFRACTION DATA FOR $PuAl_3$

| *hk.l* | $\sin^2\theta$ | | *I* | |
|---|---|---|---|---|
| | Calc. | Obs. | Obs.* | Calc.† |
| 10.1 | 0.0243 | 0.0250 | w | 2.4 |
| 00.3 | 0.0258 | — | abs. | 0 |
| 10.2 | 0.0329 | 0.0337 | s | 5.0 |
| 00.4 | 0.0459 | — | abs. | 0 |
| 10.3 | 0.0472 | 0.0478 | s | 4.4 |
| 11.0 | 0.0643 | 0.0652 | s | 4.5 |
| 11.1 | 0.0672 | 0.0681 | m | 0 |
| 10.4 | 0.0673 | | | 2.1 |
| 00.5 | 0.0717 | — | abs. | 0 |
| 11.2 | 0.0758 | — | abs. | 0 |
| 20.0 | 0.0857 | — | abs. | 0 |
| 20.1 | 0.0886 | 0.0896 | w | 1.2 |
| 11.3 | 0.0901 | — | abs. | 0 |
| 10.5 | 0.0931 | 0.0947 | vw | 0.5 |
| 20.2 | 0.0972 | 0.0981 | s | 3.0 |
| 00.6 | 0.1032 | 0.1037 | m | 1.9 |
| 20.3 | 0.1115 | 0.1121 | s | 3.4 |
| 10.6 | 0.1246 | — | abs. | 0 |
| 20.4 | 0.1316 | 0.1318 | m | 2.0 |
| 11.5 | 0.1360 | — | abs. | 0 |
| 00.7 | 0.1404 | — | abs. | 0 |
| 12.0 | 0.1501 | — | abs. | 0 |
| 12.1 | 0.1529 | 0.1540 | vw | 0.5 |
| 20.5 | 0.1574 | 0.1582 | vw | 0.5 |
| 12.2 | 0.1615 | 0.1625 | m | 1.3 |
| 10.7 | 0.1619 | | | 0.2 |
| 11.6 | 0.1675 | 0.1679 | m+ | 2.4 |
| 12.3 | 0.1758 | 0.1760 | m | 1.6 |
| 00.8 | 0.1834 | — | abs. | 0 |
| 20.6 | 0.1889 | — | abs. | 0 |
| 30.0 | 0.1929 | 0.1933 | m− | 1.0 |
| 30.1 | 0.1958 | 0.1957 | m− | 0 |
| 12.4 | 0.1959 | | | 1.0 |
| 30.2 | 0.2044 | 0.2046 | w− | 0.5 |
| 10.8 | 0.2049 | | | 0 |
| 30.3 | 0.2187 | — | abs. | 0 |
| 12.5 | 0.2217 | 0.2220 | w− | 0.3 |
| 20.7 | 0.2262 | 0.2268 | w− | 0.3 |
| 00.9 | 0.2321 | — | abs. | 0 |
| 30.4 | 0.2384 | — | abs. | 0 |
| 22.0 | 0.2572 | 0.2583 | m | 1.4 |
| 13.0 | 0.2786 | — | abs. | 0 |

*$s$ = *strong*, $m$ = *medium*, $w$ = *weak*, $vw$ = *very weak*, and *abs.* = *absent*.
†$I \propto |F|^2 p[(1+\cos^2 2\theta)/\sin^2\theta \cos\theta]$.

**The equivalent positions in $P6_3/mmc$ are 2 Pu in (b), 4 Pu in (f) with $z = 1/12$, 6 Al in (h) with $x = \frac{1}{6}$, and 12 Al in (k) with $x = \frac{1}{6}$ and $z = 7/12$.*

The intensities of neighboring reflections only were compared, since no absorption correction was used in the calculations. Since the calculated intensities agreed with those observed on the powder diffraction film, the unit cell model appeared a reasonable one (see Table II).

The above solution may be considered only an approximate one, however, since weak reflections have been observed for 00.4, 00.8, 00.10, 00.14, and 00.16 by the Los Alamos group on Weissenberg patterns (8). Stambaugh found that the interplanar distances in the [00.1] direction were $0.162\pm0.002\ c_0$ for AB and CA, and $0.176\pm0.004\ c_0$ for BC, instead of the equiplanar distance of $0.167\ c_0$ (5). Unfortunately, this solution is not considered unique since satisfactory intensity checks for all *hk.l* values were not completed (5).

If all the Pu atoms were equidistant in the $PuAl_3$ cell the expected length of the $c_0$ axis would be 14.88 Å, instead of the observed 14.40 Å, to conform with the observed Pu–Pu separation in the [10.0] direction. Stambaugh's results indicate that the 0.48 Å shrinkage in $c_0$ is confined to those planes which do not have the $UAl_3$-type stacking sequence; i.e. if the shrinkage was distributed equally over the planes BAB and CAC the interplanar distances in the [00.1] direction would be $0.164\ c_0$ for AB and CA, and $0.172\ c_0$ for BC.

(*c*) *$PuAl_4$*

A 20 wt. % Pu–Al alloy was reacted with 3 *N* NaOH to dissolve the aluminum matrix. The powder diffraction pattern of the crystalline residue was complex, and similar to the $UAl_4$ pattern. Single crystals of $PuAl_4$ were prepared by cooling a molten 20% Pu–Al alloy at 100° C. per hr., and dissolving away the excess aluminum in NaOH. One of the small needlelike crystals (Fig. 3) was mounted in a quartz capillary.

A series of rotation photographs showed that $PuAl_4$ has an orthorhombic unit cell with dimensions similar to $UAl_4$ (see Table III). The calculated density is 6.10 gm. cm.$^{-3}$, assuming four molecules per unit cell. The spectra found missing by Borie (3) in the $UAl_4$ analysis were missing in the $PuAl_4$ pattern also; i.e. the reflections present were

(*a*) $h\ k\ l$, only for $h+k+l = 2n$
(*b*) $h\ k\ 0$, only for $h = 2n$ and $k = 2n$
(*c*) $h\ 0\ l$, only for $h+l = 2n$
(*d*) $0\ k\ l$, only for $k+l = 2n$.

TABLE III

UNIT CELL DIMENSIONS FOR $PuAl_4$ and $UAl_4$

| | $PuAl_4$, Å | $UAl_4$ (3), Å |
|---|---|---|
| $a_0$ | 4.42±0.02 | 4.41±0.02 |
| $b_0$ | 6.26±0.02 | 6.27±0.02 |
| $c_0$ | 13.66±0.03 | 13.71±0.03 |

These data indicate that the cell is body-centered with an 00*l* glide plane and may be described by either the space group *Ima*2 or *Imma*.

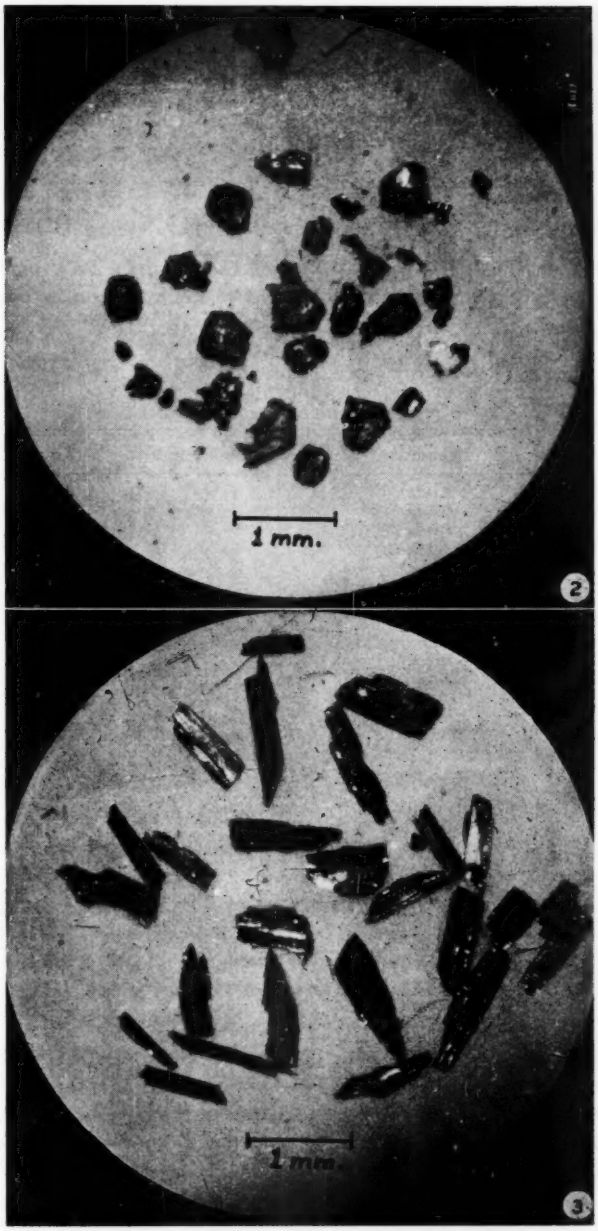


Fig. 2. Single crystals of $PuAl_3$.
Fig. 3. Single crystals of $PuAl_4$.

A visual comparison of the intensities on the $PuAl_4$ and $UAl_4$ powder patterns showed the two to be identical. Hence, Borie's description for $UAl_4$ (3) is applicable to $PuAl_4$ using atomic positions in space group *Imma*.

$(0, 0, 0; \frac{1}{2}, \frac{1}{2}, \frac{1}{2})+$
4 Pu in (*e*) $0, \frac{1}{4}, z; 0, \frac{3}{4}, \bar{z}; z = 0.111$
4 Al in (*e*) $0, \frac{1}{4}, z; 0, \frac{3}{4}, \bar{z}; z = -0.111$
4 Al in (*b*) $0, 0, \frac{1}{2}; 0, \frac{1}{2}, \frac{1}{2}$
8 Al in (*h*) $0, y, z; 0, \bar{y}, \bar{z}; 0, \frac{1}{2}+y, \bar{z}; 0, \frac{1}{2}-y, z; y = -0.033, z = 0.314.$

Singer has concluded that the value $z = 0.113$ for the 4 Pu atoms in (*e*) gives better intensity agreement than $z = 0.111$ (5). The interatomic distances are listed in Table IV.

TABLE IV
INTERATOMIC DISTANCES IN $PuAl_4$

| Atom | Neighbor | Number of neighbors | Distance, Å |
|---|---|---|---|
| Pu(4*e*) | Al(4*e*) | 2 | 3.13 |
| | Al(4*e*) | 1 | 3.03 |
| | Al(4*b*) | 4 | 3.11 |
| | Al(8*h*) | 4 | 3.01 |
| | Al(8*h*) | 2 | 3.29 |
| Al(4*e*) | Pu(4*e*) | 2 | 3.13 |
| | Pu(4*e*) | 1 | 3.03 |
| | Al(4*b*) | 4 | 3.11 |
| | Al(8*h*) | 4 | 2.79 |
| | Al(8*h*) | 2 | 3.09 |
| Al(4*b*) | Pu(4*e*) | 4 | 3.11 |
| | Al(4*e*) | 4 | 3.11 |
| | Al(4*b*) | 2 | 3.13 |
| | Al(8*h*) | 2 | 2.55 |
| Al(8*h*) | Pu(4*e*) | 2 | 3.01 |
| | Pu(4*e*) | 1 | 3.29 |
| | Al(4*e*) | 2 | 2.79 |
| | Al(4*e*) | 1 | 3.09 |
| | Al(4*b*) | 1 | 2.55 |
| | Al(8*h*) | 2 | 2.82 |
| | Al(8*h*) | 1 | 3.54 |
| | Al(8*h*) | 1 | 2.72 |

2. *Plutonium–Beryllium Alloys*

Plutonium–beryllium alloys were prepared in BeO crucibles by the reduction of plutonium trifluoride with powdered beryllium metal, 99.8% pure, in vacuum at 1100–1200° C. At these temperatures the beryllium fluoride product readily distilled, leaving a fluoride-free alloy.

The powder diffraction pattern of the intermediate phase $PuBe_{13}$ was readily interpreted since the compound is face-centered cubic and is isostructural with $UBe_{13}$. The lattice constant, $a_0$, decreases from $10.284 \pm 0.001$ Å on the Be-rich side to $10.278 \pm 0.001$ Å on the Pu-rich side, indicating some

small range of solid solubility. The calculated density, assuming eight formula weights of $PuBe_{13}$, is 4.35 gm. cm.$^{-3}$.

The compound $UBe_{13}$ has been found isostructural with $NaZn_{13}$ and is described by the space group *Fm3c* (1). The $NaZn_{13}$ parameters reported by Zintl and Hauche (15) have been refined recently by Shoemaker *et al.* (14). These refined parameters, $y = 0.1806$ and $z = 0.1192$, were used in calculating the interatomic distances in the $PuBe_{13}$ cell (Table V).

TABLE V

INTERATOMIC DISTANCES IN $PuBe_{13}$

| Atom | Neighbor | Number of neighbors | Distance, Å |
|---|---|---|---|
| $Be_I(0, 0, 0)$ | $Be_{II}(0, y, z)$ | 12 | 2.22 |
| $Be_{II}$ | $Be_{II}(0, z, \frac{1}{2}-y)$ | 2 | 2.15 |
| | $Be_I(0, 0, 0)$ | 1 | 2.22 |
| | $Be_{II}(z, \frac{1}{2}-y, 0)$ | 2 | 2.25 |
| | $Be_{II}(z, 0, y)$ | 4 | 2.31 |
| | $Be_{II}(0, y, \bar{z})$ | 1 | 2.45 |
| | $Pu(\frac{1}{4}, \frac{1}{4}, \frac{1}{4})$ | 2 | 2.99 |
| $Pu(\frac{1}{4}, \frac{1}{4}, \frac{1}{4})$ | $Be_{II}(0, y, z)$ | 24 | 2.99 |

The observed contraction of $PuBe_{13}$ on the Pu-rich side is somewhat surprising, since the Pu atom is about 35% larger than the Be atom. The isostructural $NpBe_{13}$ lattice also contracts, on the Np-rich side (12). A similar phenomenon has been observed by Bradley and Taylor (4) for the Al-rich side of the phase NiAl; i.e. the lattice spacing decreases rapidly with an increasing aluminum ratio. The latter effect has been attributed to the generation of nickel vacancies in the lattice as the aluminum ratio increases. A similar defect structure, Be-deficient, may exist in Pu-rich $PuBe_{13}$.

3. *Plutonium – Transition Metal Alloys*

Alloys of plutonium with the transition elements manganese, iron, cobalt, and nickel have been prepared by heating an intimate mixture of plutonium trifluoride and transition metal powder, 99.99% pure, in the presence of lithium vapor at 950° C. The product was then heated at 1100° C. for 15 min. Satisfactory Pu–Fe and Pu–Ni alloys were prepared in BeO crucibles. The best Pu–Co and Pu–Mn alloys, however, were prepared in Ta containers, since the latter alloys soaked into BeO.

(*a*) *$PuX_2$-type Phases*

X-ray powder photographs of alloys containing 65–70 wt. % Pu showed a face-centered cubic phase, isostructural with $UFe_2$ (2). Two separate preparations of $PuFe_2$ showed different lattice constants, indicating a range of composition for this phase. The observed lattice dimensions and calculated densities for the $PuX_2$ compounds are listed in Table VI. All four compounds have the $MgCu_2$ structure in space group *Fd3m*, with eight formula weights per unit cell. Interatomic distances are shown in Table VII.

TABLE VI

UNIT CELL SIZE AND X-RAY DENSITY FOR $PuX_2$-TYPE PHASES

| Compound | Lattice dimension, Å | Calculated density, gm. cm.$^{-3}$ |
|---|---|---|
| $PuMn_2$ | 7.290±0.005 | 11.96 |
| $PuFe_2$ | (*a*) 7.150±0.005 | 12.74 |
| | (*b*) 7.190±0.005 | 12.53 |
| $PuCo_2$ | 7.075±0.005 | 13.39 |
| $PuNi_2$ | 7.16 ±0.01 | 12.90 |

TABLE VII

INTERATOMIC DISTANCES IN THE COMPOUNDS $PuX_2$ WHERE X = Mn, Fe, Co, or Ni

| Atom | Neighbor | Number of neighbors | Distance, Å | | | | |
|---|---|---|---|---|---|---|---|
| | | | | $PuFe_2$ | | | |
| | | | $PuMn_2$ | (*a*) | (*b*) | $PuCo_2$ | $PuNi_2$ |
| Pu | Pu | 4 | 3.16 | 3.10 | 3.12 | 3.06 | 3.10 |
| | X | 12 | 3.02 | 2.96 | 2.98 | 2.93 | 2.96 |
| X | X | 6 | 2.58 | 2.53 | 2.54 | 2.50 | 2.53 |
| | Pu | 6 | 3.02 | 2.96 | 2.98 | 2.93 | 2.96 |

(*b*) *$PuNi_5$*

A powder photograph of a Pu–Ni alloy near the composition $PuNi_5$, 45 wt. % Pu, showed a single phase which was indexed on a hexagonal lattice with dimensions

$$a_0 = 4.875 \pm 0.005 \text{ Å},$$

$$c_0 = 3.970 \pm 0.005 \text{ Å}.$$

The X-ray data resembled closely those for the compound $ThNi_5$, which has the $CaZn_5$ structure (6). Calculated intensities based on this structure are in reasonable agreement with the observed powder data for $PuNi_5$, as shown in Table VIII.

Thus, $PuNi_5$ may be described by the $CaZn_5$ structure with the following atomic positions in space group $P6/mmm$:

$$1 \text{ Pu} \quad \text{in } 0, 0, 0$$

$$2 \text{ Ni}_\text{I} \quad \text{in } \tfrac{1}{3}, \tfrac{2}{3}, 0; \tfrac{2}{3}, \tfrac{1}{3}, 0$$

$$3 \text{ Ni}_\text{II} \text{ in } \tfrac{1}{2}, 0, \tfrac{1}{2}; 0, \tfrac{1}{2}, \tfrac{1}{2}; \tfrac{1}{2}, \tfrac{1}{2}, \tfrac{1}{2}.$$

The calculated density is 10.82 gm. cm.$^{-3}$.

Interatomic distances are listed in Table IX.

(*c*) *$Pu_2Ni_{17}$*

Since $PuNi_5$ proved to be isostructural with $ThNi_5$, a search was made for a Pu–Ni compound isomorphous with $Th_2Ni_{17}$. A phase with an X-ray pattern

TABLE VIII

POWDER DIFFRACTION DATA FOR $PuNi_3$

| *hk.l* | $\sin^2\theta$ | | *I* | |
|---|---|---|---|---|
| | Calc. | Obs. | Obs.† | Calc.‡ |
| 10.0 | 0.0333 | 0.0348 | m− | 246 |
| 10.1 | 0.0710 | 0.0731 | s | 1109 |
| 11.0 | 0.1000 | 0.1029 | m | 547 |
| 20.0 | 0.1307 | 0.1365 | m | 536 |
| 11.1 | 0.1377 | 0.1408 | s+ | 1400 |
| 00.2 | 0.1508 | 0.1523 | m− | 341 |
| 20.1 | 0.1711 | — | abs. | 0 |
| 10.2 | 0.1841 | 0.1881 | w− | 70 |
| 21.0 | 0.2317 | 0.2381 | w− | 51 |
| 11.2 | 0.2509 | 0.2538 | m | 275 |
| 21.1 | 0.2711 | 0.2743 | m | 312 |
| 20.2 | 0.2842 | 0.2870 | m+ | 320 |
| 30.0 | 0.3001 | 0.3031 | w+ | 102 |
| 30.1 | 0.3378 | 0.3415 | m | 321 |
| 00.3 | 0.3394 | — | abs. | 10 |
| 10.3 | 0.3727 | 0.3736 | w+ | 94 |
| 21.2 | 0.3842 | 0.3860 | w | 49 |
| 22.0 | 0.4001 | 0.4039 | m | 201 |
| 31.0 | 0.4334 | 0.4345 | vw | 21 |
| 22.1 | 0.4378 | 0.4408 | s− | 43 |
| 11.3 | 0.4394 | | | 216 |
| 30.2 | 0.4509 | 0.4525 | w+ | 109 |
| 31.1 | 0.4711 | 0.4735 | m− | 135 |
| 20.3 | 0.4727 | | | 0.2 |
| 40.0 | 0.5213 | 0.5284 | vw | 64 |
| 22.2 | 0.5509 | 0.5532 | m | 272 |
| 40.1 | 0.5712 | 0.5748 | m | 0.1 |
| 21.3 | 0.5727 | | | 111 |
| 31.2 | 0.5843 | 0.5878 | vw | 30 |
| 00.4 | 0.6028 | 0.6048 | vw | 43 |
| 32.0 | 0.6335 | — | abs. | 15 |
| 10.4 | 0.6367 | 0.6405 | m+ | 15 |
| 30.3 | 0.6383 | | | 157 |
| 32.1 | 0.6712 | 0.6746 | w | 110 |
| 40.2 | 0.6843 | 0.6875 | w | 119 |
| 41.0 | 0.7001 | 0.7038 | m | 85 |
| 11.4 | 0.7033 | | | 85 |
| 20.4 | 0.7354 | 0.7388 | s | 125 |
| 41.1 | 0.7359 | | | 335 |
| 22.3 | 0.7375 | | | 34 |
| 31.3 | 0.7715 | 0.7740* | w | 123 |
| 32.2 | 0.7830 | 0.7852* | vw | 36 |
| 50.0 | 0.8321 | — | abs. | 10 |
| 21.4 | 0.8353 | 0.8360* | vw | 40 |
| 41.2 | 0.8495 | 0.8513* | m | 227 |
| 50.1 | 0.8697 | 0.8725* | w− | 81 |
| 40.3 | 0.8713 | — | abs. | 0.6 |
| 33.0 | 0.8987 | 0.8993* | w− | 71 |
| 30.4 | 0.9019 | 0.9026* | w | 142 |
| 42.0 | 0.9319 | 0.9337* | m− | 242 |
| 33.1 | 0.9363 | 0.9374* | m+ | 334 |
| 00.5 | 0.9411 | — | abs. | 14 |
| 42.1 | 0.9696 | — | abs. | 4 |
| 32.3 | 0.9712 | 0.9714* | m+ | 354 |
| 10.5 | 0.9744 | 0.9740* | w | 186 |
| 50.2 | 0.9827 | 0.9826* | vw | 69 |

*Cu $K_{\alpha_1}$ reflection.

†*s = strong, m = medium, w = weak, vw = very weak, abs. = absent.*

‡$I \propto |F|^2 p[(1+\cos^2 2\theta)/\sin^2\theta \cos\theta]$

TABLE IX

INTERATOMIC DISTANCES IN $PuNi_5$

| Atom | Neighbor | Number of neighbors | Distance, Å |
|---|---|---|---|
| Pu | $Ni_I$ | 6 | 2.82 |
| | $Ni_{II}$ | 12 | 3.14 |
| $Ni_I$ | Pu | 3 | 2.82 |
| | $Ni_I$ | 3 | 2.82 |
| | $Ni_{II}$ | 6 | 2.44 |
| $Ni_{III}$ | Pu | 4 | 3.14 |
| | $Ni_I$ | 4 | 2.44 |
| | $Ni_{II}$ | 4 | 2.44 |

similar to, but more complex than, $PuNi_5$ was observed in alloys containing 30–35 wt. % Pu. This pattern was solved using a hexagonal lattice of dimensions

$$a_0 = 8.30 \pm 0.01 \text{ Å},$$

$$c_0 = 8.00 \pm 0.01 \text{ Å}.$$

The isomorphous phase $Th_2Ni_{17}$ has $a_0 = 8.37$ Å and $c_0 = 8.14$ Å (6). Since the intensities in the powder patterns of $Th_2Ni_{17}$ and $Pu_2Ni_{17}$ are closely related it seems reasonable to assign the $Th_2Ni_{17}$ structure to $Pu_2Ni_{17}$. The following approximate atomic positions apply in space group $P6_3/mmc$, for two molecules per unit cell:
2 $Pu_I$ in ($b$), 2 $Pu_{II}$ in ($d$), 6 $Ni_I$ in ($g$), 12 $Ni_{II}$ in ($j$) with $x = \frac{1}{3}$ and $y = 0$, 12 $Ni_{III}$ in ($k$) with $x = \frac{1}{6}$ and $z = 0$, and 4 $Ni_{IV}$ in ($f$) with $z = 0.11$.

4. *Plutonium–Silver Alloys*

Plutonium–silver alloys were prepared by heating in vacuum metallic Pu and fine-grain Ag of 99.97% purity in Ta crucibles at 1050° C. The Pu metal was prepared in 300 to 1000 mgm. amounts by the reduction of 99.5% pure $PuF_3$ with Li vapor at 950° C. During the alloying step the LiF slag covering the Pu metal distilled to the glass bulb surrounding the furnace assembly, leaving a clean alloy surface.

Powder diffraction patterns of Ag-rich alloys showed that a single phase existed at 40–45 wt. % Pu, i.e. $PuAg_3$. No attempt was made to apply graphical solution methods to the complex pattern since large hexagonal, columnar crystals could be separated from alloys approximating the composition $PuAg_3$. These proved satisfactory as single crystal X-ray specimens.

A series of rotation photographs showed that the $PuAg_3$ unit cell was hexagonal. Measurement of the layer line spacings gave lattice dimensions of

$$a_0 = 12.72 \pm 0.05 \text{ Å},$$

$$c_0 = 9.39 \pm 0.03 \text{ Å}.$$

These dimensions were refined by indexing the diffraction spots in the back reflection region of the zero layer lines. The diffraction angle, $\theta$, was measured with a steel scale on a film which had been mounted in the camera according to the method of Straumanis. The pertinent X-ray data from a rotation about

the $c_0$ axis are given in Table X. The crystal was adjusted for a rotation about the $a_0$ axis so that all but the 00.$l$ planes were tilted away from the vertical. The Cu $K_{\alpha_1}$ diffraction spot from 00.12 was indexed and $\theta$ measured on the resulting photograph. The measured $d$-spacing was 0.7835 Å. The refined unit cell dimensions are

$$a_0 = 12.730 \pm 0.003 \text{ Å},$$

$$c_0 = 9.402 \pm 0.005 \text{ Å}.$$

TABLE X

X-RAY DATA FROM A ROTATION PHOTOGRAPH OF $PuAg_3$ ABOUT THE $c_0$ AXIS

| $hk.l$ | $d_{obs.}$, Å* | $a_0$, Å |
|---|---|---|
| 87.0, 13.0.0 | 0.8479 | 12.728 |
| 96.0 | 0.8431 | 12.730 |
| 12.2.0 | 0.8405 | 12.728 |
| 10.5.0 | 0.8333 | 12.729 |
| 13.1.0 | 0.8148 | 12.727 |
| 12.3.0 | 0.8017 | 12.727 |
| 88.0 | 0.7955 | 12.728 |
| 97.0 | 0.7934 | 12.728 |
| 14.0.0, 10.6.0 | 0.7874 | 12.729 |
| 11.5.0 | 0.7776 | 12.730 |

**Obtained with Cu $K_{\alpha_1}$ radiation.*

The density of 450 mgm. of selected $PuAg_3$ crystals was measured with a pycnometer using ethylene dibromide as the immersion fluid. The resultant density was

$$\rho_{measured} = 11.16 \text{ gm. cm.}^{-3}.$$

If it is assumed that the unit cell contains 16 formula weights of $PuAg_3$, the density calculated from the X-ray data agrees closely with the measured value, i.e.

$$\rho_{calculated} = 11.33 \text{ gm. cm.}^{-3}.$$

The only systematic extinctions observed were of the type 00.$l$ where $l = 2n+1$, indicating that the possible space groups for $PuAg_3$ are $P6_3$, $P6_3/m$, and $P6_322$.

Since a structure-type suggesting a solution for the $PuAg_3$ structure was not found in the literature, no further attempt was made to establish the atom positions in the unit cell.

## DISCUSSION

Many more data on the binary intermetallic phases of neptunium, plutonium, and americium are required before the alloying systematics of the transuranic elements are understood. Sufficient information is available, however, to indicate that the alloying properties of the actinides are not necessarily similar in a specific alloy environment. The element plutonium, for example, exhibits isomorphism with uranium in the compounds $PuAl_2$ and $PuAl_4$ but not in $PuAl_3$, and with thorium in $PuNi_5$ and $Pu_2Ni_{17}$ but not in $PuNi_2$. Further marked

## APPENDIX I

X-RAY DATA FOR SOME BINARY INTERMETALLIC COMPOUNDS OF PLUTONIUM

| Compound | Structure type | Crystal system | Lattice constants, Å | Formula weights per unit cell | Space group | American results (5), Å | Russian results (9), Å |
|---|---|---|---|---|---|---|---|
| $PuAl_2$ | $MgCu_2$ | F.C.C.* | $a_0 = 7.831 \pm 0.005$ | 8 | $Fd3m$ | Pu-rich: $a_0 = 7.838 \pm 0.001$<br>Al-rich: $a_0 = 7.848 \pm 0.001$ | |
| $PuAl_3$ | $PuAl_3$ | Hexagonal | $a_0 = 6.08 \pm 0.01$<br>$c_0 = 14.40 \pm 0.03$ | 6 | $P6_3/mmc$ (8) | $a_0 = 6.17 \pm 0.02$<br>$c_0 = 14.5 \pm 0.1$ | |
| $PuAl_4$ | $UAl_4$ | Orthorhombic | $a_0 = 4.42 \pm 0.02$<br>$b_0 = 6.26 \pm 0.02$<br>$c_0 = 13.66 \pm 0.03$ | 4 | $Ima2$ or $Imma$ | $a_0 = 4.40$<br>$b_0 = 6.28$<br>$c_0 = 13.79$ | |
| $PuBe_{13}$ | $NaZn_{13}$ | F.C.C. | Pu-rich: $a_0 = 10.278 \pm 0.001$<br>Be-rich: $a_0 = 10.284 \pm 0.001$ | 8 | $Fm3c$ | Be-rich: $a_0 = 10.282 \pm 0.001$ | $10.274 \pm 0.002$ |
| $PuCo_2$ | $MgCu_2$ | F.C.C. | $a_0 = 7.075 \pm 0.005$ | 8 | $Fd3m$ | Pu-rich: $a_0 = 7.081 \pm 0.001$ | |
| $PuFe_2$ | $MgCu_2$ | F.C.C. | (*a*) $a_0 = 7.150 \pm 0.005$<br>(*b*) $a_0 = 7.190 \pm 0.005$ | 8 | $Fd3m$ | Pu-rich: $a_0 = 7.191 \pm 0.001$ | 7.179 |
| $PuMn_2$ | $MgCu_2$ | F.C.C. | $a_0 = 7.290 \pm 0.005$ | 8 | $Fd3m$ | Pu-rich: $a_0 = 7.292 \pm 0.001$ | 7.28 |
| $PuNi_2$ | $MgCu_2$ | F.C.C. | $a_0 = 7.16 \pm 0.01$ | 8 | $Fd3m$ | Pu-rich: $a_0 = 7.141 \pm 0.001$<br>Ni-rich: $a_0 = 7.115 \pm 0.001$ | 7.14 |
| $PuNi_5$ | $CaZn_5$ | Hexagonal | $a_0 = 4.875 \pm 0.005$<br>$c_0 = 3.970 \pm 0.005$ | 1 | $P6/mmm$ | Pu-rich: $a_0 = 4.872 \pm 0.002$<br>$c_0 = 3.980 \pm 0.001$<br>Ni-rich: $a_0 = 4.861 \pm 0.002$<br>$c_0 = 3.982 \pm 0.001$ | |
| $Pu_2Ni_{17}$ | $Th_2Ni_{17}$ | Hexagonal | $a_0 = 8.30 \pm 0.01$<br>$c_0 = 8.00 \pm 0.01$ | 2 | $P6_3/mmc$ | $a_0 = 8.29 \pm 0.02$<br>$c_0 = 8.01 \pm 0.02$ | |
| $PuAg_2$ | | Hexagonal | $a_0 = 12.730 \pm 0.003$<br>$c_0 = 9.402 \pm 0.005$ | 16 | $P6_3$, $P6_3/m$, or $P6_322$ | | |

*F.C.C. = *face-centered cubic.*

differences in alloying properties are illustrated by the absence of compounds of the type PuAl (5, 13) and AmAl (13), and $Pu_2Al$ (5) in the systems U–Al and Np–Al.

Variable alloying characteristics in the early members of the actinide series might be expected, according to Mott (10), because of a variable valency resulting from an electron interchange between the 5*f* and 6*d* shells. Since existing evidence indicates that the binding energies for 5*f* and 6*d* electrons are nearly equal at neptunium, alloy data for neptunium and plutonium should prove especially important in characterizing the metallurgical systematics of the actinides.

## SUMMARY

X-ray data for eleven binary intermetallic compounds of plutonium have been obtained. These are listed in Appendix I, and are compared with American results from the Los Alamos Laboratory (5). Russian results (9) for $PuBe_{13}$, $PuFe_2$, $PuMn_2$, and $PuNi_2$ are included in the Appendix.

Nine of the compounds are isostructural with the corresponding uranium compounds. $PuAl_3$ has a structure not previously reported. $PuAg_3$ appears also to have a new structure but a complete structure determination was not carried out.

## ACKNOWLEDGMENT

The author is indebted to J. Baird and R. R. Boucher for their assistance in the preparation of the alloy specimens.

## REFERENCES

1. Baenziger, N. C. and Rundle, R. E. Acta Cryst. 2: 258. 1949.
2. Baenziger, N. C., Rundle, R. E., Snow, A. I., and Wilson, A. S. Acta Cryst. 3: 34. 1950.
3. Borie, B. S. Trans. Am. Inst. Mining Engrs. 191: 800. 1951.
4. Bradley, A. J. and Taylor, A. Proc. Roy. Soc. A, 159: 56. 1937.
5. Coffinberry, A. S. and Ellinger, F. H. Intern. Conf. on the Peaceful Uses of Atomic Energy, Paper No. P/826. August, 1955.
6. Florio, J. V. and Rundle, R. E. U.S. Atomic Energy Comm. Rept. ISC-273. June, 1952.
7. International Tables for X-Ray Crystallography. Kynoch Press, Birmingham. 1952.
8. Jette, E. R. Private communication. June 20, 1955.
9. Konobeevsky, S. T. Proc. Acad. Sci. U.S.S.R. on the Peaceful Uses of Atomic Energy, Chem. Science Vols. 1–5: p. 362. July, 1955.
10. Mott, B. W. Research, 6: 238. 1953.
11. Rundle, R. E. and Wilson, A. S. Acta Cryst. 2: 148. 1949.
12. Runnalls, O. J. C. Acta Cryst. 7: 222. 1954.
13. Runnalls, O. J. C. Unpublished data.
14. Shoemaker, D. P., Marsh, R. E., Ewing, F. J., and Pauling, L. Acta Cryst. 5: 637. 1952.
15. Zintl, E. and Hauche, W. Naturwissenschaften, 25: 717. 1937.

# THEORY OF THE TRANSIENT PHASE IN KINETICS, WITH SPECIAL REFERENCE TO ENZYME SYSTEMS

## II. THE CASE OF TWO ENZYME–SUBSTRATE COMPLEXES[1]

By Ludovic Ouellet and Keith J. Laidler

ABSTRACT

A theoretical treatment is worked out for the kinetic scheme

$$E + S \rightleftarrows (ES)_1 \rightleftarrows (ES)_2 \rightarrow E + P$$

in which two enzyme–substrate complexes are formed consecutively. The steady-state rate equations are obtained, and equations are given for the transient phase subject to the condition that the substrate concentration is greatly in excess of that of the enzyme. Some kinetic consequences of the resulting equations are discussed.

In a previous paper (3) the reaction scheme

$$E + S \rightleftarrows ES \rightarrow E + P$$

has been considered from the standpoints of the conditions under which the steady-state theory applies, and of the kinetic behavior during the transient phase which exists prior to the establishment of the steady state. Since several recent publications (1, 2, 4) have referred to the possibility that there may be several enzyme–substrate complexes formed in consecutive reactions we have thought it of interest to consider briefly the steady-state and transient-phase equations for such a system. We have confined our considerations to the case of two enzyme–substrate complexes, since the transient-phase equations become very complicated if more complexes are assumed.

## THEORY

The system under consideration is

$$\underset{e_0-y_1-y_2}{E} + \underset{s_0}{S} \underset{k_{-1}}{\overset{k_1}{\rightleftarrows}} \underset{y_1}{(ES)_1} \underset{k_{-2}}{\overset{k_2}{\rightleftarrows}} \underset{y_2}{(ES)_2} \overset{k_3}{\rightarrow} \underset{e_0-y_1-y_2}{E} + \underset{p}{P}.$$

It is to be noted that the complexes are formed reversibly, the final products irreversibly. The concentrations of the various substances are indicated above. As discussed in the previous paper (3) the substrate concentration can be assumed to be essentially $s_0$ during the transient phase provided that the initial concentration of substrate is much greater than that of the enzyme.

The kinetic equations applicable to the above system are

[1] $$\dot{y}_1 = k_1 s_0(e_0 - y_1 - y_2) - (k_{-1} + k_2)y_1 + k_{-2}\, y_2$$

[2] $$\dot{y}_2 = k_2\, y_1 - (k_{-2} + k_3)y_2$$

[3] $$\dot{p} = k_3\, y_2.$$

[1]*Manuscript received October 17, 1955.*
*Contribution from the Department of Chemistry, The University of Ottawa, Ottawa, Canada.*

*Steady State*

The steady-state equations are obtained by setting $\dot{y}_1$ and $\dot{y}_2$ equal to zero and solving Eqs. [1] and [2]. The solution for $y_2$ is

$$[4] \qquad y_2 = \frac{k_1 k_2 e_0 s_0}{k_1(k_{-2}+k_2+k_3)s_0+(k_{-1}k_{-2}+k_{-1}k_3+k_2k_3)}$$

and the rate is therefore

$$[5] \qquad \dot{p} = \frac{k_1 k_2 k_3 e_0 s_0}{k_1(k_{-2}+k_2+k_3)s_0+(k_{-1}k_{-2}+k_{-1}k_3+k_2k_3)}.$$

This may be expressed in the familiar form

$$[6] \qquad \dot{p} = \frac{V s_0}{K_m+s_0}$$

where $V$, the maximum rate, is given by

$$[7] \qquad V = \frac{k_2 k_3 e_0}{k_{-2}+k_2+k_3}$$

and $K_m$, the Michaelis constant, is

$$[8] \qquad K_m = \frac{k_{-1}k_{-2}+k_{-1}k_3+k_2k_3}{k_1(k_{-2}+k_2+k_3)}.$$

If $k_3$ is very large the second complex $(ES)_2$ has no stable existence, and the relationships then reduce to the familiar forms

$$[9] \qquad V = k_2 e_0$$

$$[10] \qquad K_m = (k_{-1}+k_2)/k_1$$

applicable to the case of the single complex.

*The Transient Phase*

The kinetic equations for the transient phase are obtained as follows. Elimination of $y_1$ between Eqs. [1] and [2] gives rise to

$$[11] \qquad \ddot{y}_2+\dot{y}_2(k_1 s_0+k_{-1}+k_2+k_{-2}+k_3) \\ +y_2[k_1(k_2+k_{-2}+k_3)s_0+k_{-1}k_{-2}+k_2k_3]-k_1 k_2 s_0 e_0 = 0.$$

This may be written as

$$[12] \qquad \ddot{y}_2+P\dot{y}_2+Qy_2-R = 0.$$

The solution of this is

$$[13] \qquad y_2 = +(R/Q)+M \exp\{\tfrac{1}{2}[-P+\sqrt{(P^2-4Q)}]\,t\}+N \\ \exp\{\tfrac{1}{2}[-P-\sqrt{(P^2-4Q)}]t\}$$

where $M$ and $N$ are constants to be determined from the boundary conditions. The condition $t = 0$, $y_2 = 0$ leads to

$$M+N = -R/Q \tag{14}$$

and $t = 0$, $\dot{y}_2 = 0$ leads to

$$\frac{M}{N} = \frac{P+\sqrt{(P^2-4Q)}}{-P+\sqrt{(P^2-4Q)}}. \tag{15}$$

The solution of Eqs. [14] and [15] leads to

$$M = -\frac{R}{Q}\cdot\frac{P+\sqrt{(P^2-4Q)}}{-P+\sqrt{(P^2-4Q)}} \tag{16}$$

and

$$N = -\frac{R}{Q}\cdot\frac{\sqrt{(P^2-4Q)}-P}{2\sqrt{(P^2-4Q)}}. \tag{17}$$

The expression for $y_2$ is therefore

$$y_2 = \frac{R}{Q}\left[1-\frac{P+\sqrt{(P^2-4Q)}}{2\sqrt{(P^2-4Q)}}\exp\{\tfrac{1}{2}[-P-\sqrt{(P^2-4Q)}]t\}\right. \\ \left.-\frac{\sqrt{(P^2-4Q)}-P}{2\sqrt{(P^2-4Q)}}\exp\{\tfrac{1}{2}[-P-\sqrt{(P^2-4Q)}]t\}\right]. \tag{18}$$

This is of the form

$$y_2 = (R/Q)+M\,e^{Ft}+N\,e^{Gt} \tag{19}$$

where $R$, $Q$, $M$, and $N$ are defined above and $F$ and $G$ are given by

$$F=\tfrac{1}{2}[P-\sqrt{(P^2-4Q)}] \tag{20}$$

$$G=\tfrac{1}{2}[+P+\sqrt{(P^2-4Q)}]. \tag{21}$$

Insertion of Eq. [19] in Eq. [3] followed by integration then gives rise to the following expression for $p$ as a function of time:

$$p = \frac{k_3R}{Q}t+\frac{k_3M}{F}(e^{-Ft}-1)+\frac{k_3N}{G}(e^{-Gt}-1). \tag{22}$$

The general form of this relationship is as shown in Fig. 1. When $t$ is sufficiently large the exponential terms vanish (since $F$ and $G$ are necessarily positive) and the equation reduces to

$$p = \frac{k_3R}{Q}t-\frac{k_3M}{F}-\frac{k_3N}{G}. \tag{23}$$

This linear relationship between $p$ and $t$ corresponds to the establishment of the steady state. If this linear portion of the curve is extrapolated back to the time axis the intercept, which may be referred to as the induction period for the reaction, is given by

$$\tau = \frac{Q}{R}\left(\frac{M}{F}+\frac{N}{G}\right). \tag{24}$$

If the expressions for $F$, $G$, $M$, $N$, $Q$, and $R$ are inserted into this relationship it is found that

[25] $$\tau = P/Q$$

[26] $$= \frac{k_1 s_0 + k_{-1} + k_2 + k_{-2} + k_3}{k_1(k_2 + k_{-2} + k_3)s_0 + k_{-1}k_{-2} + k_1 k_3 + k_2 k_3}.$$

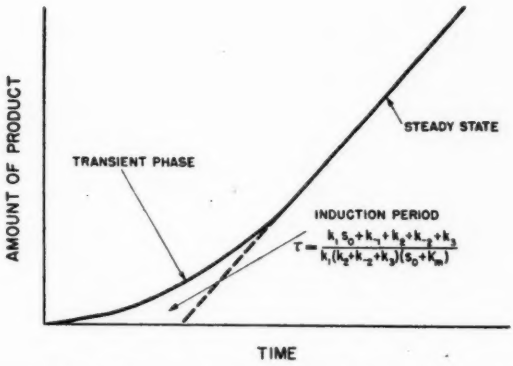


FIG. 1. Schematic plot of amount of product against time, for the case in which there are two successive enzyme–substrate complexes.

Using Eq. [8] this may be written as

[27] $$\tau = \frac{k_1 s_0 + k_{-1} + k_2 + k_{-2} + k_3}{k_1(k_2 + k_{-2} + k_3)(s_0 + K_m)}.$$

*Periodic Solutions*

The interesting possibility of periodic behavior can be shown to arise if $P^2 - 4Q$ is less than zero. Algebraic analysis shows that this can happen only if $k_2 > k_{-1}$. The necessary conditions can then be written as

[28] $$k_2 + k_{-2} + k_3 - 2\sqrt{[(k_2 - k_{-1})k_3]} < k_1 s_0 + k_{-1} < k_2 + k_{-2} + k_3 + \sqrt{[(k_2 - k_{-1})k_3]}.$$

Under these conditions, Eq. [18] can be written as

[29] $$y_2 = \frac{R}{Q} - \frac{R}{Q}\left[\exp -\frac{Pt}{2}\right]\left(\cos\frac{\sqrt{(4Q - P^2)}}{2} \cdot t + \frac{RP}{Q\sqrt{(4Q - P^2)}} \sin\frac{\sqrt{(4Q - P^2)}}{2} \cdot t\right).$$

This is the equation of a damped periodic variation, the period $T$ of which is given by

[30] $$T = 4\pi/\sqrt{(4Q - P^2)}.$$

Eqs. [25] and [30] yield, in terms of the measurable quantities $\tau$ and $T$,

$$Q = \frac{2 \mp 2\sqrt{[1-(4\pi^2\tau^2/T^2)]}}{\tau^2} \qquad [31]$$

and

$$P = \frac{2 \mp 2\sqrt{[1-(4\pi^2\tau^2/T^2)]}}{\tau}. \qquad [32]$$

$P$ and $Q$ are not complex quantities, so that

$$T > 2\pi\tau \qquad [33]$$

is a necessary relation between the measurable quantities $T$ and $\tau$. The fact that $T$ must be so much greater than $\tau$ makes it difficult to detect the periodicity experimentally. In ideal cases a plot of $P$ against $s$, by extrapolation to $s = 0$, gives

$$P_{s=0} = k_{-1}+k_2+k_{-2}+k_3 \qquad [34]$$

and the slope of the line will give $k_1$ directly. A similar plot for $Q$ yields

$$Q_{s=0} = k_{-1}(k_{-2}+k_3)+k_2 k_3 \qquad [35]$$

and the slope of the line is $k_1(k_2+k_{-2}+k_3)$. Equations [7], [8], [34], [35] and the slopes of $P$ vs. $s_0$ and $Q$ vs. $s_0$ provide six relations to determine five constants.

## DISCUSSION

Certain special cases of the above equations are of some interest. In the first place, in the event that $k_3$ is very large (i.e. that the complex $(ES)_2$ has only a fleeting existence) the induction period is given by

$$\tau = 1/[k_1(s_0+K_m)]. \qquad [36]$$

This equation was previously quoted by Gutfreund (2), and it follows directly from Eq. [48] of the previous paper (3). Since Eq. [36] is of the same form as Eq. [27] it is clearly not possible to tell, from a study of the induction period, anything about the existence of the second complex.

Another result of interest is obtained if $s_0$ is sufficiently large. The induction period is then

$$\tau = 1/(k_2+k_{-2}+k_3). \qquad [37]$$

A plot of $\tau(s_0+K_m)$ against $s_0$ would give this quantity as its slope. In the event that one of these three rate constants is much larger than the others the induction period is thus, at high $s_0$, equal to the reciprocal of that constant.

## REFERENCES

1. GUTFREUND, H. Trans. Faraday Soc. 51: 441. 1955.
2. GUTFREUND, H. Discussions Faraday Soc. 1955. In press.
3. LAIDLER, K. J. Can. J. Chem. 33: 1614. 1955.
4. LUMRY, R., SMITH, E. L., and GLANTZ, R. R. J. Am. Chem. Soc. 73: 4330. 1951.

# VAPOR PRESSURES OF AQUEOUS SOLUTIONS OF SILVER NITRATE, OF AMMONIUM NITRATE, AND OF LITHIUM NITRATE[1]

By A. N. Campbell, J. B. Fishman, G. Rutherford, T. P. Schaefer,[2] and L. Ross

ABSTRACT

This paper is devoted to the direct determination of the vapor pressures of solutions of the nitrates of silver, of ammonium, and of lithium, at temperatures varying from 30° C. to 105° C. and at concentrations varying from 10 to 85 weight % (for lithium nitrate, the limited solubility precluded measurements beyond 65%). From the vapor pressures, the enthalpies of evaporation of water (by a modification of the Clapeyron–Clausius equation), the differential heats of dilution, and the activities of water (as compared with the mole fractions of the solvent) have been calculated. From the results we conclude that the water of hydration of the ammonium and silver ions (if, indeed, these ions are hydrated at all) is very loosely attached, while that of the lithium ion is strongly bound.

The present work was undertaken because it was thought that a knowledge of the vapor pressures at a series of temperatures would yield the heat of evaporation of water from solutions of different concentrations and hence throw some light, if only of a qualitative nature, on the firmness with which the different ions held their water of hydration. As the concentration of an electrolytic solution is increased there will be fewer molecules of water left for ionic hydration; at extremely high concentration there will be strong competition for the remaining water molecules. Using the concept of Stokes and Robinson (8) that the ions adsorb layers of water molecules in accordance with the Brunauer, Emmet, and Teller equation, it should become progressively more difficult to strip away the successive layers of water surrounding the ions; the last and most firmly bound layer should require a large amount of energy to remove it. Application of the Clapeyron–Clausius equation (though not in its normal form: see Discussion) to the vapor pressures of concentrated solutions should give the heat of evaporation and hence, perhaps, a measure of the difficulty of removing water from the ions.

The problem of finding vapor pressures was first attempted by finding boiling points at different fixed pressures. After spending a year, however, on this method of attack we abandoned it because we found that, although we could control pressure and boiling point to any desired degree of constancy, we had no certainty as to the composition of the equilibrium liquid. Indeed, the work about to be described showed that we occasionally had composition errors equivalent to an error of 0.5° in boiling point.

Because of this uncertainty in the composition variable of the boiling point method, we decided to turn to a method in which the composition factor would be known and invariable. The direct determination of vapor pressure in a closed system offers such a method. The loss of water by evaporation to produce one atmosphere pressure in a closed system is negligible, even in the strongest solutions used.

[1]*Manuscript received October 3, 1955.*
*Contribution from the Chemistry Department, University of Manitoba, Winnipeg, Manitoba.*
[2]*Holder of a N.R.C. Bursary.*

There has been surprisingly little experimental work done on the vapor pressure of aqueous electrolytic solutions, especially over a range of temperature. Most of that which has been done is confined to the isopiestic measurement of vapor pressures for the determination of activity at 25° C.

Our vapor pressure measurements have been utilized to calculate the heat of evaporation of water from the various solutions, the heat of dilution, and the activity of water as given by the ratio $p/p_0$.

## EXPERIMENTAL PROCEDURE

The sources and purity of our materials have frequently been described elsewhere (1). All solutions were made up by direct weighing, using salts which, after purification, had been thoroughly dried; the lithium nitrate was always fused before use. For the determination of the vapor pressures of the more dilute solutions the differential manometer of Hartung (4) was used. It was possible to use this up to concentrations of 60% by weight for silver nitrate solutions but only up to 40% concentration for lithium nitrate. In the differential manometer one limb contains pure water and the other the solution.

Fig. 1 represents Hartung's apparatus as used by us. The method of use is described by Hartung but certain modifications are mentioned here. For instance, since we used mineral oil in our thermostat and worked up to temperatures of 105°, it was impossible to use ordinary rubber in the thermostat and neoprene was used for the bung through which the long limb of the mano-

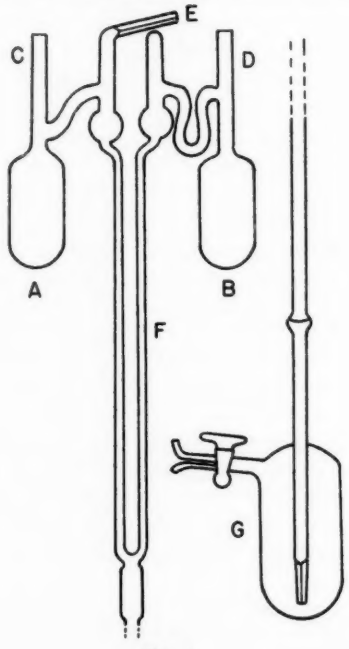


Fig. 1.

meter passes. The long limb was also severed, about 10 cm. above the mercury reservoir, and a ball and socket joint introduced; this facilitated the installation and dismantling of the apparatus, which had to be done every time a new solution was introduced. A little silicone oil was allowed to float on top of both mercury levels in the manometer. This had the dual advantage of preventing the condensation of small amounts of water on the mercury surfaces (which, we found, produced distortion in the field of vision of the cathetometer) and, when silver nitrate solutions were used, of preventing mercury vapor entering the solutions and causing decomposition, as it does very readily.

The necessity of removing the last trace of air in all vapor pressure measurements is well known, and for this purpose the procedure adopted was to freeze both bulbs in dry ice. The mercury level was then lowered and both bulbs evacuated continuously for the space of half an hour. The mercury level was then raised and the contents of the bulbs allowed to thaw. The above procedure was repeated at least four times. Finally the capillary leading to the pump was sealed off and the contents allowed to thaw for the last time. The solution was then agitated to ensure homogeneity.

With the more concentrated solutions (70% by weight for silver nitrate, 40% for lithium nitrate) it was impossible to use the differential manometer, since the limbs of the U-tube were only 20 cm. long, and with highly concentrated solutions at higher temperatures the difference in vapor pressure from that of water became greater than 20 cm. of mercury. A direct barometric apparatus therefore became necessary.

The apparatus is shown in Fig. 2. Dissolved air was removed by the same treatment as already described. In the more concentrated solutions now used,

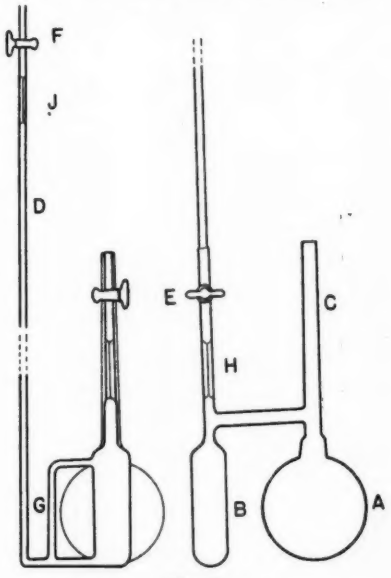


Fig. 2.

the 'salting-out' effect rendered the solubility of air much less and the difficulty of removing dissolved air was proportionately reduced.

All manometers were completely immersed in a tall rectangular copper tank furnished with glass sides. Because the thermostatic fluid was mineral oil it was necessary to use Buna-N rubber as gasket material for the glass windows. Measurements were made between 30° C. and 105° C. The usual procedure of using an immersion heater to keep temperature slightly below the operating temperature and controlling an electric light bulb as the source of extra heat, together with the use of three stirrers, gave a temperature fluctuation of not more than ±0.02° C., over the whole range of temperature.

Two cathetometers were used to measure differences in mercury levels, one a short range instrument which could be read to 0.01 mm., and another of greater range which could be read to 0.1 mm. Successive readings showed that it required about two hours to obtain equilibrium at the lower temperatures, while half an hour sufficed at the higher temperatures. All mercury columns were reduced to 0° C. The probable error does not exceed 0.2% and this makes the data good enough for most purposes.

## EXPERIMENTAL RESULTS

The experimental results are given in Table I.

TABLE I

THE VAPOR PRESSURES OF SOLUTIONS OF SILVER NITRATE, OF AMMONIUM NITRATE, AND OF LITHIUM NITRATE AT DIFFERENT TEMPERATURES

| Silver nitrate | | | Ammonium nitrate | | | Lithium nitrate | | |
|---|---|---|---|---|---|---|---|---|
| Conc., wt. % | Temp., ° C. | Press., mm. Hg | Conc., wt. % | Temp., ° C. | Press., mm. Hg | Conc., wt. % | Temp., ° C. | Press., mm. Hg |
| 9.98 | 30.06 | 31.64 | 10.00 | 30.00 | 31.51 | 10.00 | 30 | 30.48 |
| | 40.00 | 54.63 | | 40.00 | 54.48 | | 40 | 52.57 |
| | 50.00 | 91.37 | | 50.00 | 90.70 | | 50 | 87.83 |
| | 60.00 | 147.4 | | 60.00 | 145.90 | | 60 | 141.76 |
| | 70.00 | 230.4 | | 70.00 | 227.17 | | 70 | 221.40 |
| | 80.00 | 349.8 | | 80.00 | 344.10 | | 80 | 335.90 |
| | 90.00 | 517.5 | | 90.00 | 508.2 | | 90 | 497.20 |
| | 101.00 | 774.8 | | 100.00 | 733.2 | | 100 | 718.35 |
| | | | | 101.40 | 770.5 | | 102 | 771.08 |
| 19.98 | 30.06 | 31.57 | 20.00 | 30.00 | 30.90 | 20.00 | 30 | 27.83 |
| | 40.00 | 54.36 | | 40.00 | 53.84 | | 40 | 48.35 |
| | 50.00 | 90.81 | | 50.00 | 88.94 | | 50 | 80.67 |
| | 60.00 | 146.0 | | 60.00 | 141.8 | | 60 | 130.60 |
| | 70.00 | 227.5 | | 70.00 | 219.3 | | 70 | 203.93 |
| | 80.00 | 344.9 | | 80.00 | 330.5 | | 80 | 309.12 |
| | 90.00 | 509.0 | | 90.00 | 486.5 | | 90 | 456.21 |
| | 101.00 | 760.7 | | 100.00 | 699.8 | | 100 | 658.05 |
| | | | | 102.00 | 750.6 | | 105 | 784.04 |
| 30.00 | 30.00 | 30.30 | 30.00 | 30.00 | 30.43 | 30.00 | 30 | 23.08 |
| | 40.00 | 52.63 | | 40.00 | 52.00 | | 40 | 40.22 |
| | 50.00 | 87.77 | | 50.00 | 84.78 | | 50 | 66.79 |
| | 60.00 | 141.3 | | 60.00 | 134.7 | | 60 | 109.42 |
| | 70.00 | 220.6 | | 70.00 | 208.2 | | 70 | 171.32 |
| | 80.00 | 334.8 | | 80.00 | 313 0 | | 80 | 261.16 |
| | 90.00 | 495 0 | | 90.00 | 459.6 | | 90 | 388.41 |
| | 102.00 | 767 5 | | 100.00 | 659.9 | | 100 | 562.25 |
| | | | | 104.00 | 758.4 | | | |

TABLE I (*Concluded*)

| Silver nitrate | | | Ammonium nitrate | | | Lithium nitrate | | |
|---|---|---|---|---|---|---|---|---|
| Conc., wt. % | Temp., ° C. | Press., mm. Hg | Conc., wt. % | Temp., ° C. | Press., mm. Hg | Conc., wt. % | Temp., ° C. | Press., mm. Hg |
| 40.00 | 30.00 | 29.50 | 40.00 | 30.00 | 26.25 | 40.00 | 30 | 19.18 |
| | 40.00 | 51.18 | | 40.00 | 45.30 | | 40 | 33.11 |
| | 50.00 | 85.40 | | 50.00 | 75.09 | | 50 | 55.73 |
| | 60.00 | 137.5 | | 60.00 | 120.8 | | 60 | 89.34 |
| | 70.00 | 214.5 | | 70.00 | 188.0 | | 70 | 140.45 |
| | 80.00 | 325.7 | | 80.00 | 284.6 | | 80 | 215.06 |
| | 90.00 | 481.4 | | 90.00 | 420.0 | | 90 | 320.30 |
| | 103.00 | 772.8 | | 100.00 | 604.3 | | 100 | 463.97 |
| | | | | 105.71 | 736.9 | | 105 | 556.78 |
| 50.00 | 30.00 | 28.68 | 50.00 | 30.00 | 25.65 | 50.00 | 30 | 13.59 |
| | 40.00 | 49.78 | | 40.00 | 43.39 | | 40 | 23.37 |
| | 50.00 | 82.95 | | 50.00 | 71.68 | | 50 | 39.93 |
| | 60.00 | 133.6 | | 60.00 | 113.4 | | 60 | 64.66 |
| | 70.00 | 208.6 | | 70.00 | 176.0 | | 70 | 102.21 |
| | 80.00 | 316.3 | | 80.00 | 265.7 | | 80 | 157.20 |
| | 90.00 | 466.9 | | 87.91 | 358.9 | | 90 | 236.10 |
| | 103.00 | 749.1 | | 100.00 | 555.7 | | 104 | 400.57 |
| 59.29 | 31.04 | 29.33 | 60.00 | 30.00 | 21.72 | 57.28 | 30 | 9.21 |
| | 40.09 | 47.87 | | 40.00 | 36.96 | | 40 | 16.61 |
| | 50.14 | 79.70 | | 50.00 | 61.54 | | 50 | 28.49 |
| | 60.28 | 129.2 | | 60.00 | 98.36 | | 60 | 46.86 |
| | 70.37 | 202.7 | | 70.00 | 152.8 | | 70 | 75.77 |
| | 80.50 | 308.6 | | 80.00 | 231.0 | | 80 | 118.25 |
| | 90.56 | 457.5 | | 90.00 | 339.5 | | 90 | 179.31 |
| | 100.65 | 662.0 | | 100.00 | 486.7 | | 100 | 264.20 |
| | 105.60 | 787.1 | | | | | 105 | 319.87 |
| 69.99 | 30.00 | 26.15 | 70.00 | 40.00 | 31.62 | 64.953 | 30 | |
| | 40.00 | 45.88 | | 50.00 | 52.10 | | 40 | 11.14 |
| | 50.00 | 75.79 | | 60.00 | 82.20 | | 50 | 19.01 |
| | 60.00 | 122.0 | | 70.00 | 128.6 | | 60 | 31.74 |
| | 70.00 | 189.6 | | 80.00 | 193.8 | | 70 | 50.77 |
| | 80.00 | 286.2 | | 90.00 | 285.6 | | 80 | 79.77 |
| | 90.00 | 421.5 | | 100.00 | 405.5 | | 90 | 122.22 |
| | 100.00 | 606.6 | | | | | 100 | 182.06 |
| | | | | | | | 105 | 221.34 |
| 80.05 | 60.00 | 107.2 | 80.00 | 60.00 | 63.82 | | | |
| | 65.00 | 134.2 | | 70.00 | 98.13 | | | |
| | 70.00 | 166.8 | | 80.00 | 146.4 | | | |
| | 75.00 | 206.2 | | 90.00 | 213.5 | | | |
| | 80.00 | 252.6 | | 100.00 | 304.8 | | | |
| | 85.00 | 307.9 | | | | | | |
| | 90.00 | 372.4 | | | | | | |
| | 95.00 | 447.9 | | | | | | |
| | 100.00 | 534.8 | | | | | | |
| 85.07 | 75.00 | 183.1 | 90.00 | 100.00 | 201.2 | | | |
| | 80.00 | 223.8 | | 105.00 | 240.2 | | | |
| | 82.00 | 246.6 | | 110.00 | 281.9 | | | |
| | 85.00 | 271.8 | | 115.00 | 330.0 | | | |
| | 87.50 | 298.8 | | 120.00 | 385.7 | | | |
| | 90.00 | 328.6 | | 125.00 | 445.7 | | | |
| | 92.50 | 360.8 | | 130.00 | 512.0 | | | |
| | 100.00 | 471.6 | | | | | | |
| 90.00 | 120.00 | 716.1 | | | | | | |
| | 124.80 | 820.2 | | | | | | |
| | 126.58 | 866.3 | | | | | | |
| | 130.00 | 950.4 | | | | | | |

## DISCUSSION

In order to obtain $\Delta H_1$ (the molar enthalpy of evaporation of water from the different solutions) the following procedure was adopted: Using the Clapeyron–Clausius equation, in its classical form, the calculation must be restricted to a small range of temperature over which $\Delta H$ may be regarded as constant; such a restriction magnifies the experimental error. A very useful application of the Clapeyron–Clausius equation for the correlation of vapor pressure and latent heat data has, however, been given by Othmer (7). Using the symbols $\Delta H_1$ and $\Delta H_2$ for the molar enthalpies of evaporation of water from solution and from pure water respectively and rearranging the differential form of the Clapeyron equation, the following expression results:

$$[1] \qquad (1/\Delta H_1)(dP_1/P_1) = dT/RT^2.$$

The same expression may be written for any other material at the same temperature as:

$$[2] \qquad (1/\Delta H_2)(dP_2/P_2) = dT/RT^2.$$

$P_1$ and $P_2$ are the vapor pressures of the two substances at the same temperature $T$. Equating equations [1] and [2] and rearranging, equation [3] is obtained:

$$[3] \qquad dP_1/P_1 = (\Delta H_1/\Delta H_2)(dP_2/P_2).$$

With the usual assumptions as to the vapor being an ideal gas and the volume of the condensed phase being negligible, one obtains, in logarithmic form,

$$[4] \qquad d(\log P_1)/d(\log P_2) = \Delta H_1/\Delta H_2.$$

If $\Delta H_1/\Delta H_2$ is considered constant, equation [4] may be integrated to give equation [5],

$$[5] \qquad \log P_1 = (\Delta H_1/\Delta H_2) \log P_2 + C.$$

Hence, if the logarithm of the vapor pressure, $P_1$, of a solution is plotted against the logarithm of the vapor pressure of water, $P_2$, at the same temperature, a straight line results which has for its slope the ratio of the molar enthalpies of evaporation. This line is straight if the ratio $\Delta H_1/\Delta H_2$ is constant over the temperature range in question and this is reasonably near the truth for water and aqueous solutions. Knowing the value of the ratio, and that of the latent heat of evaporation of pure water, $\Delta H_1$, the latent heat of evaporation of water from solution is obtained. The best data for the latent heats of evaporation of water, and for vapor pressure, are contained in a paper by Goff and Gratch (3); they give an equation for vapor pressure of water in terms of temperature, which we have used throughout. The slopes of log $P_1$ versus log $P_2$ were calculated analytically by the method of moments instead of by the more inaccurate graphical method.

In Table II are given the values of $\Delta H_1$, the latent heat of evaporation of water from the various solutions, for a mean temperature of 50° C. For this temperature we have taken $\Delta H_2$, the heat of evaporation of pure water, to be 10,245 cal.; this is the average of several direct calorimetric determinations by Johnson and Molstad (6). An examination of Table II shows that, for silver nitrate, $\Delta H$ for solution is not much different from that for pure water. The

slight difference is positive and increases with increasing concentration, i.e., less heat is required to evaporate water from solution than from pure water. Similar results have been obtained before. Thus, Hirschler (5) showed that the vapor pressures of certain saturated aqueous solutions, when plotted as

TABLE II

THE SLOPES $\Delta H_1/\Delta H_2$ OF LOG $P_1$ VERSUS LOG $P_2$, AND THE VALUE OF $\Delta H_1$, AT 50° C. ($\Delta H_2$ = 10,245 CAL./MOLE)

| Conc., wt. % | Slope $\Delta H_1/\Delta H_2$ | $\Delta H_1$ | $\Delta H_2-\Delta H_1$ |
|---|---|---|---|
| | Silver nitrate | | |
| 9.98 | 0.9982 | 10227 | 18 |
| 19.98 | 0.9929 | 10172 | 73 |
| 30.00 | 0.9960 | 10204 | 41 |
| 40.00 | 0.9958 | 10202 | 43 |
| 50.00 | 0.9948 | 10192 | 53 |
| 59.29 | 0.9948 | 10192 | 53 |
| 69.99 | 0.9895 | 10138 | 107 |
| 80.05 | 0.9893 | 10135 | 110 |
| 85.07 | 0.9799 | 10039 | 206 |
| | Ammonium nitrate | | |
| 10.00 | 0.9916 | 10158 | 87 |
| 20.00 | 0.9811 | 10047 | 198 |
| 30.00 | 0.9702 | 9948 | 297 |
| 40.00 | 0.9889 | 10130 | 115 |
| 50.00 | 0.9613 | 9832 | 413 |
| 60.00 | 0.9817 | 10054 | 191 |
| 70.00 | 0.9765 | 9999 | 246 |
| 80.00 | 0.9611 | 9834 | 411 |
| 90.00 | 0.9523 | 9759 | 486 |
| | Lithium nitrate | | |
| 10.00 | 0.9967 | 10211 | 34 |
| 20.00 | 0.9969 | 10213 | 32 |
| 30.00 | 1.0078 | 10325 | − 79 |
| 40.00 | 1.0063 | 10310 | − 64 |
| 50.00 | 1.0225 | 10476 | −225 |
| 57.28 | 1.0585 | 10844 | −566 |
| 64.953 | 1.0700 | 10962 | −670 |

log $P$ vs. $1/T$, give straight lines parallel to a similar plot for water. Since $\Delta H_2-\Delta H_1$ is a small positive quantity and increases with increasing concentration, this means that heat is adsorbed when a mole of water is added to a large amount of solution (differential heat of dilution) and this amount of heat increases with increasing concentration. For ammonium nitrate, the differential heat of dilution is also positive, but rather more pronounced, amounting to half a kilocalorie at the highest concentration. For lithium nitrate the heat of dilution is negative. Heat is evolved when lithium nitrate solutions are diluted and this seems to be in harmony with the accepted belief in the strongly hydrated lithium ion.

In Table III, the activity of the water in solution, derived from the vapor pressure and the corresponding vapor pressure of pure water, is compared with the mole fraction of water (calculated on the assumption of non-ionized salt).

For silver nitrate, the agreement is surprisingly good between the mole fraction and the activity coefficient and it is essentially independent of temperature, i.e., Raoult's law is obeyed, throughout the concentration range, far more closely than it should be for a solution of an electrolyte. Campbell and Kartz-

TABLE III

THE ACTIVITY OF WATER $P/P_0$ IN SOLUTIONS AT VARIOUS CONCENTRATIONS AND TEMPERATURES

| Conc., mole fraction of water* | Temperature (° C.) | | | | | | | |
|---|---|---|---|---|---|---|---|---|
| | 30 | 40 | 50 | 60 | 70 | 80 | 90 | 100 |
| **Silver nitrate** | | | | | | | | |
| 0.9883 | .9906 | .9872 | .9872 | .9860 | .9855 | .9845 | .9842 | |
| 0.9742 | .9884 | .9823 | .9811 | .9766 | .9731 | .9707 | .9680 | |
| 0.9565 | .9519 | .9510 | .9482 | .9452 | .9435 | .9423 | .9414 | |
| 0.9340 | .9268 | .9248 | .9226 | .9197 | .9175 | .9167 | .9156 | |
| 0.9041 | .9010 | .8995 | .8962 | .8936 | .8922 | .8902 | .8880 | |
| 0.8017 | .8216 | .8291 | .8188 | .8161 | .8109 | .8055 | .8016 | |
| 0.7015 | | | | .7171 | .7134 | .7109 | .7083 | |
| 0.6234 | | | | | | .6299 | .6250 | |
| **Ammonium nitrate** | | | | | | | | |
| 0.9756 | .9901 | .9845 | .9799 | .9759 | .9717 | .9686 | .9663 | .9648 |
| 0.9467 | .9709 | .9729 | .9609 | .9486 | .9380 | .9304 | .9251 | .9199 |
| 0.9120 | .9560 | .9398 | .9160 | .9012 | .8905 | .8810 | .8739 | .8683 |
| 0.8695 | .8248 | .8187 | .8113 | .8082 | .8041 | .8009 | .7987 | .7951 |
| 0.8163 | .8059 | .7841 | .7745 | .7590 | .7528 | .7478 | .7392 | .7312 |
| 0.7478 | .6825 | .6679 | .6649 | .6581 | .6537 | .6502 | .6456 | .6404 |
| 0.6557 | | .5714 | .5629 | .5500 | .5498 | .5455 | .5432 | .5335 |
| 0.5262 | | | | .4270 | .4197 | .4120 | .4060 | .4011 |
| **Lithium nitrate** | | | | | | | | |
| 0.9719 | .9577 | .9500 | .9490 | .9485 | .9470 | .9455 | .9455 | .9452 |
| 0.9387 | .8743 | .8737 | .8716 | .8738 | .8723 | .8701 | .8675 | .8659 |
| 0.8993 | .7251 | .7269 | .7216 | .7321 | .7328 | .7351 | .7386 | .7398 |
| 0.8518 | .6027 | .5983 | .6021 | .5977 | .6007 | .6053 | .6091 | .6105 |
| 0.7928 | .4269 | .4224 | .4314 | .4326 | .4372 | .4425 | .4490 | |
| 0.7406 | .2893 | .3009 | .3078 | .3135 | .3241 | .3328 | .3410 | .3476 |
| 0.67373 | | .2013 | .2054 | .2123 | .2172 | .2245 | .2324 | .2396 |

**Calculated on the assumption of no ionization, i.e., the weight of silver nitrate is divided by the molecular weight.*

mark (2) have calculated the extent of ion-pair formation in silver nitrate solutions, but this is far from complete at concentrations for which the calculation is valid and therefore it is impossible to account for the above observation on the assumption that silver nitrate is only slightly ionized. For ammonium nitrate, however, the activity drops markedly with rising temperature and, for concentrations of 80 and 90% (mole fractions of 0.6557 and 0.5262 water) the activity is much lower than the mole fraction. For lithium nitrate, the discrepancy between activity and mole fraction is still greater. Since activity and concentration are related, it would appear that the concentration of (free) water is somewhat less in ammonium nitrate solutions than the mole fraction would imply and, in lithium nitrate solutions, very much less. This

can be accounted for on the assumption that the silver ion is not (or very feebly) hydrated, the ammonium ion a little more, and the lithium ion very strongly hydrated.

Finally, in Fig. 3, the vapor pressures of all three electrolytes, at different temperatures, have been plotted against mole fraction of solute. The figure brings out very clearly the fact that, at corresponding mole fraction and

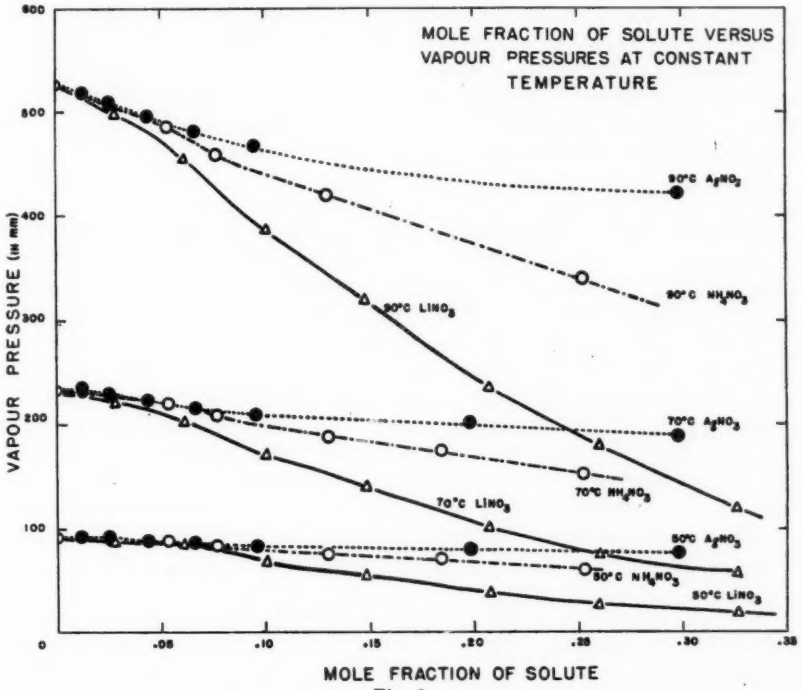


Fig. 3.

temperature, the vapor pressures of the lithium nitrate solutions are much lower than those of the silver nitrate and ammonium nitrate solutions. The most obvious explanation of this is the one given above, viz. that the lithium ion holds its water of hydration much more firmly than do the silver and ammonium ions. The high viscosity of lithium nitrate solutions points in the same direction.

## REFERENCES

1. CAMPBELL, A. N. and KARTZMARK, E. M. Can. J. Research, B, 28: 43. 1950. CAMPBELL, A. N., DEBUS, G., and KARTZMARK, E. M. Can. J. Chem. 33: 1508. 1955.
2. CAMPBELL, A. N. and KARTZMARK, E. M. Can. J. Chem. 33: 887. 1955.
3. GOFF, J. A. and GRATCH, S. Trans. Am. Soc. Heating Ventilating Engrs. 52: 95. 1946.
4. HARTUNG, E. J. Trans. Faraday Soc. 15: 150. 1920.
5. HIRSCHLER, A. E. J. Am. Chem. Soc. 58: 2472. 1936.
6. JOHNSON, E. F. and MOLSTAD, M. C. J. Phys. & Colloid Chem. 55: 257. 1951
7. OTHMER, D. F. Ind. Eng. Chem. 36: 858. 1944.
8. STOKES, R. H. and ROBINSON, R. A. J. Am. Chem. Soc. 70: 1870. 1948

# THE NUMBER OF POLYPEPTIDE CHAINS IN BOVINE PLASMA ALBUMIN[1]

By M. E. Reichmann[2] and J. Ross Colvin

## ABSTRACT

The molecular weight of performic acid oxidized bovine plasma albumin, dispersed in 0.08 *M* borate + 0.2 *M* sodium chloride buffer, pH 7.4, was estimated as 30,000 by light-scattering and sedimentation equilibrium methods, 19,000 by osmotic pressure. Sedimentation velocity analyses and electrophoresis showed that the component polypeptide chains of the material are similar in mass and charge density so the polydispersity must be attributed to labile aggregates. The results indicate that here are at least three and probably four similar polypeptide chains in the molecule of native bovine plasma albumin, held together by disulphide bonds.

## INTRODUCTION

Knowledge of the number of polypeptide chains in a protein molecule is prerequisite to an understanding of its structure but unequivocal data are available for only a few of these substances (5). Even for readily available bovine plasma albumin (B.P.A.) information is scanty. Previous estimates from end group analyses (33, 37), or from viscosity measurements after the disulphide links between chains were broken by performic acid (19), agree that the most probable figure is one. However, the first method may be misleading because of terminal substitution, and unequivocal interpretation of the second is difficult. Therefore, the number of polypeptide chains in B.P.A. has been redetermined by estimating the molecular weight of the product of performic acid oxidation (29) of B.P.A. by light-scattering, sedimentation equilibrium, and osmotic pressure techniques. The results were supplemented by sedimentation velocity and electrophoretic measurements.

## METHODS AND MATERIALS

Previous studies have shown that the disulphide links between amino acid residues in a protein may be destroyed without significant hydrolysis of the peptide bonds (3, 30). Accordingly, the component polypeptide chains were separated by a modification of Sanger's method of oxidizing disulphide bridges (30) on the assumption that any other covalent links, such as phosphate, (22) were absent.

Five grams of B.P.A. (Armour and Co., Chicago, Lot R370295B) was dissolved in 180 ml. of 90% formic acid and 30 ml. of 30% hydrogen peroxide was added. The reaction was allowed to proceed 25 min. at room temperature, then 50 ml. of 95% ethanol was added and the oxidized protein was precipitated by adding 200 ml. of 5 *M* NaCl. The addition of ethanol prevented frothing and loss of material. After the evolution of oxygen stopped, an additional 400 ml. of 5 *M* NaCl was added to ensure complete precipitation. The

[1] *Manuscript received October 25, 1955.*
*Contribution from the Division of Applied Biology, National Research Laboratories, Ottawa, Canada. Issued as N R C No. 3838 Presented at the Sixth Canadian High Polymer Forum, St Catharines Ontario, April 15, 1955*
[2] *National Research Council of Canada Postdoctorate Fellow, 1954–55*

precipitate was separated from the supernatant liquid by centrifugation, resuspended in water, and dialyzed against distilled water for 36 hr. Analysis of the outer liquid showed that less than 1.5% of the precipitated nitrogen passed through the membrane during dialysis. Similar analysis of the supernatant liquid from centrifugation showed that less than 2.0% of the total nitrogen failed to be precipitated by the salt solution. Finally, the oxidized, dialyzed B.P.A. was freeze dried. Ninety-five per cent of the initial nitrogen was recovered. The slightly yellow, fluffy powder was initially insoluble in water at neutrality to pH 9.5. However, the protein did not reprecipitate when the pH was adjusted to neutrality by dialysis. The oxidized protein was also readily soluble in formamide, and 90% formic acid. Three separate preparations, made as described above, plus one sample oxidized for 60 min. were examined during the study. No differences were observed between any of the preparations.

During the study, it was necessary to oxidize crystalline lysozyme (Armour and Co., Chicago) as above, except that the oxidized protein was precipitated by 180 ml. of saturated $Na_2SO_4$ per gram of lysozyme and dialysis times were extended in order to remove the sulphate ion completely.

An aliquot of the first preparation of oxidized B.P.A. was hydrolyzed by refluxing in 3 *N* HCl in 50% formic acid for 24 hr. and the hydrolyzate analyzed qualitatively for sulphydryl or disulphide bonds by the methods of Toennies and Kolb (35). Neither cysteine nor cystine was detectable with the nitroprusside reagent or potassium cyanide indicating complete conversion of these two amino acid residues to cysteic acid. Examination of trial preparations which were oxidized at room temperature for 5, 10, 15, and 20 min. showed that complete conversion to cysteic acid required about 20 min. under these conditions.

The free $\alpha$-amino terminal groups were determined in both native and oxidized B.P.A., using Sanger's technique (29). Only aspartic acid residues were detected in both samples. Attempts to determine the number of aspartic acid residues per protein molecule by this method were unsatisfactory owing to appreciable breakdown of the D.N.P.-aspartic acid. However, for a given set of conditions, the number of N-terminal aspartic acid residues appeared to be equal in oxidized and native B.P.A., thus strengthening the assumption that no peptide bonds were broken during the oxidation reaction.

Protein solutions were prepared by dissolving oxidized B.P.A. in formamide and dialyzing against several changes of the appropriate buffer. Protein concentrations were estimated by micro-Kjeldahl analysis (accuracy, $\pm 1\%$ of the total nitrogen present) assuming the total nitrogen content of the protein to be 16.1% (36).

A Brice and Speiser light-scattering photometer (8) was used to estimate weight average molecular weights. A blue filter (Corning No. 3389, 2.5 mm.) inserted in front of the phototube eliminated fluorescent light. All measurements were made at 4360Å. The refractive index increment, $dn/dc$, of oxidized B.P.A. was measured in a B.S. differential refractometer. The same value was obtained as that reported for native B.P.A., 0.195 (23), giving $K = 2\pi^2 n_0^2 (dn/dc)^2 / N\lambda^4$ the value of $6.2 \times 10^{-7}$ ($n_0$ = refractive index of solvent, $N$ = Avogadro's number, $\lambda$ = wavelength of light used). All measurements

were made in the standard 30 mm. square cells. Other details of the technique were as described previously (25).

Sedimentation coefficients were estimated from observations in a Spinco ultracentrifuge at 59,780 r.p.m. A one degree adjustment for adiabatic cooling of the rotor (6, 38) was included in the standard corrections of the coefficients to water at 20° (32). Three determinations of the sedimentation coefficient $S_{20}$, of native B.P.A. in 0.05 *M* phosphate buffer, 0.2 *M* NaCl, pH 6.6, at concentrations 0.33%, 0.50%, and 1.0% gave the values 4.10, 4.08, and $3.91\times10^{-13}$ respectively. These values and their extrapolation to $4.3\times10^{-13}$ at zero concentration are in agreement with previous determinations (21). However, repeated similar determinations of the coefficient of native B.P.A. in 0.08 *M* borate, 0.2 *M* NaCl, yielded a value of $S^{\circ}_{20}$ of $4.6\times10^{-13}$. The sedimentation coefficients reported for oxidized B.P.A. in 0.08 *M* borate +0.2 *M* NaCl, pH 7.4, may therefore be 10% too high. Cause of the discrepancy is unknown. In spite of this qualification, the borate buffer was used because of the difficulties of cleaning phosphate or more alkaline buffers for light-scattering.

Archibald (4) has shown that in sedimentation equilibrium experiments the weight average molecular weight may be estimated from the polymer concentrations near the ends of the cell, prior to complete attainment of equilibrium. The method has been applied successfully to bacitracin (24), digitonin (9), and lysozyme (31). In addition, the procedure gives information on polydispersity of the sample since, for heterogeneous samples, the molecular weight at the base of the cell will be higher than at the meniscus and the difference will increase with time. This technique was therefore applied to oxidized B.P.A. The ultracentrifuge and cells were the same as in the sedimentation velocity experiments. Speed of the rotor was 5300 r.p.m. Photographs were taken every four hours in the interval from 12 to 40 hr. From the sedimentation patterns, a function $\delta = (1/rc)\ (dc/dr)$ was calculated (9), ($r$ is the distance of a given point in the cell from the center of rotation, $c$ is the concentration in gm./ml. at that point, and $dc/dr$ is the concentration gradient). The weight average molecular weights at the meniscus and base of the cell were estimated from the extrapolated values of $\delta$ by the relation $\delta = M(1-V\rho)/\omega^2RT$. (Here, $V$ is the partial specific volume of the protein, $\rho$ is the density of the solution, $\omega$ is the angular velocity, $R$ is the gas constant, $T$ is the absolute temperature, and $M$ is the molecular weight.) Partial specific volume of oxidized B.P.A. was assumed to be the same as that of the native protein, 0.734 (11).

Osmotic pressures were measured at equilibrium using osmometers previously described (13). In some preliminary experiments (26), Visking dialysis bags were used but later proved unsatisfactory because of flexibility. Parloidin (Mallinckrodt Chem. Works) membranes prepared by Adair's method (1) were substituted. Pressures were determined at 7.5±0.1°C. after 16 hr. of equilibration and confirmed after an additional 12 hr. Equilibrium was reached from both sides and the osmotic pressures thus obtained agreed within experimental error

Electrophoretic examinations were carried out at 0.15°C. in a Tiselius schlieren apparatus as modified by Longsworth (20). Dialysis for one day against buffer solutions prepared according to Clark's method (10) preceded examination. The pH of each solution was checked by a Beckman Model G pH meter calibrated by commercial standards.

## RESULTS

Results typical of the light-scattering data for oxidized B.P.A. in concentrated salt solutions and in water at pH 7.4 are shown in Fig. 1. $Kc/R_{90}$ is plotted as a function of protein concentration where $R_{90}$ is the reduced intensity of

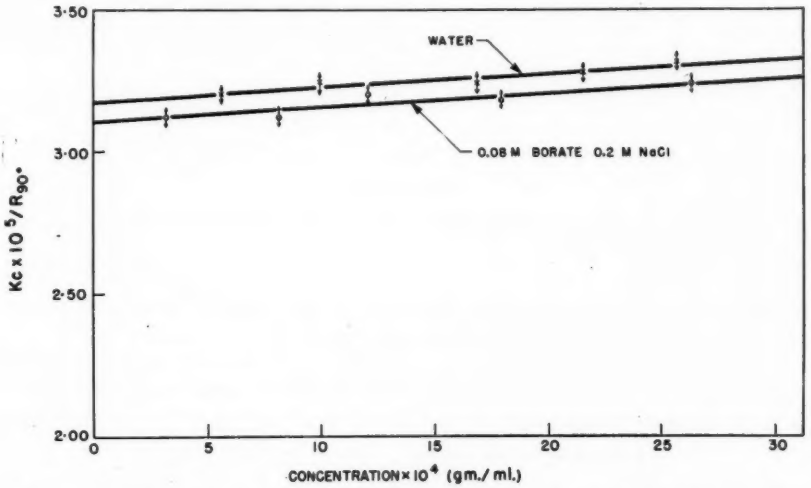


FIG. 1. Light-scattering of oxidized B.P.A. in 0.08 *M* borate + 0.2 *M* sodium chloride, and in water, both at pH 7.4.

the light scattered at 90°, $K$ is as defined previously, and $c$ is the concentration of the protein. The extrapolated value of $Kc/R_{90}$ at zero protein concentration is an estimate of the reciprocal of the weight average molecular weight while the slope of the line is proportional to the second virial coefficient (14). The slope is therefore a measure of the net particle interactions.

Two preparations oxidized for 20 min. and one oxidized for 60 min. were studied by light-scattering. All three oxidized samples had identical weight average molecular weights, 32,000±2000. Under the same conditions native B.P.A. had a molecular weight of 77,000 in good agreement with previous results (16).

Results typical of osmotic pressure experiments on the three samples are shown in Fig. 2. Here $P/cRT$ is plotted as a function of concentration; the osmotic pressure, $P$, being expressed in dyne/cm.$^2$. The extrapolated value of $P/cRT$ at zero protein concentration was $5.2\pm0.4\times10^{-5}$ which corresponds to a number average molecular weight of 19,000±1500. Under the same

conditions, native B.P.A. had a number average molecular weight of 67,000 in agreement with previous results (18). The difference between this value and that for the weight average molecular weight 77,000 has been attributed to a small proportion of high molecular weight material present in some

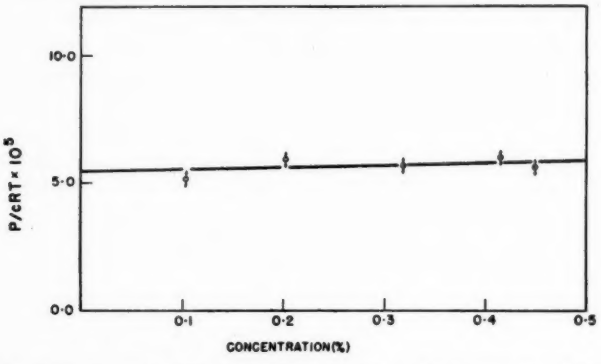


FIG. 2. Osmotic pressure of oxidized B.P.A. as a function of concentration, in 0.08 *M* borate buffer + 0.2 *M* NaCl, pH 7.4.

samples of native B.P.A. (16). Presence of this fraction in our sample was confirmed by sedimentation velocity experiments.

A single peak was observed in sedimentation velocity experiments with oxidized B.P.A. (Fig. 3), which sedimented with a mean coefficient, $S^{\circ}_{20}$, of $1.49 \pm 0.05 \times 10^{-13}$ in 0.08 *M* borate, 0.2 *M* NaCl, pH 7.4. The sedimentation

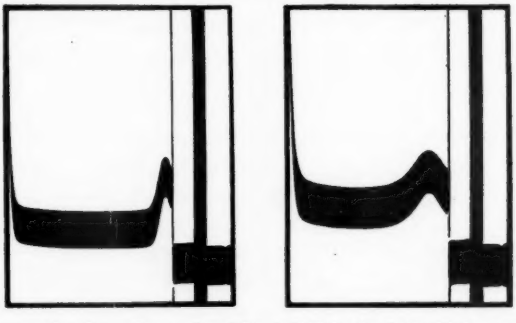

FIG. 3. Sedimentation boundary of oxidized B.P.A. in 0.08 *M* borate + 0.2 *M* NaC pH 7.4.

coefficient was independent of protein concentration over the range 0.3% to 1.0%. The threefold reduction in the value of the coefficient compared with native B.P.A. (21) suggested that oxidation separated the protein into fragments. An estimate of the distribution of the sedimentation coefficients of such fragments of oxidized B.P.A., made by the method of Williams *et al.* (39), showed only a single peak about the mean value. The peak was not

sharp but the significance which may be attributed to this is doubtful because of inherent uncertainties of extrapolation in the method. A justifiable conclusion is that the sedimentation differences among the molecules are small or else the various types are in rapid equilibrium (2).

Fig. 4 summarizes the data from an experiment using Archibald's approach to sedimentation equilibrium at pH 7.4. The function $(1/rc)(dc/dr)$ is plotted versus $r$, the distance from the center of rotation, and extrapolated

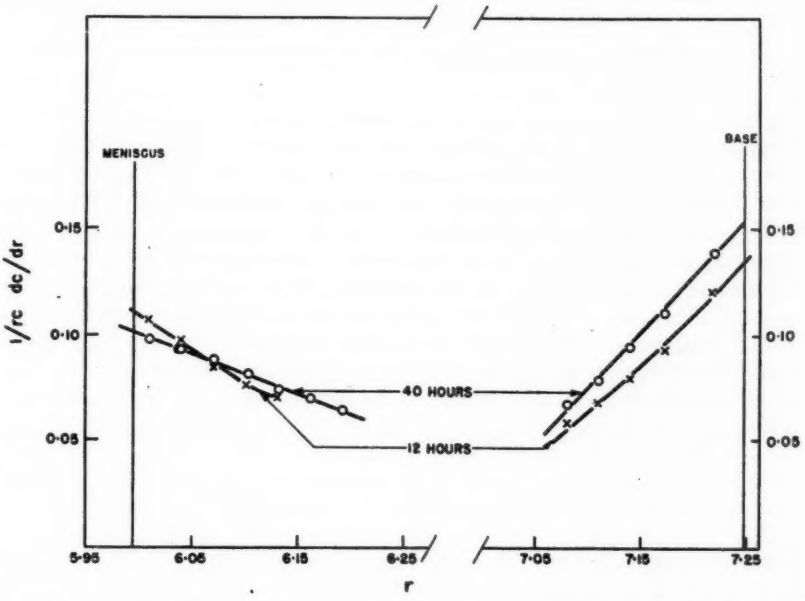


FIG. 4. Archibald's approach to sedimentation equilibrium with oxidized B.P.A. in 0.08 *M* borate + 0.2 *M* NaCl, pH 7.4.

to the meniscus and base of the cell. Twelve hours after the beginning of the run the molecular weight at the meniscus was 33,000 and at the base, 40,000. After 40 hr. of sedimentation, the molecular weight decreased to 30,000 at the meniscus and increased to 45,000 at the base. Similar results were obtained at pH 9.0 in aqueous ammonia. These observations are in agreement with those from light-scattering and are consistent with the sedimentation velocity experiments.

Oxidized B.P.A. was examined electrophoretically over the pH range from 4.7 to 7.4 in 0.05 *M* acetate, phosphate, or borate buffers. Varying concentrations of sodium chloride were added to adjust the field strength. A typical pattern for the material under all conditions is shown in Fig. 5. A single symmetrical peak was observed, suggesting that the charge densities of all the components of oxidized B.P.A. are similar.

Previous studies of the structure of insulin (30) and of ribonuclease (3) have shown that performic acid under the conditions employed does not hydrolyze peptide bonds appreciably. However these two proteins do not contain the labile tryptophane residue (34) whereas two such residues are found per B.P.A. molecule (36). Performic acid oxidation was therefore

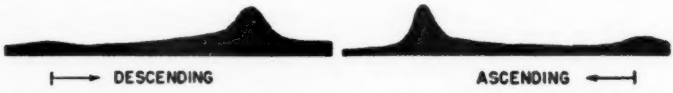


FIG. 5. Ascending and descending electrophoretic boundaries of oxidized B.P.A. in 0.05 *M* acetate buffer, pH 5.5. Field strength 6.3 volts/cm. Time 116 min.

applied to lysozyme (8 tryptophane residues per 15,000 gm. (36)), to see if the single chain of the molecule (17) was broken by the procedure. The oxidized protein was insoluble in water from pH 2.0 to 8.0. Light-scattering measurements of native and oxidized lysozyme were therefore made in 90% formic acid. The molecular weight of the oxidized protein was about five times *higher* than that of the native protein assuming the same values for the refractive index increment in both materials. The data from two experiments using Archibald's approach to sedimentation equilibrium on oxidized and native lysozyme, dissolved in formamide, are summarized in Fig. 6. After 45 hr. at 12,000 r.p.m. the function $\delta$ at the meniscus is about 1.7 times higher for the oxidized protein compared to the native. Consequently, assuming the

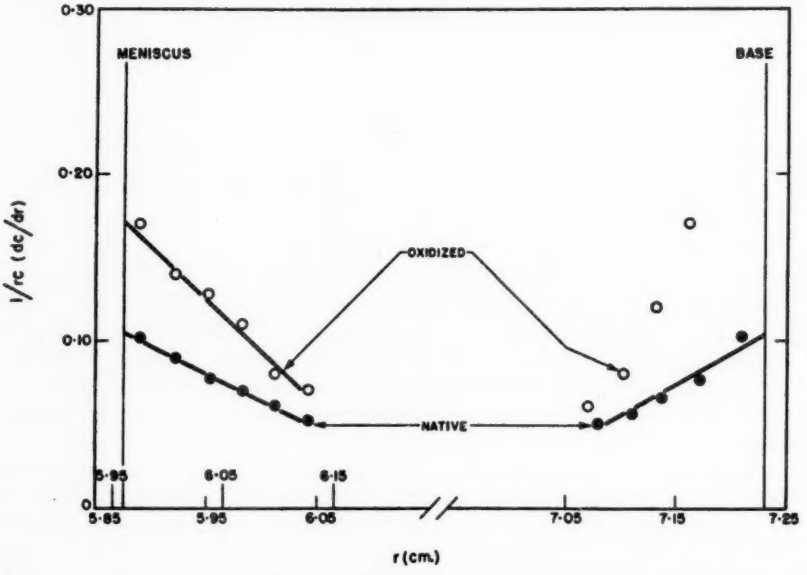


FIG. 6. Archibald's approach to sedimentation equilibrium with oxidized and native lysozyme in formamide.

same partial specific volume for both proteins, the data indicate a molecular weight about 1.7 times that of the native for the oxidized protein. The values of $\delta$ at the base of the cell indicate monodispersity of the native sample and extensive aggregation in the oxidized sample. Similar results were obtained with globin (27) which contains 5 tryptophane residues per 68,000 gm. (36) but the extent of aggregation in the oxidized sample was much smaller than in lysozyme. This evidence together with the absence of additional $\alpha$-amino terminal groups in oxidized B.P.A. strongly indicates that no scission of the polypeptide chain(s) occurred.

## DISCUSSION

We tentatively assume, on the basis of the foregoing evidence, that no splitting of the polypeptide chains takes place during oxidation. Then the lower molecular weight of oxidized B.P.A., compared to that for the native albumin, indicates that previous suggestions that this protein consists of a single chain (19, 37) must be reconsidered. The earlier conclusions were based on either an assumption of fully accessible, completely unsubstituted terminal groups or the assumption of a Staudinger viscosity coefficient unmodified by the oxidation procedure. In the light of later work (7, 12, 28), it would not be surprising if either or both assumptions were invalid.

The electrophoretic patterns over a wide range of pH show that the polypeptide chains of oxidized B.P.A. are similar in charge density and therefore probably in amino acid composition. In addition, the single peak in the sedimentation patterns as well as the single maximum in the distribution function of sedimentation coefficients of oxidized B.P.A. indicates that the chains of native B.P.A. are approximately equal in weight. If the chains are similar in size, the discrepancy between the weight average and number average molecular weights of oxidized B.P.A. may be explained by interactions between the chains to produce a small proportion of aggregates of varying degrees of stability. Attractive forces, favoring formation of such aggregates, are shown by the difficulty of dissolving the material in water and by the zero value for the second virial coefficient in light-scattering experiments in water at pH 7.4, in spite of the high negative charge carried by the chains (15). Most of the aggregates are in rapid equilibrium with the smaller subunits, as shown by the single peak in sedimentation velocity experiments, and cause only a spreading of the boundary (2). However, the difference between the molecular weights at the meniscus and the base of the cell in the approach to sedimentation equilibrium shows that dissociation of a fraction of these aggregates is very slow, probably because of mechanical entanglement of the random coils. Thus the molecular weight at the meniscus in sedimentation equilibrium deviates only slightly from the light-scattering value, while at the base the weight average molecular weight increases with time.

Assuming therefore a molecular weight of 66,000 for native B.P.A. (15, 18) which contains polypeptide chains of equal size, the observed number average molecular weight shows that there are three or four such chains per molecule. However, four chains is the more probable figure because aggregation of

components would tend to raise the estimated number average molecular weight of the oxidized material. A larger number of chains is excluded because no diffusion of protein through the osmometer membranes could be detected after seven days, although ribonuclease (mol. wt. 13,000) (32) passed through fairly rapidly under the same conditions.

The chains are presumably held together by some of the 14 disulphide bridges in B.P.A. (36) but no information is yet available on their number and location. Furthermore, because Van Vunakis and Brand found only one N-terminal amino acid residue per molecule (37), the results indicate that the other three chain ends are either substituted or inaccessible to reaction with dinitrofluorobenzene under the conditions employed.

The foregoing conclusions rest on the assumption that no polypeptide bonds were broken by performic acid oxidation. Presently available evidence for this assumption is substantial but does not exclude the possibility that tryptophane residues in a polypeptide chain may be particularly labile when linked to specific amino acids. A general investigation of the possibility is desirable.

## ACKNOWLEDGMENTS

The authors should like to thank their colleagues Dr. P. A. Charlwood and D. B. Smith for discussions, advice, and criticism at all stages of the study. They are also particularly indebted to Prof. J. T. Edsall of Harvard University, and Dr. W. H. Cook, Director of the Division of Applied Biology, for stimulating advice and criticism of the methods and manuscript.

The technical assistance of Mr. D. Muirhead and Mr. L. Sowden is gratefully acknowledged.

## REFERENCES

1. ADAIR, G. S. Proc. Roy. Soc. (London), A, 108: 627. 1925.
2. ALEXANDER, A. E. and JOHNSON, P. Colloid science. Vol. I. The Clarendon Press, Oxford. 1949. p. 279.
3. ANFINSEN, C. B., REDFIELD, R. R., CHOATE, W. L., PAGE, J., and CARROLL, W. R. J. Biol. Chem. 207: 201. 1954.
4. ARCHIBALD, W. J. J. Phys. & Colloid Chem. 51: 1204. 1947.
5. BAILEY, K. Mededeel. Vlaam. Chem. Ver. 16: 245. 1954.
6. BIANCHERIA, A. and KEGELES, G. J. Am. Chem. Soc. 76: 3737. 1954.
7. BRICAS, E. and FROMAGEOT, C. Advances in Protein Chem. 8: 1. 1953.
8. BRICE, B. A., HALWER, M., and SPEISER, R. J. Opt. Soc. Amer. 40: 768. 1950.
9. BROWN, R. A., KRITCHEVSKY, D., and DAVIES, M. J. Am. Chem. Soc. 76: 3342. 1954.
10. CLARK, W. M. The determination of hydrogen ions. 3rd ed. The Williams & Wilkins Company, Baltimore, Md. 1928.
11. DAYHOFF, M. O., PERLMANN, G. E., and MACINNES, D. A. J. Am. Chem. Soc. 74: 2515. 1952.
12. DEBYE, P. and BUECHE, A. M. J. Chem. Phys. 16: 573. 1948.
13. DONNAN, F. G. and ROSE, R. C. Can. J. Research, B, 28: 105. 1950.
14. DOTY, P. and EDSALL, J. T. Advances in Protein Chem. 6: 35. 1951.
15. EDSALL, J. T. *In* The proteins. Vol. 1. Pt. B. *Edited by* H. Neurath and K. Bailey. Academic Press, Inc., New York. 1953.
16. EDSALL, J. T., EDELHOCH, H., LONTIE, R., and MORRISON, P. R. J. Am. Chem. Soc. 72: 4641. 1950.
17. FRAENKEL-CONRAT, H., MOHAMMAD, A., DUCAY, E. D., and MECHAM, D. K. J. Am. Chem. Soc. 73: 625. 1951.
18. GUTFREUND, H. Trans. Faraday Soc. 50: 628. 1954.
19. HAUROWITZ, F. Experientia, 5: 347. 1949.
20. LONGSWORTH, L. G. Ind. Eng. Chem. Anal. Ed. 18: 219. 1946.
21. MILLER, G. L. and GOLDER, R. H. Arch. Biochem. and Biophys. 36: 249. 1952.

22. PERLMANN, G. E. Nature, 174: 273. 1954.
23. PERLMANN, G. E. and LONGSWORTH, L. G. J. Am. Chem. Soc. 70: 2719. 1948.
24. PORATH, J. Acta Chem. Scand. 6: 1237. 1952.
25. REICHMANN, M. E. and CHARLWOOD, P. A. Can. J. Chem. 32: 1092. 1954.
26. REICHMANN, M. E. and COLVIN, J. R. Can. J. Chem. 33: 163. 1955.
27. REICHMANN, M. E. and COLVIN, J. R. Can. J. Chem. In press.
28. RISEMAN, J. and KIRKWOOD, J. G. J. Chem. Phys. 18: 512. 1950.
29. SANGER, F. Biochem. J. (London), 39: 507. 1945.
30. SANGER, F. Biochem. J. (London), 44: 126. 1949.
31. SMITH, D. B. Private communication.
32. SVEDBERG, T. and PEDERSEN, K. The ultracentrifuge. Oxford University Press, London. 1940.
33. THOMPSON, E. O. P. J. Biol. Chem. 208: 565. 1954.
34. TOENNIES, G. and HOMILLER, R. P. J. Am. Chem. Soc. 64: 3054. 1942.
35. TOENNIES, G. and KOLB, J. J. Anal. Chem. 23: 823. 1951.
36. TRISTRAM, G. R. *In* The proteins. Vol. 1. Pt. A. *Edited by* H. Neurath and K. Bailey. Academic Press, Inc., New York. 1953.
37. VAN VUNAKIS, H. and BRAND, E. Abstr. 119th Meeting Am. Chem. Soc. p. 28*c*. April, 1951.
38. WAUGH, D. F. and YPHANTIS, D. A. Rev. Sci. Instr. 23: 609. 1952.
39. WILLIAMS, J. W., BALDWIN, R. L., SAUNDERS, W. M., and SQUIRE, P. G. J. Am. Chem. Soc. 74: 1542. 1952.

# THE VIBRATIONAL SPECTRA OF THE FORMATE, ACETATE, AND OXALATE IONS[1]

By K. Ito[2] and H. J. Bernstein


## ABSTRACT

The infrared spectra of the formate, acetate, and oxalate ions have been obtained for both the solid and aqueous solution. The Raman spectra of these ions with depolarization ratios have been obtained in aqueous solution. Vibrational assignments have been made which differ slightly for the acetate ion and more markedly for the oxalate ion from earlier work. The depolarization ratios confirm Fonteyne's assignment for the formate ion.


## INTRODUCTION

The Raman spectra of aqueous solutions of formate (4, 7), acetate (16), and oxalate (5, 8, 11) ions, and the infrared spectra of solid metal-formate (3), -acetate (10), and -oxalate (2) have been studied in the past but no reliable assignment has been made for the oxalate ion and in some respects the rather complete assignments for $CH_3COONa$ and $CD_3COONa$ in the solid state (10) and that for the formate ion merit reinvestigation.

Infrared spectra of solid sodium formate, light and heavy sodium acetate, and sodium oxalate, and their saturated solutions in $H_2O$ and $D_2O$ were obtained from 3–35$\mu$. The Raman spectra of the aqueous solutions with depolarization ratios were also obtained. From these more complete vibrational data and comparison of spectra with the isoelectronic molecules nitromethane and nitrogen tetroxide vibrational assignments have been made for acetate and oxalate ions. The depolarization ratios for the Raman bands of the formate ion confirmed the assignment of Fonteyne (7).

## EXPERIMENTAL

The infrared spectra were obtained with a Perkin-Elmer Model 12C double pass spectrometer with CsBr, NaCl, and LiF optics. The Raman spectra were photoelectrically recorded on a White Raman spectrometer (18) and depolarization ratios measured by comparing Raman spectra obtained with polaroid film wrapped round the sample tube first with its axis in a direction parallel to the sample tube and then perpendicular to it (6). These ratios were corrected for convergence error in a manner previously described (1, 14).

The reported infrared spectra of the aqueous solutions are not as complete as those for the solids because of the strong $H_2O$ and $D_2O$ absorption. The solid infrared spectra were taken of films deposited from $H_2O$ or $CH_3OH$ on AgCl plates or polystyrene film. Raman spectra were obtained for the saturated aqueous solutions only and the depolarization ratios of all fundamentals measured.

[1]*Manuscript received August 23, 1955.*
*Contribution from the Division of Pure Chemistry, National Research Council, Ottawa, Canada. Issued as N.R.C. No. 3844. Presented at the Symposium on Molecular Structure, Columbus, Ohio, June 1955.*
[2]*National Research Laboratories Postdoctorate Research Fellow 1954–55.*

We are indebted to Dr. L. C. Leitch for the sample of $CD_3COONa$. All other compounds were c.p. grade.

*Acetate Ion*

The Raman spectrum of a saturated solution of $CH_3COONa$ in $H_2O$ is shown in Fig. 1 and the Raman data for solutions of $CH_3COONa$ and $CD_3COONa$ given in Table I.

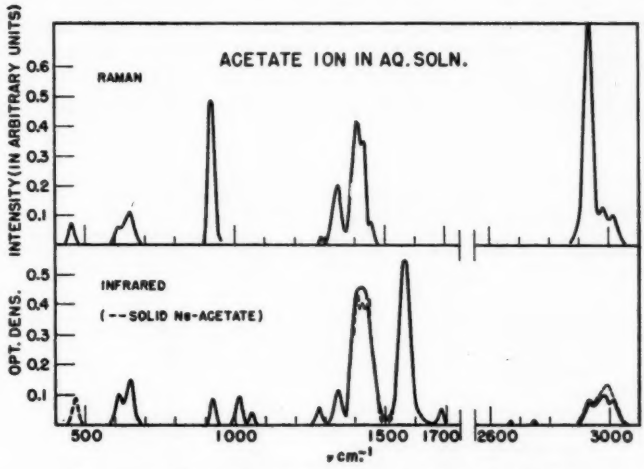


FIG. 1. The Raman and infrared spectra of the acetate ion.

TABLE I

RAMAN SPECTRA OF $CH_3COONa$ AND $CD_3COONa$ IN $H_2O$

| $CH_3COO^-$ | | $CD_3COO^-$ | |
|---|---|---|---|
| $\nu$(cm.$^{-1}$) | $\rho$ | $\nu$(cm.$^{-1}$)[a] | $\rho$ |
| 3013 | $0.8_0$ (D) | 2264 (3.2) | $0.7_4$ (D) |
| 2980 | $0.8_6$ (D) | 2231 (4.2) | $0.7_4$ (D) |
| 2933 | $0.1_2$ (P) | 2185[b] (6.4) | $0.1_8$ (P) |
| 1456 | D | 2111 (10.0) | 0.08 (P) |
| 1429 | D (?) | 2068[c] (2.3) | 0.08 (P) |
| 1414 | $0.4_9$ (P) | 1545 (0.61) | $0.8_9$ (D) |
| 1344 | $0.5_8$ (P) | 1457[d] (0.50) | $0.5_7$ (P) |
| 1289 | — | 1432[e] (1.5) | $0.8_6$ (D) |
| 927 | $0.2_0$ (P) | 1405 (8.1) | $0.3_8$ (P) |
| 649 | 0.5 (P) | 1085 (3.6) | $0.1_7$ (P) |
| 621 | $0.8_9$ (D) | 1049 (0.98) | $0.8_0$ (D) |
| 471 | D | 1031 (8.6) | $0.7_1$ (D) |
| | | 883 (4.8) | $0.1_3$ (P) |
| | | 832 (0.61) | $0.6_8$ (D?) |
| | | 619 (2.6) | $0.3_8$ (P) |
| | | 526 (0.68) | $0.7_1$ (D) |
| | | 419 (0.61) | $0.8_9$ (D) |

[a] *Values in brackets are the relative intensities referred to the 2111 cm.$^{-1}$ band.*

[b,c,d,e] *Combination bands explained as* $2\nu_2 = 2170$ $(A_1)$, $2\nu_{13} = 2062$ $(A_1)$, $\nu_{14}+\nu_{15} = 1466$ $(A_1)$, *or* $\nu_9+\nu_{11} = 1466$ $(A_1)$ *and* $\nu_5+\nu_{10} = 1461$ $(B_1)$, *respectively (see Table II).*

The infrared spectrum of the saturated solution of $CH_3COONa$ in $H_2O$ and $D_2O$ is shown also in Fig. 1. Only the part of the spectrum of the solid that differs sensibly from that of the solution is shown in Fig. 1. The band at 480 cm.$^{-1}$ in the spectrum of the solid is not found in solution because of the strong water absorption in this region. The spectrum of the solid agrees with that found by Jones and McLaren (10) and the band positions have been used in Table II in the column giving their assignment. The infrared spectrum of solid $CD_3COONa$ is the same as that previously reported (10), and bands were observed at 2267 (m), 2288 (w), 1546 (s), 1408 (s), 1084 (w), 1043 (w), 940 (m), 883 (w), and 833 (m) cm.$^{-1}$ in the infrared spectrum of $CD_3COONa$ in $H_2O$. In Table II the assignment for $CH_3COO^-$ (solid) by Jones and McLaren

TABLE II

VIBRATIONAL ASSIGNMENT OF THE ACETATE ION

| $C_{2v}$ | $\left(\begin{matrix}O\\ \diagdown\\ \quad C—CH_3\\ \diagup\\ O\end{matrix}\right)^-$ | $CH_3COO^-$ (solid)[a] Jones, McLaren | $CH_3COO^-$ (solution) This work | $CH_3NO_2$ (gas) Wells, Wilson | $CD_3COO^-$ (solution) This work | Teller–Redlich product rule ratios | |
|---|---|---|---|---|---|---|---|
| | | | | | | Obs. | Theor. |
| $a_1$ $\nu_1$ | C—H stretching | 2936 | 2935 (P) | 2965 | 2111 (P) | | |
| $\nu_2$ | $CH_3$ deformation | 1430 | 1344 (P) | 1413 | 1085 (P) | | |
| $\nu_3$ | C—O stretching | 1414 | 1413 (P) | 1384 | 1406 (P) | 1.91 | 1.95 |
| $\nu_4$ | C—C stretching | 924 | 926 (P) | 921 | 883 (P) | | |
| $\nu_5$ | COO deformation | 646 | 650 (P) | 647 | 619 (P) | | |
| $a_2$ $\nu_6$ | Torsion | — | — | — | — | | |
| $b_1$ $\nu_7$ | C—H stretching | 2989 | 3010 (D) or 2981 (D) | 3048 | 2264 (D) or 2231 (D) | | |
| $\nu_8$ | C—O stretching | 1578 | 1556 | 1582 | 1545 (D) | | |
| $\nu_9$ | $CH_3$ deformation | 1443 | 1429 (D) | 1449 | 1047 (D) | 2.53 | 2.58 |
| $\nu_{10}$ | $CH_3$ rocking | 1009 | 1020 | 1097 | 832 (D?) | | |
| $\nu_{11}$ | COO rocking (in-plane) | 460 | 471 (D) | 476 | 419 (D) | | |
| $b_2$ $\nu_{12}$ | C—H stretching | 2989 | 2981 (D) or 3010 (D) | 3048 | 2231 (D) or 2264 (D) | | |
| $\nu_{13}$ | $CH_3$ deformation | 1498 | 1456 (D) | 1488 | 1031 (D) | 2.49 | 2.53 |
| $\nu_{14}$ | $CH_3$ rocking | 1042 | 1052 | 1153 | 940 | | |
| $\nu_{15}$ | COO rocking (out-of-plane) | 615 | 621 (D) | 599 | 526 (D) | | |

[a] *In this assignment the frequencies measured here have been used.*

(but using our measured frequencies), that for $CH_3NO_2$ by Wells and Wilson (17), and the present assignments for $CH_3COO^-$ and $CD_3COO^-$ are given. The assignments are based on $C_{2v}$ point group symmetry (17). The new information provided by the above spectra and comparison with the fundamentals of the isoelectronic $CH_3NO_2$ molecule have been the basis for the present assignment and as can be seen from Table II it differs from that of Jones and McLaren for $CH_3COO^-$ in several respects. In particular, $\nu_2$, the fairly strong polarized Raman band at 1344 cm.$^{-1}$, is taken as a fundamental here instead of the rather weak infrared band at 1498 cm.$^{-1}$ which is not observed in the Raman spectrum. This band at 1498 cm.$^{-1}$ is then to be interpreted as a difference tone (see Table III). The present assignments for $\nu_2$ and $\nu_3$ were confirmed from the depolarization ratios and comparison of the Raman spectra of $CH_3COO^-$ and $CD_3COO^-$. Other changes are to assign the band at 1429 cm.$^{-1}$, which is found to be depolarized, as $\nu_9$ and the band at 1443 cm.$^{-1}$ in the infrared spectrum of the solid as $\nu_{13}$. One other small

modification is introduced by the fact that three bands in the CH stretching region are observed in the infrared and Raman spectra of the solution whereas there are only two in the infrared spectrum of the solid (see Fig. 1). Assuming all three to be fundamentals, $\nu_1$ is readily assigned because of its depolarization ratio but a choice is left for $\nu_7$ and $\nu_{12}$ as indicated in Table II.

Of the two COO rocking modes $\nu_{11}$ and $\nu_{15}$ the higher was taken as the out-of-plane mode $\nu_{15}$, since it was expected that the $\pi$ electron cloud in the $COO^-$ group accumulating in the direction perpendicular to the $COO^-$ plane gives rise to more repulsion in the potential energy function for the out-of-plane mode than for the in-plane mode. The moment of inertia argument used by Wells and Wilson for the corresponding assignment in $CH_3NO_2$ leads to this result also (which was recognized also by Jones and McLaren in their assignment).

Our assignment for $CD_3COO^-$ is essentially the same as that reported by Jones and McLaren except for the CD stretching modes. From Raman spectrum and depolarization ratios (see Table I) the band at 2231 cm.$^{-1}$

TABLE III

COMBINATION AND DIFFERENCE FREQUENCIES FOR INFRARED BANDS OF $CH_3COO^-$

| Aqueous solution | | Solid (Na salt) | | Assignment | Irred. representation |
|---|---|---|---|---|---|
| Obs. | Calc. | Obs. | Calc. | | |
| 2746 | 2757 | 2740 | 2752 | $\nu_2+\nu_3$ | $A_1$ |
| 2668 | 2688 | 2653 | 2676 | $2\times\nu_2$ | $A_1$ |
| 2583 | 2576 | 2605 | 2587 | $\nu_8+\nu_{10}$ | $A_1$ |
| | | 2557 | 2550 | $\nu_7-\nu_{11}$ | $A_1$ |
| 2486 | 2482 | 2495 | 2499 | $\nu_8+\nu_4$ | $B_1$ |
| 2416 | 2433 | 2424 | 2423 | $\nu_3+\nu_{10}$ | $B_1$ |
| 1911 | 1915 | | 1927 | $\nu_1-\nu_{10}$ | $B_1$ |
| 1693 | 1702 | | 1688 | $\nu_5+\nu_{14}$ | $B_2$ |
| | | 1498 | 1506 | $\nu_1-\nu_2$ | $A_1$ |
| | | | 1493 | $\nu_1-\nu_9$ | $B_1$ |
| 1289* | 1300 | 1300 | 1292 | $2\times\nu_5$ | $A_1$ |
| 1277 | 1271 | 1254 | 1261 | $\nu_5+\nu_{15}$ | $B_2$ |

*Observed in the Raman spectrum.*

assigned by the above authors to $\nu_1$ must be either $\nu_7$ or $\nu_{12}$. In Table III the combination bands for $CH_3COO^-$ observed in the infrared spectrum are given with plausible assignments.

The present assignments for light and heavy acetate ion (solution) are consistent with the product rule as shown in the last column of Table II. The theoretical ratios are taken from the paper of Jones and McLaren (10) which were calculated using dimensions of the solid ion. Since these ratios are very insensitive to small changes in molecular dimensions they will be very nearly the same for the solid ion and the ion in solution.

*Oxalate Ion*

The Raman spectrum of a saturated solution of potassium oxalate in $H_2O$ is shown in Fig. 2 and the Raman data given in Table IV. The infrared spectrum of saturated solutions of potassium and cesium oxalate in $H_2O$

and $D_2O$ is shown also in Fig. 2. The frequencies of the fundamentals are given in Table IV and those of the combination bands in Table V. The infrared spectrum of solid sodium oxalate is listed in Table IV (fundamentals) and

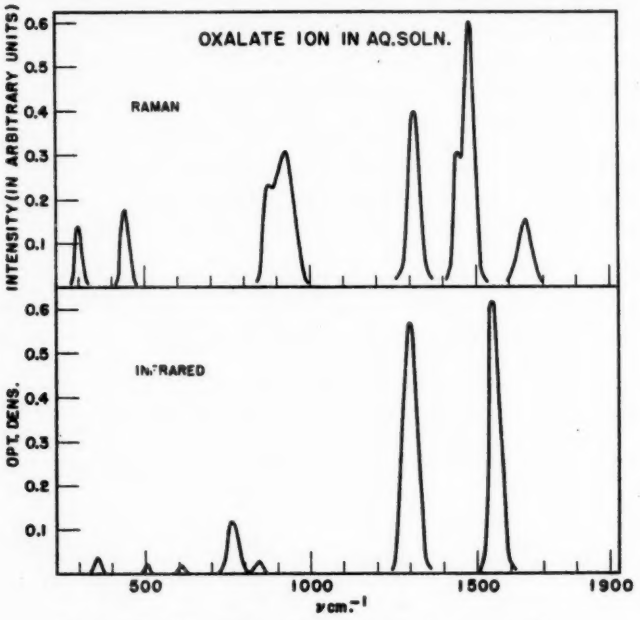


FIG. 2. The Raman and infrared spectra of the oxalate ion.

Table V (combination tones). The principal difference between the solid and solution infrared spectra is that the band at 507 cm.$^{-1}$ in the solid is by

TABLE IV

VIBRATIONAL ASSIGNMENT OF THE OXALATE ION

| Irred. rep. ($D_{2h}$) | $\cdot\left(\begin{smallmatrix} O & & O \\ & C-C & \\ O & & O \end{smallmatrix}\right)^{--}$ | $C_2O_4^{--}$ Solid Na salt | Aq. soln. | Dep. ratio | $N_2O_4$ gas | Previous assignment for $C_2O_4^{--}$ by Lecomte *et al.* | |
|---|---|---|---|---|---|---|---|
| $a_g$ | $\nu_1$ C—O stretching | | 1488 | 0.3$_s$ (P) | 1360 | ~1480 | Raman active |
| | $\nu_4$ COO deformation | | 904 | 0.1$^a$ (P) | 813 | ~ 900 | |
| | $\nu_8$ C—C stretching | | 445 | 0.5$^a$ (P) | 283 | ~ 320 | |
| $b_{1g}$ | $\nu_5$ C—O stretching | | 1660 | 0.8$_s^b$ (D) | 1724 | ~1640 | |
| | $\nu_9$ COO rocking (in-plane) | | 300 | 0.8$_s$ (D) | 500 | 525–575 | |
| $b_{2g}$ | $\nu_6$ COO rocking (out-of-plane) | | 1305 | 0.8$_s$ (D) | (1480) | ~ 450 | |
| $a_u$ | $\nu_7$ Torsion | | — | | — | | |
| $b_{1u}$ | $\nu_3$ COO rocking (out-of-plane) | 507 | 500 | | (680) | 665 | Infrared active |
| $b_{2u}$ | $\nu_2$ C—O stretching | 1640$^a$ 1405 | 1555 | | 1749 | 1500–1600 | |
| | $\nu_{10}$ COO rocking (in-plane) | | (160) | | 380 | ~ 370 | |
| $b_{3u}$ | $\nu_{11}$ C—O stretching | 1319 | 1300 | | 1265 | 1200–1300 | |
| | $\nu_{12}$ COO deformation | 766 | 766 | | 752 | 750–800 | |

$^a$*Split by the Fermi resonance into two bands with equal intensity.*

far the strongest band in this region, whereas in solution it is weak (at 500 cm.$^{-1}$) and comparable in intensity to the bands at 361 and 605 cm.$^{-1}$. Because of its strong absorption in the solid this band was chosen as a fundamental. Another feature in the infrared spectrum of the solid is the doublet

TABLE V

COMBINATION AND DIFFERENCE FREQUENCIES FOR THE INFRARED BANDS OF $C_2O_4^{--}$

| Aqueous solution | | Solid Na salt, | Assignment | Irred. |
|---|---|---|---|---|
| Obs. | Calc. | obs. | | rep. |
| | | 3134 | | |
| | | 3054 | | |
| | 2960 | 2935 | $\nu_4+\nu_{11}$ | $B_{2u}$ |
| 2860 | | 2862 | ? | |
| 2782 | 2788 | 2767 | $\nu_1+\nu_{11}$ | $B_{3u}$ |
| 2604 | 2605 | | $\nu_6+\nu_{11}$ | $B_{1u}$ |
| 2474 | | 2479 | ? | |
| | | 1885 | ? | |
| 1452* | 1460 | | $\nu_{10}+\nu_{11}$ | $B_{1g}$ |
| | 1255 | 1249 | $\nu_9-\nu_5$ | $B_{3u}$ |
| | | 1029 | ? | |
| | 894 | 898 | $\nu_4-\nu_{12}$ | $B_{2u}$ |
| | | 873 | ? | |
| 888* | 890 | | $2\nu_3$ | $A_{1g}$ |
| 846 | 855 | 854 | $\nu_{11}-\nu_3$ | $B_{3u}$ |
| 605 | 605 | 611 | $\nu_3+\nu_{10}$ | $B_{2u}$ |
| | 539 | 533 | $\nu_6-\nu_{12}$ | $B_{1u}$ |
| 361 | 360 | 363 | $\nu_4-\nu_{11}$ | $B_{2u}$ |

*Observed in the Raman spectrum.

1405 and 1640 cm.$^{-1}$ which may be explained on the basis of Fermi resonance of $\nu_9$ ($b_{2u}$) with $\nu_{11}+\nu_5$ ($B_{2u}$). In solution, only one strong band at 1555 cm.$^{-1}$ is observed. The oxalate ion has $D_{2h}$ symmetry in the solid sodium salt (9) and is assumed to have the same symmetry in solution. This is borne out by the infrared and Raman spectra which exhibit the character of mutual exclusion. In Table IV the assignment for $C_2O_4^{--}$ is given for the solid and solution made on the basis of the selection rules, depolarization ratios, and comparison with the spectrum of isoelectronic $N_2O_4$ (15). In the last column of the table the previous assignment of Lecomte *et al.* (2) is given for comparison. Since our infrared investigation covered a larger region than that investigated previously (2) and since our depolarization data are more complete than those of an earlier investigation (8), several differences between the present and the earlier (2) assignments are not unexpected. In particular the depolarization ratio of the band at 445 cm.$^{-1}$ established it as $\nu_3$. By analogy with $N_2O_4$ the other low lying Raman band is $\nu_5$ and the high one at 1305 cm.$^{-1}$ is then $\nu_6$. The band at 665 cm.$^{-1}$ reported by Lecomte *et al.* (2) occurring in the region of $CO_2$ absorption was not observed here. As $\nu_8$ we choose the strong infrared band (solid) at 507 cm$^{-1}$. The $\nu_{10}$ mode was calculated here as ~160 cm.$^{-1}$ and estimated previously (2) to be ~370 cm$^{-1}$. The calculation for $\nu_{10}$ follows from the Urey Bradley treatment by Shimanouchi *et al.* (12) for $D_{2h}$ molecules. Here it was shown that the ratio of the product of the two $b_{1g}$ frequencies to

that of the two $b_{2u}$ frequencies is a function of masses and geometry only and independent of force constants if the interaction between COO groups on different C atoms is neglected. The structural parameters used to calculate this ratio are given below (9):

$$r_{CC} = 1.56\ \text{Å},\ r_{CO} = 1.24\ \text{Å},\ \angle OCO = 125°.$$

The value of $\nu_{10} = 160$ cm.$^{-1}$ is further supported by the assignment of two observed combination tones at 1452 cm.$^{-1}$ in the Raman spectrum and 605 cm.$^{-1}$ (solution), 611 cm.$^{-1}$ (solid) in the infrared spectrum. Other interpretations of these bands are not readily forthcoming.

In Table V the combination bands observed in the infrared spectrum are listed with plausible assignments. The bands at 2862, 2479, 1885, 1029, and 873 cm.$^{-1}$ in the infrared spectrum of the solid cannot be interpreted in terms of binary combinations of the listed fundamentals.

*Formate Ion*

The Raman spectrum of a saturated solution of potassium or sodium formate in $H_2O$ is shown in Fig. 3 and the frequencies and depolarization ratios

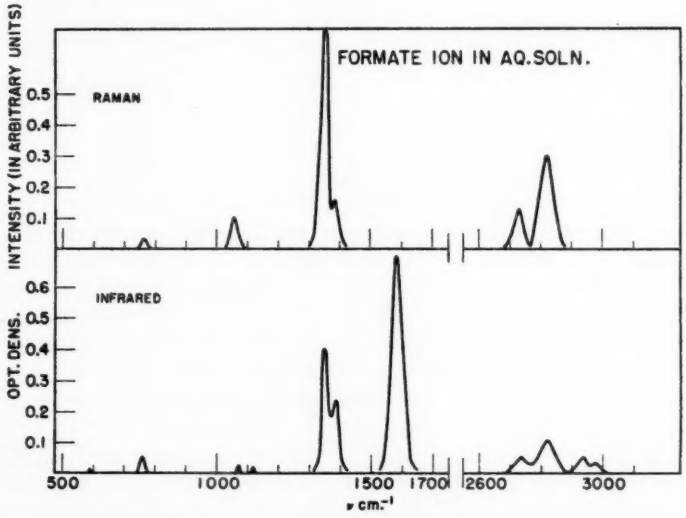


FIG. 3. The Raman and infrared spectra of the formate ion.

given in Table VI. The infrared spectrum of a saturated solution of these salts in $H_2O$ and $D_2O$ is given also in Fig. 3 and the frequencies in Table VI (fundamentals) and Table VII (combination tones). The infrared spectrum of solid sodium formate is given in Table VI (fundamentals) and in Table VII (combination tones).

The present assignment for the formate ion made on the basis of $C_{2v}$ symmetry and the measured depolarization ratios is given in Table VI.

Of the two rocking frequencies, $\nu_5$ and $\nu_6$, the higher one might be expected to be the out-of-plane mode analogous to the acetate and oxalate ions but these were assigned as shown in the table because of the results of Newman (13) obtained from the polarized infrared spectra of solid sodium formate. The present assignment for the aqueous solution is the same as that by

TABLE VI

VIBRATIONAL ASSIGNMENT OF THE FOMATE ION

| Irred. reptn. | | $\left(\begin{matrix}O\\O\end{matrix}\!\!>\!C\!-\!H\right)^-$ | Raman $\Delta\nu$ | Infrared | | | |
|---|---|---|---|---|---|---|---|
| | | | | Dep. ratio (aq. soln. of K salt) | $\nu$ (aq. soln. of K salt) | $\nu$ (solid Na salt) This work | $\nu$ (solid Na salt) Newman |
| $a_1$ | $\nu_1$ | C—H stretching | 2803 | 0.3$_7$ (P) | 2803 | 2841 | 2870 |
| | $\nu_2$ | C—O stretching | 1349 | 0.2$_9$ (P) | 1351 | 1366 | 1377 |
| | $\nu_3$ | COO deformation | 762 | 0.4$_3$ (P) | 760 | 772 | 784 |
| $b_1$ | $\nu_4$ | C—O stretching | | | 1585 | 1567 | 1620 |
| | $\nu_5$ | COO rocking (C—H bending, in-plane) | 1380 | 0.8$_6$ (D) | 1383 | 1377 | 1365 |
| $b_2$ | $\nu_6$ | COO rocking (C—H bending, out-of-plane) | 1066 | 0.8$_5$ (D) | 1069 | 1073 | 1070 |

Fonteyne (7) which was made on the basis of the Raman spectrum of the light and heavy formate ion in aqueous solution without measuring the depolarization ratios. Newman's assignments (last column of Table VI) of

TABLE VII

COMBINATION AND DIFFERENCE FREQUENCIES FOR THE INFRARED BANDS OF $HCOO^-$

| Aqueous solution | | | | Solid (Na salt) | | |
|---|---|---|---|---|---|---|
| Obs. | Calc. | Assignment | Irred. rep. | Obs. | Calc. | Assignment |
| | | | | 4313 | 4319 | $2953+\nu_3$ |
| 4180 | 4186 | $\nu_1+\nu_5$ | $B_1$ | 4200 | 4218 | $\nu_1+\nu_5$ |
| 4091 | 4111 | $2728+\nu_5$ | $A_1$ | 4085 | 4097 | $2720+\nu_5$ |
| | | | | 3611 | 3613 | $\nu_1+\nu_2$ |
| 3181 | 3178 | $2\nu_4$ | $A_1$ | 3190 | 3194 | $2\nu_4+60$ |
| | | | | 3070 | 3074 | $2\nu_4-60$ |
| 2974 | 2972 | $\nu_4+\nu_5$ | $A_1$ | 2953 | 2944 | $\nu_4+\nu_5$ |
| | | | | 2791 | 2781 | $\nu_1-60$ |
| 2728 | 2734 | $\nu_2+\nu_5$ | $B_1$ | 2720 | 2743 | $\nu_2+\nu_5$ |
| | | | | 2599 | 2600 | $2720-2\times60$ |
| 2415 | 2420 | $\nu_2+\nu_6$ | $B_2$ | 2435 | 2439 | $\nu_2+\nu_6$ |
| | | | | 2134 | 2138 | $\nu_2+\nu_3$ |
| | | | | 1700 | 1707 | $\nu_4+140$ |
| | | | | 1620 | 1627 | $\nu_4+60$ |
| | | | | 1514 | 1517 | $\nu_5+140$ |
| | | | | 1226 | 1237 | $\nu_5-140$ |
| | | | | 1013 | 1013 | $\nu_5-60$ |
| | | | | 958 | 953 | $\nu_5-2\times60$ |
| | | | | 923 | 930 | $\nu_5-140$ |
| | | | | 898 | 892 | $\nu_3+2\times60$ |
| | | | | 840 | 832 | $\nu_3+60$ |

the $a_1$ C—O stretching and the $b_1$ COO rocking were reversed as shown in the seventh column of Table VI because of the analogy with the corresponding fundamentals in the aqueous solution.

The infrared spectra of solid sodium formate were obtained of the solid films deposited from $H_2O$, a mixture of $H_2O$ and $CH_3OH$, or a mixture of $H_2O$ and acetone, on AgCl and NaCl plates. All solid samples were dried over $P_2O_5$ in a desiccator and had no absorption band in the O—H stretching region, 3100–3800 cm.$^{-1}$, showing that the samples were indeed anhydrous. The infrared spectra of these samples seemed to change slightly from sample to sample depending on the method of preparation, in contrast to the infrared spectra of the acetate and oxalate salts. In particular the $b_1$ C—O stretching mode shows a rather complicated behavior and has two bands at 1567 cm.$^{-1}$ and 1514 cm.$^{-1}$ in some samples. The intensity of the latter band was increased by dehydration in a desiccator and was even stronger in some cases than that at higher wave numbers. However, the band at 1567 cm.$^{-1}$ was assigned as a fundamental by analogy with the fundamentals for the aqueous solution. The band at 1620 cm.$^{-1}$ which was assigned as a fundamental by Newman was observed only in some samples as a weak band or a small shoulder.

Table VII shows the combination and difference bands observed in the infrared spectrum and a possible assignment. In the case of the infrared spectrum of the solid, it is necessary to assume lattice vibrational modes coupling with the internal vibrational modes of the formate ion in order to explain the observed combination bands satisfactorily. Two lattice frequencies at 140 cm.$^{-1}$ and 60 cm.$^{-1}$ have been assumed in the seventh column of Table VII which are used to interpret 13 of the 21 combination tones. There are several possible choices of the assignments for some bands in the solid infrared spectrum but only one is shown rather arbitrarily.

## REFERENCES

1. Bernstein, H. J. and Allen, G. J. Opt. Soc. Amer. 45: 237. 1955.
2. Douville, F., Duval, C., and Lecomte, J. Compt. rend. 212: 697. 1941.
3. Duval, C., Lecomte, J., and Douville, F. Ann. phys. 17: 5. 1937.
4. Edsall, J. T. J. Chem. Phys. 4: 1. 1936.
5. Edsall, J. T. J. Chem. Phys. 5: 508. 1937.
6. Edsall, J. T. and Wilson, E. B., Jr. J. Chem. Phys. 6: 124. 1938.
7. Fonteyne, R. Naturwissenschaften, 31: 441. 1943.
8. Gupta, J. Indian J. Phys. 10: 199. 1936.
9. Jeffrey, G. A. and Parry, G. S. J. Chem. Soc. 4864. 1952.
10. Jones, L. H. and McLaren, E. J. Chem. Phys. 22: 1796. 1954.
11. Kohlrausch, K. W. F. Ramanspektren. Akademische verlagsgesellschaft Becker und Erler Kom.-Ges., Leipzig. 1943.
12. See, for instance, Morino, Y., Kuchitsu, K., and Shimanouchi, T. J. Chem. Phys. 20: 726. 1952.
13. Newman, R. J. Chem. Phys. 1663. 1952.
14. Rank, D. H. and Kagarise, R. E. J. Opt. Soc. Amer. 40: 89. 1950.
15. Sutherland, G. B. B. M. Proc. Roy. Soc. A, 141: 342. 1933.
16. Theimer, R. and Theimer, O. Monatsh. Chem. 81: 314. 1950.
17. Wells, A. J. and Wilson, E. B. J. Chem. Phys. 9: 314. 1941.
18. White, J. U., Alpert, N., and DeBell, A. G. J. Opt. Soc. Amer. 45: 154. 1955.

## NOTES

### SYNTHESIS OF METHYL-$d_3$ FORMATE*

By R. Renaud and L. C. Leitch

In earlier papers of this series (1, 2) Nolin reported the preparation of several deuterated methyl and ethyl acetates from the alkyl iodides and silver acetate. On account of the instability of silver formate the method is not directly applicable to the synthesis of methyl-$d_3$ formate. This ester has now been prepared in moderately good yields by the acid-catalyzed transesterification of methyl-$d_3$ butyrate and *n*-butyl formate:

$$C_3H_7CO_2CD_3 + HCO_2C_4H_9 \rightarrow HCO_2CD_3 + C_3H_7CO_2C_4H_9.$$

The methyl-$d_3$ butyrate was prepared in nearly quantitative yield from methyl-$d_3$ bromide and silver butyrate. The methyl-$d_3$ bromide was in turn prepared by the brominative decarboxylation of silver acetate-$d_3$ in carbon tetrachloride as described in the experimental part rather than by the method reported in reference (3).

It is of interest to compare the mass spectra of methyl and methyl-$d_3$ formates:

| $HCOOCH_3$ | | $HCOOCD_3$ | |
|---|---|---|---|
| 60 | 100 | 63 | 100.0 |
| 59 | 1.86 | 62 | 4.56 |
| | | 61 | 0.1 |

Since the intensity of the 61 peak—due to loss of D—is so small in methyl-$d_3$ formate the peaks at 59 in the spectrum of methyl formate and 62 in the spectrum of methyl-$d_3$ formate must be due to loss of H in the formoxy group rather than in the methyl group.

#### EXPERIMENTAL

*Silver Butyrate*

Silver butyrate was prepared by adding a solution of 77 gm. of silver nitrate in 400 ml. of water in small portions to a stirred solution of 40 gm. of *n*-butyric acid in 200 ml. of water containing sufficient aqueous ammonia for neutralization. The salt was recrystallized from boiling water, dried for a day over phosphorus pentoxide in a vacuum desiccator, and stored in an amber bottle. The yield was nearly theoretical.

*Methyl-$d_3$ Bromide*

Silver acetate-$d_3$ (34.0 gm., 0.2 mole) was placed in a 500 ml. four-necked round-bottomed flask equipped with a funnel, a thermometer, a mechanical

*Issued as N.R.C. No. 3821.

stirrer with a graphite packed gland, and a reflux condenser. Three spiral traps, two of which were cooled in dry ice and carbon dioxide at −78° and the third at −30°C., were connected to the outlet of the condenser. A solution of 11 ml. of dry bromine in 75 ml. of dry carbon tetrachloride was added to the stirred silver salt at the rate of about a drop every two seconds. The temperature of the reaction mixture was kept at 27–30°. Addition of the bromine required about four hours. The reaction mixture was then slowly heated to the boiling point and refluxed from one to one and one-half hours while a current of dry nitrogen was passed in. The contents of the first trap were then distilled into the second. The third trap was generally empty. The crude product was distilled on the vacuum line through ascarite to remove dissolved carbon dioxide and bromine. The distillate was redistilled twice from a bath at −40°C. into a trap cooled in liquid nitrogen. The weight of crude methyl-$d_3$ bromide was 19.0 gm. After another distillation from a trap at −78° the vapor pressure of the product at 0° was 679 mm. There was little change in the vapor pressure of various fractions distilled at 0°C. The yield was 17.5 gm. (89.3% of the theoretical amount). Mass analysis showed a purity of 97.8 mol. % $CD_3Br$ or 99.2 atom % D.

*Methyl-$d_3$ Butyrate*

Silver butyrate (8.3 gm., 0.04 mole) was heated with 4.1 gm. (0.04 mole) of methyl-$d_3$ bromide in a sealed tube for 16 hr. at 80°C. in a rocking furnace. The methyl-$d_3$ butyrate was isolated by attaching the opened tube to a Stock trap cooled in liquid nitrogen on a vacuum manifold and evacuating to a pressure of 0.1 mm. The yield of ester recovered in the trap, $n_D^{20}$ 1.3879, vapor pressure 30 mm. at 22°C., was quantitative. Methyl butyrate prepared in the same way had $n_D^{20}$ 1.3874.

*Methyl-$d_3$ Formate*

A mixture of 4.5 gm. of *n*-butyl formate, 4.1 gm. of methyl-$d_3$ butyrate, and three drops of concentrated sulphuric acid was distilled in a column packed with glass helices. The yield of methyl-$d_3$ formate, b.p. 31–32°C., $n_D^{20}$ 1.3431, was 1.5 gm. (61% of the theoretical). Its mass spectrum gave a deuterium content of 97.6 mol. % or 99.07 at. %.

ACKNOWLEDGMENTS

The authors are indebted to Miss F. Gauthier and Dr. F. P. Lossing for the mass analyses.

1. NOLIN, B. Can. J. Chem. 31: 1257. 1953.
2. NOLIN, B. Can. J. Chem. 32: 1. 1954.
3. NOLIN, B. and LEITCH, L. C. Can. J. Chem. 31: 153. 1953.

RECEIVED OCTOBER 14, 1955.
DIVISION OF PURE CHEMISTRY,
NATIONAL RESEARCH COUNCIL,
OTTAWA, CANADA.

# SYNTHESIS OF DEUTERATED DIMETHYL CARBONATE*

By R. Renaud and L. C. Leitch

The well-known synthesis of alkyl carbonates from phosgene and alcohols is not suitable for the preparation of deuterated dimethyl carbonate because methyl-$d_3$ alcohol is not readily available. Since methyl-$d_3$ bromide is now easily obtained by a method reported previously by one of us (2) it seemed worth while to attempt the preparation of dimethyl carbonate from methyl bromide and silver carbonate. Diethyl carbonate labelled with $C^{14}$ was recently prepared by Eisenhauer, Pepper, Jaques, and Spinks (1) by refluxing a suspension of silver carbonate-$C^{14}$, ethyl iodide, and triethylamine under nitrogen. In the present work it was found that no reaction took place when methyl iodide and silver carbonate were heated under reflux for a day. However, when these reactants were treated for 65 hr. in a sealed tube at 60°, a 75% yield of dimethyl carbonate was obtained. With methyl bromide the yield was nearly quantitative, possibly because the product was more easily separated from unchanged methyl bromide. Similar results were obtained when methyl-$d_3$ bromide was employed. Dehalogenation of hexachloromethyl carbonate with zinc-dust and acetic acid did not give the desired product. Evolution of carbon dioxide took place presumably because of hydrolysis of the ester and no dimethyl carbonate could be isolated.

## EXPERIMENTAL

### *Dimethyl Carbonate*

#### (*a*) *From Methyl Iodide and Silver Carbonate*

Methyl iodide (14.7 gm., 0.11 mole) was distilled on a vacuum manifold into a tube containing 13.8 gm. (0.05 mole) of dry silver carbonate. The tube was sealed and heated in a rocking furnace at 60°C. for 65 hr. The liquid phase was distilled off on a vacuum line into a distilling flask. Fractional distillation of the distillate through a small column packed with glass helices afforded a 75% yield of dimethyl carbonate, b.p. 89–91°C., $n_D^{20}$ 1.3694.

#### (*b*) *From Methyl Bromide and Silver Carbonate*

A similar experiment with methyl bromide gave a nearly quantitative yield of dimethyl carbonate. An attempt to shorten the reaction time by raising the temperature to 90°C. resulted in decomposition of the silver carbonate with evolution of carbon dioxide.

### *Dimethyl-$d_3$ Carbonate*

A mixture of 5.6 ml. (10.0 gm., 0.12 mole) of methyl-$d_3$ bromide prepared as described in reference (2) and 13.8 gm. of silver carbonate was heated for 65 hr. at 60°C. The reaction product was isolated and purified as already described. The yield of deuterated dimethyl carbonate, b.p. 89–90°C., $n_D^{20}$

*Issued as N.R.C. No. 3822.

1.3677, was 4.3 g.m. A sample analyzed by mass spectrometry showed a deuterium content of 98 atom %.

ACKNOWLEDGMENTS

The authors are indebted to Miss F. Gauthier and Dr. F. P. Lossing of this Division for the mass analysis.

1. EISENHAUER, R. H., PEPPER, J. M., JAQUES, L. B., and SPINKS, J. W. T. Can. J. Chem. 30: 245. 1953.
2. RENAUD, R. and LEITCH, L. C. Can. J. Chem. 34: 179. 1956.

RECEIVED OCTOBER 14, 1955.
DIVISION OF PURE CHEMISTRY,
NATIONAL RESEARCH COUNCIL,
OTTAWA, CANADA.

## CHOLESTEROL FROM ASCARIS LUMBRICOIDES (NEMATODA)*

BY DONALD FAIRBAIRN AND R. NORMAN JONES

Conclusive evidence for the existence of sterols in any species belonging to the phylum Nematoda was not available until it was shown (1) that the reproductive organs of the common pig roundworm, *Ascaris lumbricoides*, contain small amounts of a mixture of saturated and unsaturated sterols in the approximate ratio 1:3. Although infrared analysis of the mixed sterol acetates suggested that cholesterol might be one component of the mixture, insufficient material was available for positive identification.

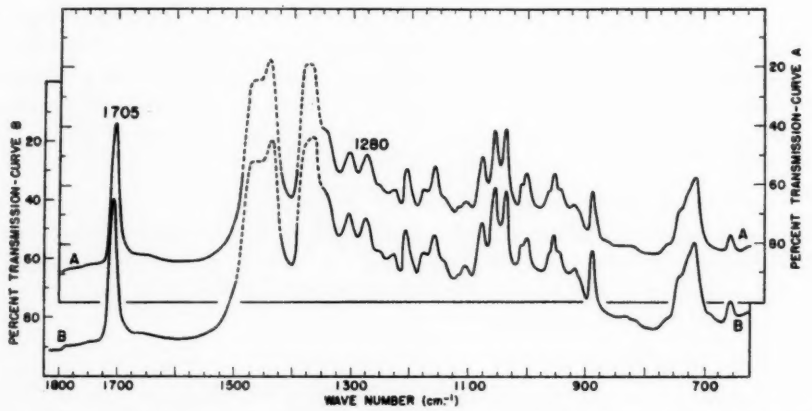


FIG. 1. Curve A. Infrared spectrum of sample of cholesterol dibromide prepared concurrently with ascaris sterol dibromide.
Curve B. Infrared spectrum of ascaris sterol dibromide. (Nujol mulls. - - -region of Nujol absorption.)

*Issued as N.R.C. No. 3829.*

An extension of the investigation has resulted in the isolation and identification of cholesterol as the dibromide. From the total lipids extracted from the blended muscle and reproductive tissues of mature female parasites, total sterols were precipitated as the digitonides and subsequently recovered in the free form (4). The recrystallized mixture was then brominated (3), insoluble bromides separated, and saturated sterols isolated as the digitonides. Recrystallization of the bromide from ether and glacial acetic acid yielded a product identical in melting point and mixed melting point with cholesterol dibromide. The saturated sterol(s) has not yet been identified.

The infrared spectra of the ascaris sterol dibromide and a sample of cholesterol dibromide prepared concurrently are shown in Curves A and B of Fig. 1. The similarity of these curves confirms the identification of the ascaris sterol, but both curves show absorption at 1705 and 1280 cm.$^{-1}$ which is not present in Fig. 2, obtained from a second sample of cholesterol dibromide immediately following crystallization from ethyl acetate – methanol at room temperature.* This difference is attributed to the partial photolysis or autoxidation of the first two samples during transshipment prior to analysis.

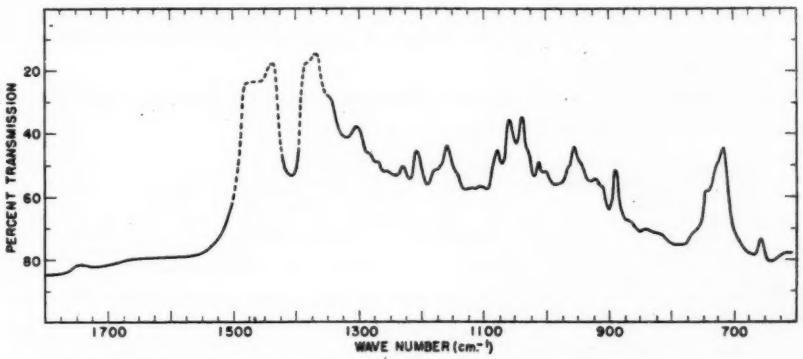


FIG. 2. Infrared spectrum of freshly prepared cholesterol 5$\alpha$,6$\beta$-dibromide.

The bromination method employed resulted in characteristically low yields of ascaris sterol bromide, which were necessarily accepted because it was desirable to isolate saturated sterols quantitatively from the mother liquor. For this reason the identification of cholesterol as the main unsaturated sterol depended upon the provision of auxiliary evidence such as (1) the similarly low yield obtained by bromination of pure cholesterol, (2) the iodine number and rate and intensity of color development with the Schoenheimer-Sperry reagent (1, 2), and (3) the infrared spectrum of the mixed acetates (1), which resembled closely that of authentic cholesterol acetate. These observations led to the conclusion that large amounts of unsaturated sterols other than cholesterol were absent.

*We wish to thank Dr. A. Nickon for the preparation of this material.

## EXPERIMENTAL

Thirty grams of the fats obtained by extraction of 2 kgm. of ascaris muscle and reproductive tissue (representing 2.6 kgm. of adult female parasites) was shaken vigorously with five volumes of ethanol (twice), after which the clear solution was treated with 1% digitonin in ethanol. The sterol digitonides so obtained were washed twice by centrifugation with ethanol–ether (1:2) and three times with ether, dried, decomposed in a minimum volume of dry pyridine at 70°, and the free digitonin precipitated by addition of 10 volumes of dry, ethanol-free ether. The supernatant solution contained 260 mgm. of mixed sterols which were recrystallized once from 80% methanol (m.p. 123–124°). Bromination of 216 mgm. of this product provided 67 mgm. of sterol bromide (29% yield, calculated as cholesterol dibromide and including the necessary correction for saturated sterol content) which was recrystallized twice from ether and glacial acetic acid (1:3). Authentic cholesterol dibromide was prepared by the same procedure (yield, 31%). M.p. cholesterol dibromide 115.5–116°, ascaris sterol bromide 115–116°, mixed m.p. 115–116°; identical infrared spectra.

The mother liquor obtained from the bromination of ascaris sterols was treated with digitonin to remove saturated (unbrominated) sterol. From the resulting digitonide 54 mgm. of saturated sterol was recovered (iodine number, 2; m.p. 131–132°).

Financial assistance from the National Research Council of Canada is gratefully acknowledged.

1. Fairbairn, D. Can. J. Biochem. Physiol. 33:31. 1955.
2. Idler, D. R. and Baumann, C. A. J. Biol. Chem. 203:389. 1953.
3. Schoenheimer, R. Hoppe-Seyler's Z. physiol. Chem. 192:77. 1930.
4. Schoenheimer, R. and Dam, H. Hoppe-Seyler's Z. physiol. Chem. 215:59. 1933.

Received October 28, 1955.
Institute of Parasitology,
McGill University,
Macdonald College, Prov. of Quebec,
and
Division of Pure Chemistry,
National Research Council of Canada,
Ottawa, Canada.

## PREPARATION OF TRIBUTYL ANTIMONITE

By L. J. Carbonneau and D. C. Downing

There is only one reference in the literature to a direct preparation of antimony esters (2). In it, antimony trioxide was reacted with the corresponding alcohol, under water-removing conditions.

We attempted to carry out this preparation with butanol, without success. It was then found that the ester could be readily prepared, in high (86%) yield, by reacting butanol and antimony trichloride.

Into a 500 ml. three-necked flask, equipped with a mechanical stirrer, reflux condenser, thermometer, and provision for solid addition, was weighed 74.1 gm.

(1.0 mole, Shaw. Chem. dried) *n*-butanol. With continuous stirring, 76.0 gm. (0.33 mole, Mallinckrodt A.R.) antimony trichloride was added over a 0.5 hr. period. The temperature rose from 26–30° C. No cooling was used. Stirring was continued for an additional 0.5 hr. Ammonia gas was then bubbled through the stirred mixture until no more gas was absorbed (excess ammonia coming through), using external cooling to keep the reaction below 25° C. During precipitation of ammonium chloride, 250 ml. of isoheptane was added to thin the mixture. The mixture was filtered on a Büchner funnel, and the precipitate washed with 5×50 ml. of isoheptane.

The filtrate was distilled without a column at 200 mm. up to a pot temperature of 140° C., to remove isoheptane and unreacted butanol. The pressure was then reduced to 5.5 mm. and the fraction boiling at 139–141° C., collected, 97.0 gm. (86% of theory), $n_D^{20} = 1.4792$. The previously reported boiling point is 138.5–139.5° C. at 5.5 mm. (1).

1. ARBUZOV, B. A. and VINOGRADOVA, V. S. Chem. Abstr. 46: 7995. 1952.
2. MACKEY, J. F. J. Chem. Soc. 95: 604. 1909.

RECEIVED NOVEMBER 7, 1955.
RESEARCH LABORATORIES,
SHAWINIGAN CHEMICALS LIMITED,
SHAWINIGAN FALLS, QUE.

## THE CRYSTAL STRUCTURE OF DES-(OXYMETHYLENE)-LYCOCTONINE HYDRIODIDE MONOHYDRATE*

BY MARIA PRZYBYLSKA AND LÉO MARION

Des-(oxymethylene)-lycoctonine hydriodide monohydrate, $C_{24}H_{39}O_6N.HI.H_2O$, (1) crystallizes from a mixture of methanol and acetone in colorless, fine, monoclinic sphenoidal prisms, elongated along [010]. There are two optically active molecules per unit cell and since the only reflections absent are $0k0$ with $k$ odd, the space group is $P2_1$. The unit cell dimensions are

$$a = 12.79 \text{ Å},$$
$$b = 9.44 \text{ Å},$$
$$c = 11.00 \text{ Å},$$
$$\beta = 97°45'.$$

Three-dimensional data were obtained from Weissenberg photographs and the number of reflections observed amounted to 68% of those theoretically possible. The $x$ and $z$ co-ordinates of the iodine atom were derived from a Patterson projection on (010).

A three-dimensional Fourier synthesis was carried out using the phases based on the iodine contributions only. By placing the iodine atom at $y=0.250$ the elements of symmetry of space group $P2_1/m$ were introduced and the Fourier pattern showed in addition to real atoms at $x$, $y$, $z$, and $-x$, $\frac{1}{2}+y$,

*Issued as N.R.C. No. 3842.

$-z$, unreal peaks at $-x$, $-y$, $-z$, and $x$, $\frac{1}{2}-y$, $z$. The interpretation of these results gave for its free base (des-(oxymethylene)-lycoctonine) the structure represented by the schematic drawing and by the photograph of the molecular model.

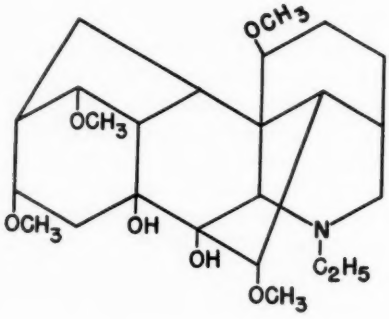


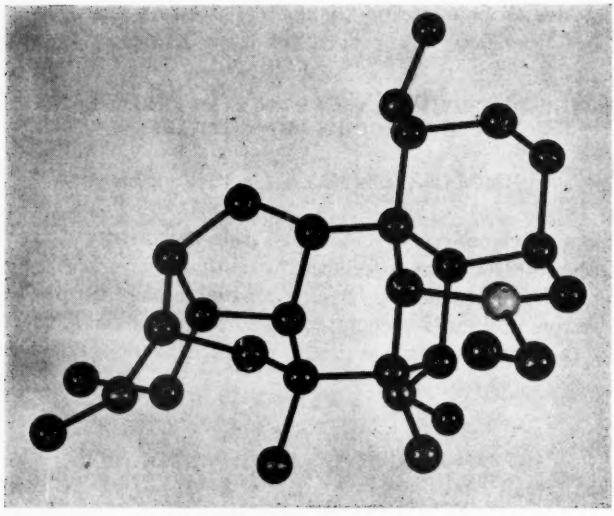

FIG. 1. The stereochemical configuration of des-(oxymethylene)-lycoctonine.

A $h0l$ difference synthesis using $(F_0-F_c)$ as coefficients was then computed, the structure-factor calculations having been based on $f$ values for carbon and iodine only. The pattern obtained indicated clearly all six oxygen atoms of the molecule and the oxygen atom of water of crystallization. Thus the ethyl group was identified and since it has been chemically proved to be attached to the nitrogen atom (2), the latter was indirectly located. No other chemical assumptions were made in this investigation.

The atomic parameters were subsequently refined by Fourier and $(F_o - F_c)$ projections along the three axes of the unit cell and the reliability index, defined as $R = \Sigma||F_o| - |F_c|| \div \Sigma|F_o|$, is now about 0.20 for each of these zones.

This work will be published in fuller detail at a later date in a different journal.

Grateful acknowledgment is made to Dr. W. H. Barnes for the use of the equipment in his laboratory and to Dr. O. E. Edwards for his interest and for the pure, chemically analyzed sample of the salt. Thanks are also due to Miss I. Ourom for her part in carrying out the computations.

1. EDWARDS, O. E. and MARION, L. Can. J. Chem. 30: 627. 1952.
2. EDWARDS, O. E. and MARION, L. Can. J. Chem. 32: 1146. 1954.

RECEIVED NOVEMBER 4, 1955.
DIVISION OF PURE CHEMISTRY,
NATIONAL RESEARCH COUNCIL,
OTTAWA, CANADA.

# CANADIAN JOURNAL OF CHEMISTRY

## Notes to Contributors

### Manuscripts

(i) ***General.*** Manuscripts, in English or French, should be typewritten, double spaced, on paper 8½ × 11 in. **The original and one copy are to be submitted.** Tables and captions for the figures should be placed at the end of the manuscript. Every sheet of the manuscript should be numbered.

Style, arrangement, spelling, and abbreviations should conform to the usage of this journal. Names of all simple compounds, rather than their formulas, should be used in the text. Greek letters or unusual signs should be written plainly or explained by marginal notes. Superscripts and subscripts must be legible and carefully placed.

Manuscripts and illustrations should be carefully checked before they are submitted. Authors will be charged for unnecessary deviations from the usual format and for changes made in the proof that are considered excessive or unnecessary.

(ii) ***Abstract.*** An abstract of not more than about 200 words, indicating the scope of the work and the principal findings, is required, except in Notes.

(iii) ***References.*** References should be listed **alphabetically by authors' names,** numbered, and typed after the text. The form of the citations should be that used in this journal in references to papers in periodicals, titles should not be given and only initial page numbers are required. All citations should be checked with the original articles and each one referred to in the text by the key numbers.

(iv) ***Tables.*** Tables should be numbered in roman numerals and each table referred to in the text. Titles should always be given but should be brief; column headings should be brief and descriptive matter in the tables confined to a minimum. Vertical rules should be used only when they are essential. Numerous small tables should be avoided.

### Illustrations

(i) ***General.*** All figures (including each figure of the plates) should be numbered consecutively from 1 up, in arabic numerals, and each figure referred to in the text. The author's name, title of the paper, and figure number should be written in the lower left corner of the sheets on which the illustrations appear. Captions should not be written on the illustrations (see Manuscripts (i)).

(ii) ***Line Drawings.*** Drawings should be carefully made with India ink on white drawing paper, blue tracing linen, or co-ordinate paper ruled in blue only; any co-ordinate lines that are to appear in the reproduction should be ruled in black ink. Paper ruled in green, yellow, or red should not be used unless it is desired to have all the co-ordinate lines show. All lines should be of sufficient thickness to reproduce well. Decimal points, periods, and stippled dots should be solid black circles large enough to be reduced if necessary. Letters and numerals should be neatly made, preferably with a stencil (**do NOT use typewriting**) and be of such size that the smallest lettering will be not less than 1 mm. high when reproduced in a cut 3 in. wide.

Many drawings are made too large; originals should not be more than 2 or 3 times the size of the desired reproduction. In large drawings or groups of drawings the ratio of height to width should conform to that of a journal page but the height should be adjusted to make allowance for the caption.

**The original drawings and one set of clear copies (e.g. small photographs) are to be submitted.**

(iii) ***Photographs.*** Prints should be made on glossy paper, with strong contrasts. They should be trimmed so that essential features only are shown and mounted carefully, with rubber cement, on white cardboard with no space or only a **very** small space (less than 1 mm.) between them. In mounting, full use of the space available should be made (to reduce the number of cuts required) and the ratio of height to width should correspond to that of a journal page (4¾ × 7½ in.); however, allowance must be made for the captions. Photographs or groups of photographs should not be more than 2 or 3 times the size of the desired reproduction.

**Photographs are to be submitted in duplicate;** if they are to be reproduced in groups one set should be mounted, the duplicate set unmounted.

### Reprints

A total of 50 reprints of each paper, without covers, are supplied free. Additional reprints, with or without covers, may be purchased.

Charges for reprints are based on the number of printed pages, which may be calculated approximately by multiplying by 0.6 the number of manuscript pages (double-spaced typewritten sheets, 8½ × 11 in.) and including the space occupied by illustrations. An additional charge is made for illustrations that appear as coated inserts. The cost per page is given on the reprint requisition which accompanies the galley.

Any reprints required in addition to those requested on the author's reprint requisition form must be ordered officially as soon as the paper has been accepted for publication.

## *Contents*


Page

The Syntheses of Sugars from Smaller Fragments. Part X. Synthesis of L-*Glucoheptulose*—*J. K. N. Jones and R. B. Kelly* - - - 95

Organic Deuterium Compounds. XIV. Preparation of Deuterated Methyl Benzenes—*R. Renaud and L. C. Leitch* - - - - - - 98

The Reactions of Trifluoromethyl Radicals with Propane, *n*-Butane, and Isobutane—*P. B. Ayscough and E. W. R. Steacie* - - - 103

The Polymerization of Styrene in the Presence of $\alpha$- and $\beta$-Bromostyrene—*M. H. Jones* - - - - - - - - - - - - - - - 108

The Photolysis of Ketene in the Presence of Hydrogen—*H. Gesser and E. W. R. Steacie* - - - - - - - - - - - - - - - 113

An Oxygen-18 Study of Acetal Formation and Hydrolysis—*Fred Stasiuk, W. A. Sheppard, and A. N. Bourns* - - - - - - - - 123

Depolarization by Mercaptoacetic Acid During Electrodeposition of Copper—*A. J. Sukava and C. A. Winkler* - - - - - - - - 128

The Crystal Structures of Some Intermetallic Compounds of Plutonium—*O. J. C. Runnalls* - - - - - - - - - - - - - 133

Theory of the Transient Phase in Kinetics, with Special Reference to Enzyme Systems. II. The Case of Two Enzyme–Substrate Complexes—*Ludovic Ouellet and Keith J. Laidler* - - - - - 146

Vapor Pressures of Aqueous Solutions of Silver Nitrate, of Ammonium Nitrate, and of Lithium Nitrate—*A. N. Campbell, J. B. Fishman, G. Rutherford, T. P. Schaefer, and L. Ross* - - - 151

The Number of Polypeptide Chains in Bovine Plasma Albumin—*M. E. Reichmann and J. Ross Colvin* - - - - - - - - - - 160

The Vibrational Spectra of the Formate, Acetate, and Oxalate Ions—*K. Ito and H. J. Bernstein* - - - - - - - - - - - - - 170

Synthesis of Methyl-$d_1$ Formate—*R. Renaud and L. C. Leitch* - - 179

Synthesis of Deuterated Dimethyl Carbonate—*R. Renaud and L. C. Leitch* - -- - - - - - - - - - - - - - - - - - - - 181

Cholesterol from *Ascaris lumbricoides* (Nematoda)—*Donald Fairbairn and R. Norman Jones* - - - - - - - - - - - - - - 182

Preparation of Tributyl Antimonite—*L. J. Carbonneau and D. C. Downing* - - - - - - - - - - - - - - - - - - - - - 184

The Crystal Structure of Des-(oxymethylene)-lycoctonine Hydriodide Monohydrate—*Maria Przybylska and Léo Marion* - - - 185


*Printed* in Canada *by* University of Toronto Press